

# **STRESS ANALYSIS OF COMPOSITE LAMINATES**

By

**Shulong Liu *B.Eng., M.Eng., M.Sc.***

*Thesis submitted to The University of Nottingham*

*for the degree of Doctor of Philosophy*

*September 2001*

# Contents

<b>List of Tables</b>	v
<b>List of Figures</b>	vii
<b>List of symbols and abbreviations</b>	x
<b>Abstract</b>	xii
<b>Acknowledgement</b>	xiii
<b>Chapter 1: Introduction</b>	1
1.1 Composite plate theories subject to mechanical loading	2
1.2 Composite plate theories subject to thermal loading	6
1.3 A predictor-corrector method	8
1.4 An overview into chapters	10
<b>Chapter 2: Generalized plate theories subject to mechanical loadings</b>	13
2.1 Introduction	13
2.2 General considerations	13
2.3 Development of general six-degree-of-freedom plate theory	16
2.3-1 Displacement field, kinematic relations	16
2.3-2 Definition of the force and moment resultants	18
2.3-3 Equilibrium equations and boundary conditions	19
2.4 A brief reduction into general five-degree-of-freedom plate theory	22
2.4-1 Displacement field, kinematic relations	22
2.4-2 Equilibrium equations and boundary conditions	23

<b>Chapter 3 Solutions to the cylindrical bending problem of laminated composite plates using several versions of generalized beam theories</b>	<b>25</b>
3.1 Introduction	25
3.1.1 External loading	28
3.1.2 Displacement field of conventional beam/plate theories	29
3.1.3 Shape functions in classical beam theory subject to mechanical loading	30
3.1.4 Shape functions in uniform shear deformable beam theory subject to mechanical loading	30
3.1.5 Shape functions in parabolic shear deformable beam theory subject to mechanical loading	31
3.2 General three-degree-of-freedom beam theory for cross-ply laminated beams subject to mechanical loading	31
3.2.1 Formulation	31
3.2.2 Determination of shape functions subject to mechanical loading	33
3.3 General four-degrees-of-freedom beam theory for cross-ply laminated beams subjected to mechanical and thermal loadings	35
3.3.1 Formulation	35
3.3.2 Determination of shape functions subject to mechanical and thermal loadings	39
3.4 General five-degree-of-freedom beam theory for angle-ply laminated beams subject to mechanical loading	43
3.4.1 Formulation	43
3.4.2 Determination of shape functions subject to mechanical loading	46

<b>Chapter 4 A predictor-corrector method for accurate stress analysis of</b>	<b>49</b>
<b>    composite beams and plates</b>	
4.1. Introduction	49
4.2 Predictor phase	50
4.3 Corrector phase	52
<b>Chapter 5 Application of the predictor-corrector method for cross-ply</b>	<b>56</b>
<b>    composite laminates subject to mechanical loading</b>	
5.1 Introduction	56
5.2 Assessment of certain refined models for cross-ply laminated simply	57
supported beams	
5.3 Application on general three-degree-of-freedom and four-degree-of-freedom	65
beam theory for different sets of boundary conditions	
5.4 On the generalised plane strain deformations of thick anisotropic composite	71
laminated plates	
5.5 Conclusions	75
<b>Chapter 6 Application of the predictor-corrector method for angle-ply</b>	<b>77</b>
<b>    composite laminates subject to mechanical loading</b>	
6.1 Introduction	77
6.2 General considerations	77
6.3 Numerical results and discussion	79
6.4 Conclusions	89

<b>Chapter 7 Application of general four-degree-of-freedom beam theory for</b>	<b>91</b>
<b>    cross-ply laminated composite beams subjected to thermal loading</b>	
7.1 Introduction	91
7.2 General considerations	91
7.3 Numerical results and discussion	93
7.4 Conclusions	109
<b>Chapter 8 Conclusions</b>	<b>112</b>
<b>Appendix 1 General solution of general three-degree-of-freedom beam theory</b>	<b>117</b>
<b>    equations</b>	
<b>Appendix 2 General solution of general four-degree-of-freedom beam theory</b>	<b>118</b>
<b>    equations</b>	
<b>Appendix 3 General solution of general five-degree-of-freedom beam theory</b>	<b>120</b>
<b>    equations</b>	
<b>References</b>	<b>122</b>

## List of Tables

5.2-1	Comparison of shear stress distributions, $\tau_{xz}(0, z)/q_1$ , for a two-layered simply supported beam	60
5.2-2	Comparison of transverse normal stress distributions, $\sigma_z(L/2, z)/q_1$ , for a two-layered simply supported beam	60
5.3-1.	Shear stress, $\tau_{xz}(L/4, z)$ , and transverse normal stress, $\sigma_z(L/2, z)$ , for a two-layered clamped-clamped beam	67
5.3-2	Shear stress, $\tau_{xz}(L/4, z)$ , and transverse normal stress, $\sigma_z(L/2, z)$ , for a two-layered clamped-free beam	67
5.4-1	Comparison of corresponding numerical results for increasing values of length to thickness ratio	70
6.3-1	Transverse shear and normal stress predictions for three-layered clamped-clamped beam ( $\alpha = 30^\circ$ )	81
6.3-2	Transverse shear and normal stress predictions for three-layered clamped-free beam ( $\alpha = 30^\circ$ )	84
6.3-3	Normalised transverse shear parameters, $\bar{\tau}_{xz}(0.25L, z)$ , of three-layered clamped-clamped beam	87
6.3-4	Normalised transverse shear parameters, $\bar{\tau}_{xz}(0.75L, z)$ , of three-layered clamped-free beam	87
7.3-1	Normalised displacements given $T_0 \sin p_1 x$ for simply supported beam	94
7.3-2	Normalised stresses given $T_0 \sin p_1 x$ for simply supported beam	95

7.3-3	Normalised displacements given $T_1 z \sin p_1 x$ for simply supported beam	96
7.3-4	Normalised stresses given $T_1 z \sin p_1 x$ for simply supported beam	97
7.3-5	Normalised displacements and stress in predictor phase given $T_0 \sin p_1 x$ for clamped-clamped beam	101
7.3-6	Normalised stresses given $T_0 \sin p_1 x$ for clamped-clamped beam	102
7.3-7	Normalised displacements and stress in predictor phase given $T_1 z \sin p_1 x$ for clamped-clamped beam	103
7.3-8	Normalised stresses given $T_1 z \sin p_1 x$ for clamped-clamped beam	104

## List of Figures

2.2-1	Coordinate system and layer numbering used for laminated plate	14
3.2-1	Coordinate system and Geometry of laminated beam	26
5.2-1	Percentage error of shear stress, $\tau_{xz}(0, z)/q_1$ , for a simply supported beam	61
5.2-2	Percentage error of shear stress, $\tau_{xz}(0, -0.1h)/q_1$ , for a simply supported beam	61
5.2-3	Percentage error of shear stress, $\tau_{xz}(0, -0.1h)/q_1$ , for a simply supported beam	63
5.2-4	Percentage error of transverse normal stress, $\sigma_z(L/2, z)/q_1$ , for a simply supported beam	63
5.2-5	Percentage error of transverse normal stress, $\sigma_z(L/2, -0.1h)/q_1$ , for a simply supported beam	64
5.2-6	Percentage error of transverse normal stress, $\sigma_z(L/2, -0.1h)/q_1$ , for a simply supported beam	64
5.3-1	Shear stress, $\tau_{xz}(L/4, -0.1h)/q_1$ , for a clamped-clamped composite beam	68
5.3-2	Transverse normal stress, $\sigma_z(L/2, -0.1h)/q_1$ , for a clamped-clamped composite beam	68
5.3-3	Shear stress, $\tau_{xz}(L/4, -0.1h)/q_1$ , for a clamped-free composite beam	70
5.3-4	Transverse normal stress, $\sigma_z(L/2, -0.1h)/q_1$ , for a clamped-free composite beam	70
6.3-1	Normalized shear stress distributions, $\bar{\tau}_{xz}$ , in corrector phase for a CC beam	82

6.3-2	Normalized transverse normal stress distributions, $\bar{\sigma}_z$ , in corrector phase for a CC beam	82
6.3-3	Normalized shear stress distributions, $\bar{\tau}_{xz}$ , in corrector phase for a CF beam	85
6.3-4	Normalized transverse normal stress distributions, $\bar{\sigma}_z$ , in corrector phase for a CF beam	85
7.3-1	In-plane displacement distributions for a simply supported beam induced by $T_0 \sin(p_1 x)$	98
7.3-2	In-plane bending stress distributions for a simply supported beam induced by $T_0 \sin(p_1 x)$	98
7.3-3	Transverse shear stress distributions for a simply supported beam induced by $T_0 \sin(p_1 x)$	99
7.3-4	In-plane displacement distributions for a simply supported beam induced by $T_1 z \sin(p_1 x)$	99
7.3-5	In-plane bending stress distributions for a simply supported beam induced by $T_1 z \sin(p_1 x)$	100
7.3-6	Transverse shear stress distributions for a simply supported beam induced by $T_1 z \sin(p_1 x)$	100
7.3-7	In-plane displacement distributions in predictor phase for a clamped- clamped beam induced by $T_0 \sin(p_1 x)$	105
7.3-8	In-plane bending stress distributions in predictor phase for a clamped- clamped beam induced by $T_0 \sin(p_1 x)$	105

7.3-9	Transverse shear stress distributions in corrector phase for a clamped-clamped beam induced by $T_0 \sin(p_1 x)$	106
7.3-10	In-plane displacement distributions in predictor phase for a clamped-clamped beam induced by $T_1 z \sin(p_1 x)$	106
7.3-11	In-plane bending stress distributions in predictor phase for a clamped-clamped beam induced by $T_1 z \sin(p_1 x)$	107
7.3-12	Transverse shear stress distributions in corrector phase for a clamped-clamped beam induced by $T_1 z \sin(p_1 x)$	107

## List of symbols and abbreviations

$q_m$	Amplitude of mechanical loading
$p_m$	Angular velocity
$L$	Beam length
$\alpha_i$	Constants of thermal expansion
$T_0, T_1$	Constants of thermal loading
$r$	Layer number
$q(x)$	Mechanical loading
$Er\%$	Percentage error
$L_x$	Plate dimension along the $x$ direction
$L_y$	Plate dimension along the $y$ direction
$h$	Plate thickness
$Q_{ij}$	Reduced elastic stiffness
$\varepsilon_j$	Strain component
$V_0$	Strain energy density function
$\sigma_i$	Stress component
$\Delta T$	Temperature change
$C_{ij}$	Three-dimensional elastic stiffness
$N$	Total number of layers
$h_r$	Transverse coordinate of interface
$u_1, v_1, w_1$	Transverse strains on the plate middle plane

$u_0, v_0, w_0$	Displacement of the plate middle plane in the $x$ , $y$ and $z$ direction
$\varphi_1, \varphi_2, \psi$	Shape functions
CLPT	Classical laminated plate theory
G3BT	General three-degree-of-freedom shear deformable beam theory
G3TC	Corrector phase of the G3BT
G3TP	Predictor phase of the G3BT
G4BT	General four-degree-of-freedom shear and transverse normal deformable beam theory
G4TC	Corrector phase of the G4BT
G4TP	Predictor phase of the G4BT
G5BT	General five-degree-of-freedom shear deformable beam theory
HSDT	Higher order shear deformable plate theory
PSDT	Parabolic shear deformable plate theory
PSDTC	Corrector phase of the PSDT
PSDTP	Predictor phase of the PSDT
USDT	Uniform shear deformable plate theory (first order shear deformable theory)
USDTC	Corrector phase of the USDT
USDTP	Predictor phase of the USDT

## **Abstract**

A general displacement-based shear and transverse normal deformable plate theory is reviewed. Shear and transverse normal deformable plate theories suitable for cylindrical bending problems have been deduced from the general plate theory by introducing certain general functions of the transverse coordinate into the displacement field approximation. This theory takes into account the transverse shear and normal deformation effects and unifies most of the classical and shear deformable theories available in the literature.

A predictor-corrector method has been used for improving the accuracy of transverse stress analysis results and assessing the accuracy of composite plate/beam theories. In more detail, uniform shear deformable plate theory, parabolic shear deformable plate theory, general three-degree-of-freedom shear deformable plate theory, general four-degree-of-freedom transverse shear and normal deformable plate theory and general five-degree-of-freedom shear deformable plate theory are employed to improving their prediction performances of transverse shear and normal stresses.

By means of the assessment of plate theories for simply supported beams, general three-degree-of-freedom shear deformable plate theory, general four-degree-of-freedom transverse shear and normal deformable plate theory are applied for other sets of boundary conditions of cross-ply laminates subject to mechanical loading. General five-degree-of-freedom shear deformable plate theory is applied for angle-ply laminates subject to mechanical loading. In addition, general four-degree-of-freedom transverse shear and normal deformable plate theory is employed for cross-ply laminates subject to thermal loading. The numerical results of the present studies are compared with the corresponding exact solution results available in the literature.

## **Acknowledgements**

I would like to thank both my supervisors, Dr. Kostas Soldatos for his great helpful and encouraging supervision, and Dr. Arthur England for his supportive guidance and supervision throughout course of my Ph.D.

I would like to thank to Prof. David Riley, Prof. John King, Dr. Richard Tew and Mrs. Anne Perkins for their warm help.

I would like to thank to Prof. Romesh Batra, Dr. Senthil Vel and Prof. Xiaoping Shu for their warm help and supplying me relative results to check the accuracy of my approach.

I would like to thank to the University of Nottingham, the School of Mathematical Science and the Division of Theoretical Mechanics for the awards of International Research Scholarships.

Many thanks to other members of staff, secretaries and postgraduate friends, all of whom created a warm and collaborative working environment in the department.

Finally, I wish to thank my wife, Wen Qin, my parents, my daughter and other members of my family, also to all of my friends who gave me necessary support and encouragement during my studies.

# Chapter 1

## Introduction

Composite materials have become increasingly important in industrial applications over recent years, particularly in the components of aircraft structures, where low weight and high strength are desired properties. Materials such as Boron-epoxy and graphite-epoxy consist of fibres (boron, graphite, etc.) and matrix (epoxy, etc.) providing the integrity of the composite by binding the fibres together. Using these types of highly fibre-reinforced materials enables the designer to control the strength and the stiffnesses of the structure. By stacking layers of different composite materials and/or changing the fibre orientation, one can form composite laminates. By construction, composite laminates have their planar dimensions one or two orders of magnitude larger than their thickness. Often laminates are used in applications which require axial and bending strength and so, composite laminates can be treated as plates.

Those composite laminated plates considered in this study are made of special orthotropic layers (i.e. cross-ply laminates) and generally orthotropic layers (i.e. angle-ply laminates). Their properties will be described in more detail in the relative chapters. The reference surface is an important feature of a composite laminate due to fact that the equations implying the deformation of the plate are defined in terms of those reference-surface deformations. The middle surface of the plate, which lies equidistant from the bounding lateral surfaces, is usually chosen as the reference surface. It may, however, be appropriate to choose the top or bottom lateral surface as the reference surface. In addition,

the edges of the plate, which cut the reference surface perpendicularly, are important in characterising the plate geometry.

Plate theories are a part of the theory of elasticity concerning the study of elastic bodies under the action of external mechanical forces. In linear plate theories, which are the main concern of this study, deformations are considered to be small compared to the plate thickness and strains are linearly proportional to stresses. Hence, Hooke's law and the theory of linear elasticity are valid throughout this study. Due to the complicated nature of three-dimensional (3D) elasticity equations for plates, their simplified two-dimensional (2D) forms have been mostly used in the literature. Taking advantage of the small thickness, 3D elasticity equations can be reduced to 2D ones, while the quantities implicated become functions of the reference surface coordinates.

### **1.1 Composite plate theories subject to mechanical loading**

Early developments in plate theories date back to the first half of the 19th century when structures were usually made of homogeneous isotropic materials whose material properties are identical in any direction. The two main approaches developed were by A. Cauchy and S. D. Poisson and subsequently by G. Kirchhoff in the latter half of the century [Love, 1952] [Novozhilov, 1964]. Their methods still provide the basis of more refined plate theories in use today.

The method proposed by Cauchy [1828] and Poisson [1829] considers the displacements and stresses to be expansions of the transverse coordinate measured from the middle surface of the plate along its thickness. Although it is theoretically possible to approach exact solutions of plate deformation by retaining a great many terms in those series expansions, the series considered may not be convergent [Novozhilov, 1964].

The second method proposed by Kirchhoff [1850] is based on several assumptions. In the classical laminated plate theory (CLPT), it is assumed that the Kirchhoff hypothesis holds. Kirchhoff's assumptions are [Reddy, 1997]:

1. Straight lines perpendicular to the middle surface (i.e., transverse normals) before deformation, remain straight after deformation.
2. The transverse normals do not experience elongation (i.e., they are inextensible).
3. The transverse normals rotate such that they remain perpendicular to the middle surface after deformation.

The first two assumptions imply that the transverse displacement is independent of the transverse (or thickness) coordinate and transverse normal strain  $\varepsilon_z = 0$ . The third assumption results in zero transverse shear strains,  $\gamma_{xz} = \gamma_{yz} = 0$ . Kirchhoff's assumptions simplify the relations describing the mechanical behaviour of plates under deformation, and solve the problem of boundary conditions encountered in the first method. Using these assumptions the deformation of the plate is reduced to studying the deformation of its middle surface only.

The extensive use of composite materials having non-homogeneous or anisotropic character (i.e., having a directional dependency) has necessitated a refinement of the existing theories. Most refined 2D shear deformable theories are a mixture of the methods of expansion and hypotheses as reviewed by Noor and Burton [1990a]. These approaches are mostly based on a displacement field approximation that involves unknown displacement components. The first part of this displacement field is involved in a corresponding classical theory, while the additional degrees of freedom are usually multiplied a-priori by a certain function of the transverse coordinate. The choices of such shear deformation "shape" functions are based on satisfying certain mechanical, material and/or geometrical constraints of the problem considered, and subsequently characterise

the degree of accuracy and sophistication of the resulting theory. Consequently, different shape functions have been utilised by different researchers. The so-called uniform shear deformable theories (USDT) (or first order shear deformable theories [Timoshenko, 1921], [Reissner, 1945] and [Mindlin, 1951]) assume a linear variation in in-plane displacements as transverse shear strains (and stresses) become uniform throughout the thickness of the plate. Hence, shear stress-free lateral boundary conditions are not satisfied and transverse shear stresses between two continuous layers are not compatible.

In higher order shear deformable theories (HSDT), the displacement field is expanded to a higher degree polynomial in thickness coordinate compared to USDT. These theories [Bickford, 1982] [Bhimaraddi and Stevens, 1984] [Reddy, 1984] [Soldatos, 1987] allow the development of a simple model for composite plates by imposing the top and bottom surfaces stress-free boundary conditions upon the displacement expansions. For that reason a parabolic variation of transverse shear strain along the thickness of the plate is assumed and the theory is referred to as the parabolic shear deformation theory (PSDT). Touratier [1992] [Soldatos, 1993] attempted the generalization of shear deformable theories by using general shape functions. When the elastic coefficients at a point have the same value for every pair of coordinate systems which are the mirror images of each other with respect to a certain plane, the material is called a monoclinic material that has only 13 independent coefficients. When three mutually orthogonal planes of material symmetry exist, the number of elastic coefficients is reduced to 9, and such materials are called orthotropic.

In dealing with laminated composite plates, the above mentioned theories cannot fulfil the continuity conditions of transverse shear stresses between two continuous layers of laminated plate. For that reason, a number of theories have been proposed in order to account for these conditions. DiSciuva [1986] proposed a zig-zag shear deformation theory

for anisotropic plates which accounted for continuity conditions between neighbouring layers. This was achieved by assuming a piecewise linear variation of in-plane displacements through the laminate thickness. This model was further improved to allow for bending in symmetric cross-ply laminated plates by Lee et al [1990]. In addition, Cho and Parmerter [1993] employed parabolic variation of transverse shear stresses instead of using a linear function of thickness coordinate for general lamination configurations of cross-ply plates. They were therefore able to satisfy the zero transverse shear stress conditions at the free lateral surfaces of the plates considered.

All of the conventional refined plate theories assume that the transverse shear deformation is distributed in the form of a lower order polynomial of the transverse coordinate,  $z$ , (some of the coefficients of which may appropriately depend on the transverse elastic moduli) or in the form of a certain elementary function of  $z$  (trigonometric or hyperbolic). Hence, they all suffer from the main stress-analysis drawback of conventional one-dimensional beam models and two-dimensional plate and shell theories; that is, they cannot accurately predict the well-known boundary layer behaviour of in-plane stress and displacement distributions either near the interfaces of a laminate or near the lateral planes of a highly reinforced structural element.

Soldatos and Watson [1997a-c] developed an advanced shear deformable plate theory that unifies most of the existing shear deformable plate and classical plate theory, i.e., by taking into consideration the effects of transverse shear or both transverse shear and normal deformation. This is achieved with the introduction of general shape functions (see also Soldatos, 1993) into the formulation of the theory. The shape functions are associated with the geometry and material properties of the composite plates or cylindrical shells.

## **1.2 Composite plate theories subject to thermal loading**

Advanced composite materials offer numerous superior properties such as high strength-to-weight ratio and nearly zero coefficient of thermal expansion in the fibre direction. Their strength and stiffness can be tailored to meet stringent design requirements for high-speed aircrafts, spacecrafts and other space structures. The properties of composite materials are frequently compromised by the environment to which they are exposed. Environmental factors that induce expansion strains are of particular concern, one such factor being fluctuations in temperature. Thermal stresses, particularly at the interface between two different materials can be a significant factor in the failure of laminated composite structures. Thus, there is a necessity to predict more accurately the thermal stresses in composite structures.

The thermal bending of homogeneous anisotropic thin plates has been investigated by Pell [1946]. Stavsky [1963] then considered the thermal deformation of laminated anisotropic plates. These early studies employed the classical laminated plate theory (CLPT) based upon the Kirchhoff-Love hypothesis. Wu and Tauchert [1980], Noor and Burton [1992], Vel and Batra [2001] used the CLPT to study the thermal deformation of laminated rectangular plates. The CLPT neglects transverse shear deformation and can lead to significant errors for even moderately thick plates. Reddy et al. [1980], Noor and Burton [1992] and Vel and Batra [2001] employed the uniform shear deformable theory (USDT) for thermal deformation and stresses (see Jones [1975], Tauchert [1991], Reddy [1997] and Vel and Batra [2001] for a historical perspective and review of various approximate theories).

Various higher-order theories for the thermal analysis of laminated plates have been reported by Cho et al. [1989], Khdeir and Reddy [1991, 1999], Noor and Burton [1992]

and Murakami [1993]. The validity of those plate theories and finite-element solutions can be assessed by comparing their predictions with the analytical solutions of the three-dimensional equations of anisotropic thermoelasticity [Murakami, 1993]; [Noor et al., 1994]; [Ali et al., 1999]. Srinivas and Rao [1972] obtained a three-dimensional solution for the flexure of laminated, isotropic, simply supported plates. Tauchert [1980] gave exact thermoelasticity solutions to the plane-strain deformation of orthotropic simply supported laminates using the method of displacement potentials. Thangjitham and Choi [1991] gave an exact solution for laminated infinite plates using the Fourier transform technique and the stiffness matrix method. Murakami [1993] generalized the work of Pagano [1970] to the cylindrical bending of simply supported laminates subjected to thermal loads. Tungikar and Rao [1994], Noor et al. [1994] and Savoia and Reddy [1995, 1997] gave exact three-dimensional solutions for thermal stresses in simply supported anisotropic rectangular laminates. For other boundary conditions, Vel and Batra [2001] analysed the generalised plane strain quasi-static thermoelastic deformations of laminated anisotropic thick plates by using the Eshelby-Stroh formalism.

The accuracy of conventional shear-deformable plate theories (USDT and PSDT) in predicting thermal deformation in cylindrical bending problem was examined by Murakami [1993]. Murakami [1993] found that the transverse displacement changes rapidly in each layer due to thermal mismatch and so conventional plate theories may lead to approximately 5% error in the predicted transverse displacements even for simply supported edges. There is therefore a need to develop a new model that is more suitable for accurate stress analysis. In this study expanding on the previous work by Soldatos and Watson [1997b, c] and taking into account thermal loading, the new derivations of general four-degree-of-freedom beam theory subject to thermal loading are established. A new set of shape functions has been chosen for a sinusoidal temperature distribution along the span

and both constant and linear variations across the thickness of the plate, yielding the exact solution [Murakami, 1993] for simply supported boundary condition. This is further confirmed by comparison between explicit solutions of the proposed method and an analytical solution [Murakami, 1993].

### 1.3 A predictor-corrector method

It is well known that conventional beam and plate theories yield poor stress analysis results when dealing with stress predictions in highly reinforced laminated components. A predictor-corrector method that can improve the accuracy of such stress analysis results has been employed by Jones [1975], Sun et al [1975], Reddy [1984], DiSciuva [1986], Noor and Burton [1990b], Savithri and Varadan [1990], Noor and Burton [1991, 1992], Heuer [1992], Noor and Malik [1999], Jane and Hong [2000]. In more detail, working on a predictor-corrector basis, the in-plane stresses that are initially predicted by means of a certain conventional beam or plate theory are substituted into the differential equations of three-dimensional elasticity, which, in a corrector phase, are integrated through the plate thickness. The resulting transverse shear and transverse normal stress distributions are expected to be improvements and therefore, more accurate stress predictions of their initially predicted counterparts. However this can only be verified by comparison with corresponding results obtained from the few existing exact elasticity solutions.

A variety of two-dimensional plate theories have been associated in references [Sun et al, 1975] [Reddy, 1984] [DiSciuva, 1986] [Noor and Burton, 1990] [Savithri and Varadan, 1990] [Heuer, 1992] [Jane and Hong, 2000] with the predictor phase of the above mentioned predictor-corrector method. The classical theory (CLPT) was employed by Jones [1975], Sun et al [1975], Reddy [1984], DiSciuva [1986] and Jane and Hong [2000],

the uniform shear deformable theory (USDT) was used by Reddy [1984], DiSciuva [1986], Noor and Burton [1990], Heuer [1992], Noor and Burton [1991, 1992] and Noor and Malik [1999], whereas the parabolic shear deformable theory (PSDT) was employed by Reddy [1984]. DiSciuva also used a theory that assumes a zig-zag displacement model [1986] whereas Savithri and Varadan [1990] used a theory that employs a piecewise cubic distribution of the in-plane displacement.

As already mentioned in Section 1.1, Soldatos and Watson [1997a, b, c] proposed some new generalised beam and plate theories which can produce the classical as well as their conventional shear deformable counterparts as particular cases. This became possible by incorporating into the theory of some general shape functions of the transverse coordinate parameter, simple forms of which were essentially the corresponding particular shape functions used in conventional theories. Moreover, they [Soldatos and Watson, 1997a, b, c] proposed a method allowing the general shape functions involved to be determined in a manner that accounts for both geometric and material properties of the highly reinforced beam or plate component to be considered. Subsequently, it is believed that the stress analysis results presented in references [Soldatos and Watson, 1997a, b, c] are particularly accurate.

As far as simply supported laminated beam and plates are concerned, the stress distributions presented in [Soldatos and Watson, 1997b, c] are identical to the corresponding exact elasticity solutions of Pagano [1969] and Srinivas and Rao [1970]. This is due to the fact that the general four-degree-of-freedom theory (G4T) employed in [Soldatos and Watson, 1997b, c] takes both the transverse shear and the transverse normal deformation effects into consideration. The corresponding general three-degree-of-freedom theory (G3T) [Soldatos and Watson, 1997a] neglects the effects of the transverse normal deformation and so the corresponding results [Soldatos and Watson, 1997a] are still

approximate even for simply supported beams and plates. There is no doubt that the predictor-corrector method could further improve the already very accurate results predicted in [Soldatos and Watson, 1997a].

In Chapter 5 the predictor-corrector method is used in connection with the most commonly used conventional shear deformable beam theories [Timoshenko, 1921] [Bickford, 1982], as well as the G3T and G4T presented in [Soldatos and Watson, 1997a, b, c]. As far as simply supported boundary conditions are concerned it allows comparisons with the results obtained from their exact elasticity counterparts. Based on the conclusions of this type of assessment, further comparisons are performed for other sets of edge boundary conditions for which explicit 3D elasticity results are intractable. These comparisons and assessment deal with the accuracy of the distribution of transverse shear and transverse normal stresses through the entire beam thickness. As far as single-layered beams are concerned, some similar preliminary comparisons with certain exact elasticity results [Vel and Bartra, 2000] are presented in [Soldatos and Liu, 2001], though they only consider displacements and stresses at particular points of the beam span. Furthermore, the correction on the transverse stresses which are predicted by general five-degree-of-freedom beam theory for angle-ply composite laminates subject to mechanical loading and four-degree-of-freedom beam theory for cross-ply composite laminates subject to thermal loading, are performed in Chapters 6 and 7.

#### **1.4 An overview into chapters**

Chapter 2 describes a theoretical unification of displacement-based plate theories, yielding the general six-degree-of-freedom plate theory (G6PT) that accounts for both transverse shear and transverse normal deformation [Soldatos and Watson, 1997b]. A

procedure of simplification from general six-degree-of-freedom plate theory into the general five-degree-of-freedom plate theory (G5PT) that ignores the transverse normal deformation [Soldatos, 1997a] is illustrated.

Chapter 3 presents general three-degree-of freedom shear deformable beam theory (G3BT) that ignores transverse normal deformation, general four-degree-of freedom beam theory (G4BT) that considers both transverse shear and transverse normal deformation, and general five-degree-of freedom shear deformable beam theory (G5BT) that ignores transverse normal deformation. These are also suitable for the study of a composite laminated plate deformed in cylindrical bending. G3BT and G5BT are simplified from G5PT, while G4BT is simplified from G6PT.

It is well known that conventional beam and plate theories yield poor results when dealing with stress analysis predictions in highly reinforced laminated components. For more accurate transverse shear and normal stresses, a correction procedure might be necessary. Chapter 4 introduces a predictor-corrector method (Section 1.3) that can improve the accuracy of transverse stress analysis results. This will be then used to improve the accuracy of the predicted transverse shear and normal stresses and hence to assess the accuracy of several composite plate/beam theories.

In Chapter 5, preliminary comparisons of USDT [Timoshenko, 1921], PSDT [Bickford, 1982] and G4T [Soldatos and Watson, 1997b, c], with certain exact elasticity results [Vel and Batra, 2000], are presented for single layered beams [Soldatos and Liu, 2001]. Based on the conclusions of this initial assessment, the application of the predictor-corrector method (Chapter 4) on general three-degree-of-freedom beam theory and general four-degree-of-freedom beam theory are made for cross-ply and other sets of boundary conditions.

Chapter 6 details applications of the predictor-corrector method (described in Chapter 4) upon general five-degree-of-freedom beam theory. The improvement of the performance of transverse shear and normal stresses for angle-ply composite laminates subject to mechanical loading is investigated.

In Chapter 7 a new method for accurate strain-stress analysis in composite laminates subject to thermal loading is proposed in the form of general four-degree-of-freedom beam theory. The predictor-corrector method described in Chapter 4 is further used for the prediction of transverse shear and normal stresses.

## Chapter 2

### Generalized plate theories subject to mechanical loadings

#### 2.1 Introduction

In this chapter a theoretical unification of displacement-based plate theories is presented (Section 2.3) in the form of the general six-degree-of-freedom plate theory introduced in [Soldatos and Watson, 1997b]. Almost all conventional plate theories including classical plate theory and refined shear deformable plate theories can be considered as particular cases or simplifications of the general six-degree-of-freedom plate theory by specializing the choice of shape functions. A procedure of simplification for the general six-degree-of-freedom plate theory into the general five-degree-of-freedom plate theory that neglects transverse normal deformation [Soldatos, 1993] is also presented (Section 2.4).

#### 2.2 General considerations

Consider a composite laminated plate of  $N$  orthotropic layers with the principal material coordinates  $(x^{(r)}, y^{(r)}, z^{(r)})$  of the  $r$ th lamina oriented at an angle  $\theta^{(r)}$  to the laminate coordinate,  $x$ . The  $r$ th layer is located between  $z = h_{r-1}$  and  $z = h_r$ , as shown in Figure 2.2-1. It is convenient to take the  $xy$ -plane of the coordinate system to be the undeformed middle plane of the laminate. The  $z$ -axis is taken to be positive in an upward

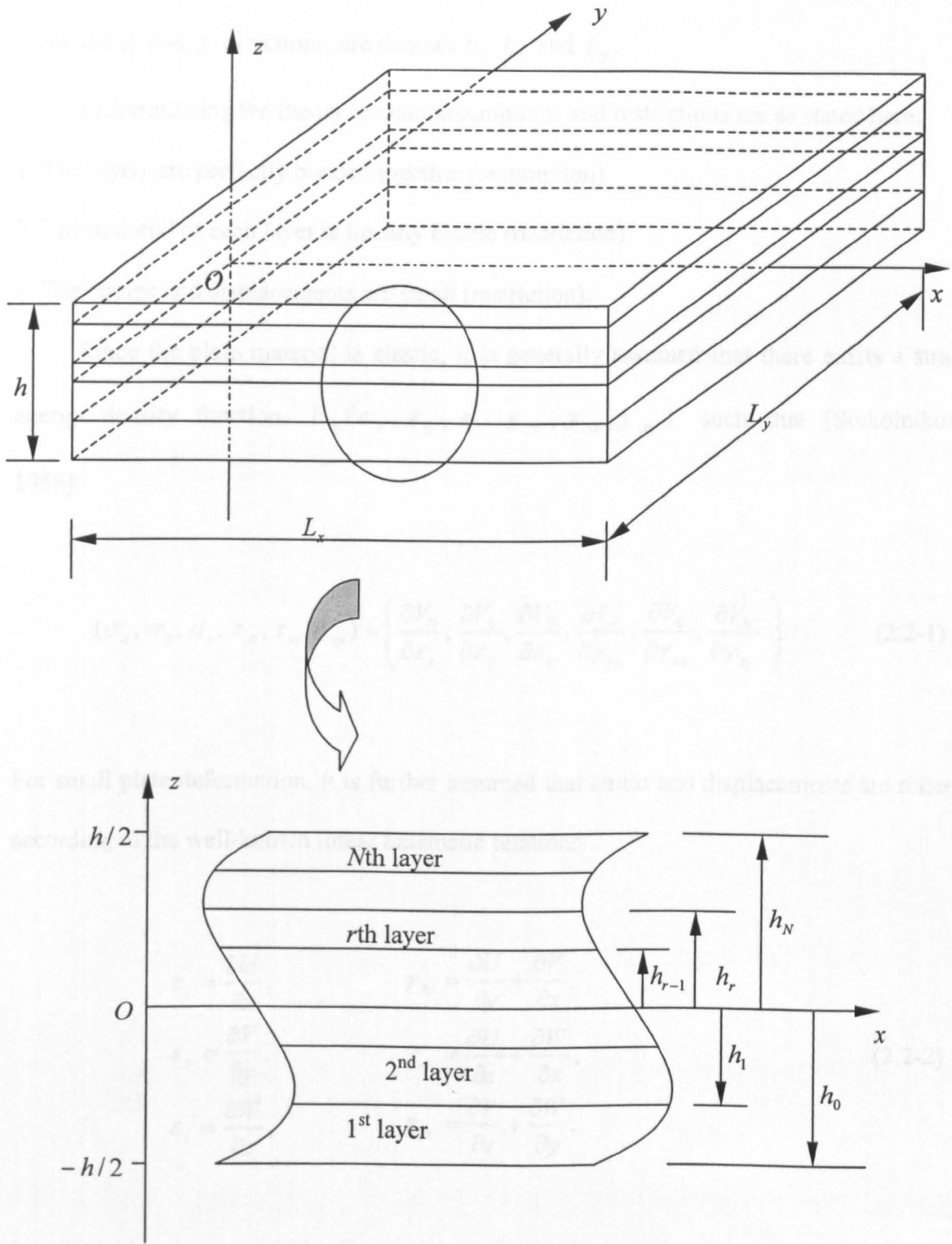


Figure 2.2-1 Coordinate system and layer numbering used for laminated plate

direction from the middle plane. The plate thickness is denoted by  $h$  while its dimensions, along the  $x$  and  $y$  directions, are denoted by  $L_x$  and  $L_y$ .

In formulating the theory, certain assumptions and restrictions are as stated here:

1. The layers are perfectly bonded together (assumption).
2. The material of each layer is linearly elastic (restriction).
3. The strains and displacements are small (restriction).

Since the plate material is elastic, it is generally assumed that there exists a strain energy density function,  $V_0(\varepsilon_x, \varepsilon_y, \varepsilon_z, \gamma_{yz}, \gamma_{zx}, \gamma_{xy})$  such that [Solkolnikoff, 1956]:

$$(\sigma_x, \sigma_y, \sigma_z, \tau_{yz}, \tau_{zx}, \tau_{xy}) = \left( \frac{\partial V_0}{\partial \varepsilon_x}, \frac{\partial V_0}{\partial \varepsilon_y}, \frac{\partial V_0}{\partial \varepsilon_z}, \frac{\partial V_0}{\partial \gamma_{yz}}, \frac{\partial V_0}{\partial \gamma_{zx}}, \frac{\partial V_0}{\partial \gamma_{xy}} \right). \quad (2.2-1)$$

For small plate deformation, it is further assumed that strain and displacements are related according to the well-known linear kinematic relations:

$$\begin{aligned} \varepsilon_x &= \frac{\partial U}{\partial x}, & \gamma_{xy} &= \frac{\partial U}{\partial y} + \frac{\partial V}{\partial x}, \\ \varepsilon_y &= \frac{\partial V}{\partial y}, & \gamma_{xz} &= \frac{\partial U}{\partial z} + \frac{\partial W}{\partial x}, \\ \varepsilon_z &= \frac{\partial W}{\partial z}, & \gamma_{yz} &= \frac{\partial V}{\partial z} + \frac{\partial W}{\partial y}. \end{aligned} \quad (2.2-2)$$

where  $\varepsilon_i$  and  $\gamma_{ij}$  ( $i, j = x, y, z$ ) denote the strain components while  $U, V$  and  $W$  represent the plate displacements in the  $x, y$  and  $z$  directions, respectively. It is finally

assumed that stresses satisfy the equilibrium equations of three-dimensional elasticity, namely:

$$\begin{aligned}\frac{\partial \sigma_x}{\partial x} + \frac{\partial \tau_{xy}}{\partial y} + \frac{\partial \tau_{xz}}{\partial z} &= 0, \\ \frac{\partial \tau_{xy}}{\partial x} + \frac{\partial \sigma_y}{\partial y} + \frac{\partial \tau_{yz}}{\partial z} &= 0, \\ \frac{\partial \tau_{xz}}{\partial x} + \frac{\partial \tau_{yz}}{\partial y} + \frac{\partial \sigma_z}{\partial z} &= 0.\end{aligned}\tag{2.2-3}$$

## 2.3 Development of general six-degree-of-freedom plate theory (G6PT)

### 2.3-1 Displacement field, kinematic relations

In dealing with a static analysis, the general-six-degree-of-freedom plate theory begins with the displacement model

$$\begin{aligned}U(x, y, z) &= u_0(x, y) - z w_{0,x}(x, y) + \varphi_1(z) u_1(x, y), \\ V(x, y, z) &= v_0(x, y) - z w_{0,y}(x, y) + \varphi_2(z) v_1(x, y), \\ W(x, y, z) &= w_0(x, y) + \psi(z) w_1(x, y),\end{aligned}\tag{2.3-1}$$

where  $(\quad)_{,x} = \frac{\partial(\quad)}{\partial x}$ , etc.  $u_0$ ,  $v_0$  and  $w_0$  represent the unknown displacements of the plate middle plane and  $u_1$ ,  $v_1$  and  $w_1$  represent the unknown values of the transverse strains on the plate middle plane. There are six main unknowns (degrees of freedom) of the theory. Here, the functions  $\varphi_1(z)$ ,  $\varphi_2(z)$  and  $\psi(z)$  are assumed to be given functions of the

transverse co-ordinate parameter that can dictate the shape of transverse shear and normal strains (see equation 2.3-4 below). At this stage, no particular forms will be assigned to these functions. For notational convenience, it is assumed that they all have dimensions of length. For the convenience of determining the constants appeared when deriving shape functions, further constraints might be imposed on  $\varphi_1(z)$ ,  $\varphi_2(z)$  and  $\psi(z)$  [Soldatos and Watson, 1997a, b, c]:

$$\varphi_1(0) = \varphi_2(0) = \psi(0) = 0, \quad (2.3-2)$$

and

$$\left. \frac{d\varphi_1}{dz} \right|_{z=0} = \left. \frac{d\varphi_2}{dz} \right|_{z=0} = \left. \frac{d\psi}{dz} \right|_{z=0} = 1. \quad (2.3-3)$$

These constraints are only potential requirement for determining the unknown constants when deriving shape functions.

Upon applying the kinematic relation of three-dimensional elasticity (Equation 2.2-2) to the displacement approximation (Equation 2.3-1), one obtains the following approximate strain field:

$$\begin{aligned} \varepsilon_x &= e_x^c + z k_x^c + \varphi_1(z) k_x^a, & \gamma_{xz} &= \varphi_1'(z) e_{xz}^a + \psi(z) k_{xz}^a, \\ \varepsilon_y &= e_y^c + z k_y^c + \varphi_2(z) k_y^a, & \gamma_{yz} &= \varphi_2'(z) e_{yz}^a + \psi(z) k_{yz}^a, \\ \varepsilon_z &= \psi'(z) e_z^a, & \gamma_{xy} &= e_{xy}^c + z k_{xy}^c + \varphi_1(z) k_{xy}^a + \varphi_2(z) k_{yx}^a, \end{aligned} \quad (2.3-4)$$

where a prime denotes ordinary differentiation with respect to  $z$ , and

$$\begin{aligned}
e_x^c &= u_{0,x}, & k_x^a &= u_{1,x}, \\
e_y^c &= v_{0,y}, & k_y^a &= v_{1,y}, \\
e_{xy}^c &= u_{0,y} + v_{0,x}, & e_z^a &= w_1, \\
& & e_{xz}^a &= u_1, & k_{xy}^a &= u_{1,y}, \\
k_x^c &= -w_{0,xx}, & e_{yz}^a &= v_1, & k_{yx}^a &= v_{1,x}, \\
k_y^c &= -w_{0,yy}, & & & k_{xz}^a &= w_{1,x}, \\
k_{xy}^c &= -2w_{0,xy}, & & & k_{yz}^a &= w_{1,y}.
\end{aligned} \tag{2.3-5}$$

### 2.3-2 Definition of the force and moment resultants

In a close connection with the 3D elasticity relations (2.2-1), the approximate stress field considered can be represented by introducing the generalized stress components [Soldatos and Watson, 1997b]:

$$\begin{aligned}
(\sigma_x^c, \sigma_y^c, \tau_{xy}^c) &= \left( \frac{\partial V_0}{\partial e_x^c}, \frac{\partial V_0}{\partial e_y^c}, \frac{\partial V_0}{\partial e_{xy}^c} \right), \\
(m_x^c, m_y^c, m_{xy}^c) &= \left( \frac{\partial V_0}{\partial k_x^c}, \frac{\partial V_0}{\partial k_y^c}, \frac{\partial V_0}{\partial k_{xy}^c} \right);
\end{aligned} \tag{2.3-6}$$

$$\begin{aligned}
(\sigma_z^a, \tau_{xz}^a, \tau_{yz}^a) &= \left( \frac{\partial V_0}{\partial e_z^a}, \frac{\partial V_0}{\partial e_{xz}^a}, \frac{\partial V_0}{\partial e_{yz}^a} \right), \\
(m_x^a, m_y^a, m_{xy}^a, m_{yx}^a, m_{xz}^a, m_{yz}^a) &= \left( \frac{\partial V_0}{\partial k_x^a}, \frac{\partial V_0}{\partial k_y^a}, \frac{\partial V_0}{\partial k_{xy}^a}, \frac{\partial V_0}{\partial k_{yx}^a}, \frac{\partial V_0}{\partial k_{xz}^a}, \frac{\partial V_0}{\partial k_{yz}^a} \right).
\end{aligned} \tag{2.3-7}$$

Applying the chain rule of partial differentiation in connection with the present approximate strain field (Equation 2.3-4), force and moment resultants are defined by integrating through the thickness as follows:

$$\begin{aligned}
(N_x^c, N_y^c, N_{xy}^c) &= \int_{-h/2}^{h/2} (\sigma_x^c, \sigma_y^c, \tau_{xy}^c) dz = \int_{-h/2}^{h/2} (\sigma_x, \sigma_y, \tau_{xy}) dz, \\
(M_x^c, M_y^c, M_{xy}^c) &= \int_{-h/2}^{h/2} (m_x^c, m_y^c, m_{xy}^c) dz = \int_{-h/2}^{h/2} (\sigma_x, \sigma_y, \tau_{xy}) z dz;
\end{aligned} \tag{2.3-8}$$

$$\begin{aligned}
(N_z^a, Q_x^a, Q_y^a) &= \int_{-h/2}^{h/2} (\sigma_z^a, \tau_{xz}^a, \tau_{yz}^a) dz \\
&= \int_{-h/2}^{h/2} (\sigma_z \psi'(z), \tau_{xz} \varphi_1'(z), \tau_{yz} \varphi_2'(z)) dz,
\end{aligned}$$

$$\begin{aligned}
(M_x^a, M_y^a, M_{xy}^a, M_{yx}^a, P_x^a, P_y^a) &= \int_{-h/2}^{h/2} (m_x^a, m_y^a, m_{xy}^a, m_{yx}^a, m_{xz}^a, m_{yz}^a) dz, \\
&= \int_{-h/2}^{h/2} (\sigma_x \varphi_1(z), \sigma_y \varphi_2(z), \tau_{xy} \varphi_1(z), \tau_{xy} \varphi_2(z), \tau_{xz} \psi(z), \tau_{yz} \psi(z)) dz.
\end{aligned} \tag{2.3-9}$$

Terms with superscript <sup>(c)</sup> are the same as those in classical plate theory, while terms with superscript <sup>(a)</sup> account for the transverse shear or normal deformation.

### 2.3-3 Equilibrium equations and boundary conditions

For convenience, it is assumed that the plate is subjected to a given stress distribution  $q(x, y)$ , which acts normally and downward on its top lateral plane ( $z = h/2$ ). It should be noted however, that any other external loading configuration could be considered and successfully treated in the same way. The six equations of equilibrium of the general six-degree-of-freedom plate theory can be obtained using the theorem of minimum potential energy [Sokolnikoff, 1956, p 382]. We define the potential energy by the formula

$$\Pi = \int_{-h/2}^{h/2} \int_0^y \int_0^x V_0(x, y, z) dx dy dz - \int_0^y \int_0^x q(x, y) W(x, y) dx dy. \quad (2.3-10)$$

Of all displacements satisfying a given set of boundary conditions, those which satisfy the equilibrium equations make the potential energy an absolute minimum, i.e.,

$$\delta \Pi = 0. \quad (2.3-11)$$

Noting that the variation of  $V_0$  is given by

$$\delta V_0 = \frac{\partial V_0}{\partial \varepsilon_x} \delta \varepsilon_x + \frac{\partial V_0}{\partial \varepsilon_y} \delta \varepsilon_y + \frac{\partial V_0}{\partial \varepsilon_z} \delta \varepsilon_z + \frac{\partial V_0}{\partial \gamma_{yz}} \delta \gamma_{yz} + \frac{\partial V_0}{\partial \gamma_{xz}} \delta \gamma_{xz} + \frac{\partial V_0}{\partial \gamma_{xy}} \delta \gamma_{xy}, \quad (2.3-12)$$

equations (2.2-1), (2.3-4) and (2.3-5) yield

$$\frac{\partial V_0}{\partial \varepsilon_x} \delta \varepsilon_x = \sigma_x (\delta u_{0,x} - z \delta w_{0,xx} + \varphi_1 \delta u_{1,x}), \quad (2.3-13)$$

with corresponding expressions for the remaining terms appearing on the right-hand side of Equation (2.3-12).

Inserting equations (2.3-10), (2.3-12) and (2.3-13) into Equation (2.3-11), integrating through the plate thickness with the simultaneous use of equations (2.3-8) and (2.3-9) and, finally, making use of the calculus of variations, the six equations of equilibrium of general six-degree-of-freedom plate theory are obtained as follows,

$$\begin{aligned}
N_{x,x}^c + N_{xy,y}^c &= 0, \\
N_{xy,x}^c + N_{y,y}^c &= 0, \\
M_{x,xx}^c + 2M_{xy,xy}^c + M_{y,yy}^c &= q(x, y), \\
M_{x,x}^a + M_{xy,y}^a - Q_x^a &= 0, \\
M_{yx,x}^a + M_{y,y}^a - Q_y^a &= 0, \\
P_{x,x}^a + P_{y,y}^a - N_z^a &= \psi(h/2) q(x, y).
\end{aligned} \tag{2.3-14}$$

Each one of the first three equations appears identical to its corresponding classical plate theory counterpart. Hence they balance conventional force and moment resultants consistent with Kirchhoff's assumptions. The last three equations address the balancing of force and moment resultants due to the transverse shear and normal deformation effects.

The equations of equilibrium (2.3-14) are accompanied by several sets of edge boundary conditions, which are obtained on the basis of a variational approach. Assuming for simplicity that the plate is rectangular with side lengths  $L_x$  and  $L_y$ , all sets of boundary conditions applicable at the edges  $x = 0, L_x$  are given as:

$u_0$	prescribed or	$N_x^c$	prescribed,	
$v_0$	prescribed or	$N_{xy}^c$	prescribed,	
$w_0$	prescribed or	$M_{x,x}^c + M_{xy,y}^c$	prescribed,	
$w_{0,x}$	prescribed or	$M_x^c$	prescribed,	(2.3-15)
$u_1$	prescribed or	$M_x^a$	prescribed,	
$v_1$	prescribed or	$M_{xy}^a$	prescribed,	
$w_1$	prescribed or	$P_x^a$	prescribed.	

Corresponding sets of boundary conditions are equally applicable on the other two plate edges  $y = 0, L_y$ .

## 2.4 A brief description of general five-degree-of-freedom plate theory (G5PT)

### 2.4-1 Displacement field, kinematic relations

Application of the second assumption of Kirchhoff's hypotheses (Section 1.1) to the three-dimensional general-six-degree-of-freedom plate theory yields in a straightforward manner the general-five-degree-of-freedom shear deformable plate theory. This procedure begins with the displacement model

$$\begin{aligned}
 U(x, y, z) &= u_0(x, y) - zw_{0,x}(x, y) + \varphi_1(z)u_1(x, y), \\
 V(x, y, z) &= v_0(x, y) - zw_{0,y}(x, y) + \varphi_2(z)v_1(x, y), \\
 W(x, y, z) &= w_0(x, y),
 \end{aligned}
 \tag{2.4-1}$$

that neglects the effects of transverse normal deformation ( $w_1 = 0$ ).  $u_0, v_0$  and  $w_0$  represent the displacements of the plate middle plane and  $u_1$  and  $v_1$  represent the values of the transverse strains of the plate middle plane. The functions  $\varphi_1(z)$  and  $\varphi_2(z)$  are again assumed to be given functions of the transverse co-ordinate parameter, and by means of derivatives they dictate the shape of transverse shear deformation effects. In the refined plate theories [Soldatos, 1993] [Soldatos and Watson, 1997a], the following remaining constraints are imposed on the displacement field (see also Section 2.3-1):

$$\varphi_1(0) = \varphi_2(0) = 0,
 \tag{2.4-2}$$

$$\frac{d\varphi_1}{dz} \Big|_{z=0} = \frac{d\varphi_2}{dz} \Big|_{z=0} = 1. \quad (2.4-3)$$

By the assumption of this displacement field (Equation 2.4-1) all those terms involving  $w_1$  and  $\psi$  in the derivations of six-degree-of-freedom plate theory are neglected.

The approximate strain field simplifies to:

$$\begin{aligned} \varepsilon_x &= e_x^c + zk_x^c + \varphi_1(z)k_x^a, & \gamma_{xz} &= \varphi_1'(z)e_{xz}^a, \\ \varepsilon_y &= e_y^c + zk_y^c + \varphi_2(z)k_y^a, & \gamma_{yz} &= \varphi_2'(z)e_{yz}^a, \\ \varepsilon_z &= 0, & \gamma_{xy} &= e_{xy}^c + zk_{xy}^c + \varphi_1(z)k_{xy}^a + \varphi_2(z)k_{yx}^a. \end{aligned} \quad (2.4-4)$$

where a prime denotes ordinary differentiation with respect to  $z$ , and all the variables and expressions in Equation (2.4-4) remain the same as defined in Equation (2.3-4) and Equation (2.3-5).

## 2.4-2 Equilibrium equations and boundary conditions

Using the same variational procedure as described in Equations (2.3-10)-(2.3-13), the five equilibrium equations of general five-degree-of-freedom plate theory are obtained [Soldatos, 1993],

$$\begin{aligned} N_{x,x}^c + N_{xy,y}^c &= 0, \\ N_{xy,x}^c + N_{y,y}^c &= 0, \\ M_{x,xx}^c + 2M_{xy,xy}^c + M_{y,yy}^c &= q(x, y), \\ M_{x,x}^a + M_{xy,y}^a - Q_x^a &= 0, \\ M_{yx,x}^a + M_{y,y}^a - Q_y^a &= 0, \end{aligned} \quad (2.4-5)$$

where the force and moment resultants are defined in Equation (2.3-8) and Equation (2.3-9). Each one of the first three equations again appears identical to its corresponding classical plate theory counterpart. Hence it deals with balancing conventional force and moment resultants consistent with Kirchhoff's assumptions. The last two equations address the balancing of force and moment resultants due to the transverse shear deformation effects.

The equations of equilibrium (2.4-5) are accompanied by several variationally admissible sets of edge boundary conditions. These can be obtained naturally on the basis of a variational approach. With disregarding the specific form of shape functions, A certain boundary condition prescription differs only with the degrees of freedom involved. Assuming that the plate is rectangular with side lengths  $L_x$  and  $L_y$ , all sets of boundary conditions applicable to the edges  $x = 0, L_x$  are given as follows:

$u_0$	prescribed or	$N_x^c$	prescribed,	
$v_0$	prescribed or	$N_{xy}^c$	prescribed,	
$w_0$	prescribed or	$M_{x,x}^c + M_{xy,y}^c$	prescribed,	
$w_{0,x}$	prescribed or	$M_x^c$	prescribed,	(2.4-6)
$u_1$	prescribed or	$M_x^a$	prescribed,	
$v_1$	prescribed or	$M_{xy}^a$	prescribed.	

Corresponding sets of variationally admissible boundary conditions are applicable on the other two plate edges  $y = 0, L_y$ .

## Chapter 3

### Solutions to cylindrical bending problem of laminated composite plates using several versions of generalized beam theories

#### 3.1 Introduction

Consider a plate strip (Figure 2.2-1) of infinite extent in the  $y$  direction, having a constant length,  $L$ , in the  $x$  direction. It is made of an arbitrary number,  $N$ , of linearly elastic layers that satisfies the generalized Hooke's law [Jones, 1975]:

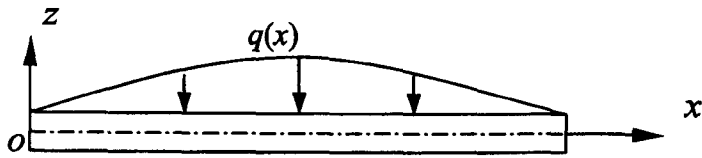
$$\sigma_i = C_{ij} \varepsilon_j \quad (i, j = 1, 2, \dots, 6) \quad (3.1-1)$$

where  $\sigma_i$  are the stress components,  $C_{ij}$  is the three-dimensional stiffness matrix, and  $\varepsilon_j$  are the strain components.

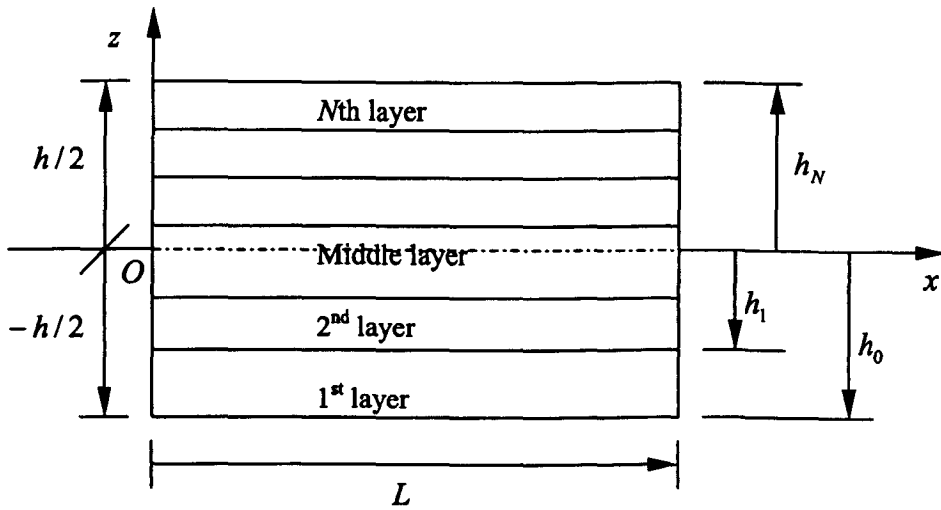
The three-dimensional constitutive equations used in G4BT [Soldatos and Watson, 1997b, c] are those of plane strain elasticity, namely [Jones, 1975]:

$$\begin{aligned} \sigma_x &= C_{11} \varepsilon_x + C_{13} \varepsilon_z, \\ \sigma_z &= C_{13} \varepsilon_x + C_{33} \varepsilon_z, \\ \tau_{xz} &= C_{55} \gamma_{xz}, \end{aligned} \quad (3.1-2)$$

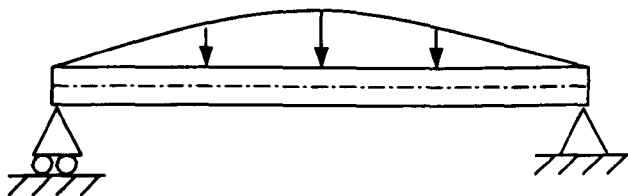
It may be worth clarifying that  $\varepsilon_i$  and  $\gamma_{ij}$  ( $i, j = 1, 2, \dots, 3$ ) in Hooke's law represent



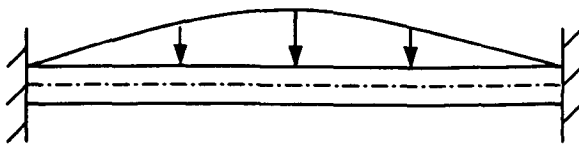
(a) Co-ordinate system



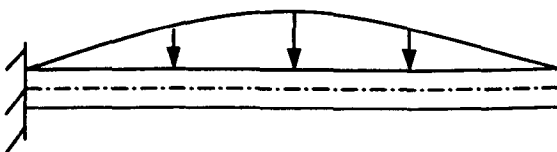
(b) Coordinate and layer numbering of a composite beam



(c) Simply supported composite beam (SS)



(d) Clamped-clamped composite beam (CC)



(e) Clamped-free composite beam (CF)

Figure 3.2-1 Coordinate system and Geometry of laminated beam

elastic strains only. For the shear deformable beam theory employed in this study, namely the G5BT [Shu and Soldatos, 2000], constitutive equations are expressed as [Jones, 1975]

$$\begin{Bmatrix} \sigma_x \\ \sigma_y \\ \tau_{xy} \end{Bmatrix} = \begin{bmatrix} Q_{11} & Q_{12} & Q_{16} \\ Q_{12} & Q_{22} & Q_{26} \\ Q_{16} & Q_{26} & Q_{66} \end{bmatrix} \begin{Bmatrix} \varepsilon_x \\ \varepsilon_y \\ \gamma_{xy} \end{Bmatrix}, \quad \begin{Bmatrix} \tau_{yz} \\ \tau_{xz} \end{Bmatrix} = \begin{bmatrix} Q_{44} & Q_{45} \\ Q_{45} & Q_{55} \end{bmatrix} \begin{Bmatrix} \gamma_{yz} \\ \gamma_{xz} \end{Bmatrix}, \quad (3.1-3)$$

Moreover, in the G3BT [Soldatos and Watson, 1997a], the USDT [Timoshenko, 1921] and the PSDT [Bickford, 1982], the corresponding constitutive relations are simplified as [Jones, 1975]:

$$\begin{aligned} \sigma_x &= Q_{11} \varepsilon_x, \\ \tau_{xz} &= Q_{55} \gamma_{xz}, \end{aligned} \quad (3.1-4)$$

where  $Q_{ij}$  ( $i, j=1, 2, \dots, 6$ ) denote the appropriate reduced elastic stiffnesses.

Assume further that the plate is subjected to a loading that acts normally and downwards on its top lateral plane but is independent of the  $y$  co-ordinate. Due to the symmetries involved in both the geometrical and loading characteristics, all the displacement components  $u_0, v_0, w_0, u_1, v_1$  and  $w_1$  of the plate, are independent of the  $y$  parameter and, therefore, all their partial derivatives with respect to  $y$  are zero. Such a plate problem in plane-strain state can be simplified to a beam problem. Therefore the stress analysis of such a plate can alternatively be performed by a beam theory. Hence the term ‘three-dimensional elasticity’ should be interpreted as ‘two-dimensional plane strain elasticity. It may worth to note that, in determination of the shape functions and derivation

of the predictor and corrector phases plain stain state is assumed. Justifications are required as different assumptions may lead to rather different results [Li, 1996].

By dropping its dependency on the  $y$  co-ordinate parameter and nullifying the minor displacement component in  $y$  direction ( $v_0$  and  $v_1$ ), the general five-degree-of-freedom shear deformable plate theory (Section 2.4) is simplified into a general three-degree-of-freedom shear deformable beam theory (G3BT) that is applicable for cross-ply laminated beams, and a general five-degree-of-freedom shear deformable beam theory (G5BT) that is applicable for angle-ply laminated beams. The general six-degree-of-freedom plate theory (Section 2.3) is simplified into a general four-degree-of-freedom beam theory (G4BT), which is suitable for cross-ply laminated beams.

### 3.1.1 External loading

Assume the  $N$ -layer linear elastic beam (Figure 3.2-1) with unit width in the  $y$  direction and finite length,  $L$ , in the  $x$  direction, is subject to the loading

$$q(x) = q_m \sin(p_m x), \quad p_m = m\pi / L, \quad m = 1, 2, \dots \quad (3.1-5)$$

which acts normally and downwards on its top lateral plane,  $z = h/2$ . This can be thought as a simple harmonic in the corresponding Fourier sine-series expansion of any relevant loading distribution.

Similarly, where thermal loading is considered, this is assumed the temperature field is of the form:

$$\Delta T(x, z) = (T_0 + T_1 z) \sin(p_m x), \quad p_m = m\pi / L, \quad (m = 1, 2, \dots). \quad (3.1-6)$$

This can be understood as being a simple harmonic in a Fourier sine-series expansion along  $x$  – direction of any relevant temperature field satisfying Fourier’s Heat Conduction Law.

### 3.1.2 Displacement field of conventional beam/plate theories

The general displacement field is defined in Equation (2.3-1) can also be given by

$$\mathbf{U} = U(x, y, z) \vec{i} + V(x, y, z) \vec{j} + W(x, y, z) \vec{k}. \quad (3.1-7)$$

Here  $\vec{i}$ ,  $\vec{j}$  and  $\vec{k}$  are unit vectors.  $U, V$  and  $W$  are displacement components, can be expressed as an expansion in a Taylor series form:

$$\begin{aligned} U(x, y, z) &= u_0(x, y) + z u_1(x, y) + z^2 u_2(x, y) + z^3 u_3(x, y) + \dots, \\ V(x, y, z) &= v_0(x, y) + z v_1(x, y) + z^2 v_2(x, y) + z^3 v_3(x, y) + \dots, \\ W(x, y, z) &= w_0(x, y) + z w_1(x, y) + z^2 w_2(x, y) + z^3 w_3(x, y) + \dots, \end{aligned} \quad (3.1-8)$$

here,  $u_0, v_0$  and  $w_0$  are reference (middle) plane displacement components. The unknown functions with sub-indices 1, 2 and 3 are the first, second and third derivatives of corresponding displacement components with respect to the transverse coordinate,  $z$ .

In principle, it is possible to extend these displacement series expansions of the thickness coordinate up to any desired degree. However, due to the algebraic complexity and computer effort involved with higher-order theories in return of marginal gain in

accuracy, conventional theories [Timoshenko, 1921] [Bickford, 1982] involve only limited numbers of terms after truncation of the above Taylor series. Additionally, the advanced shape functions of G3BT [Soldatos Watson, 1997a], G4BT [Soldatos and Watson, 1997b, c] and G5BT [Shu and Soldatos, 2000] will be detailed in the following corresponding Sections 3.2.2, 3.3.2 and 3.4.2, respectively.

### **3.1.3 Shape functions in classical beam theory subject to mechanical loading**

In the classical beam theory, it is assumed that the Kirchhoff's hypothesis holds (Section 1.1). In formulating the theory, certain assumptions or restrictions are adopted (Section 2.2). Under these assumptions and restrictions, the shape functions of classical beam are of the form:

$$\varphi_1(z) = 0, \quad \varphi_2(z) = 0, \quad \psi(z) = 0. \quad (3.1-9)$$

### **3.1.4 Shape functions in uniform shear deformable beam theory subject to mechanical loading**

In uniform shear deformable beam theory (first-order shear deformable beam theory) [Timoshenko, 1921], the Kirchhoff's hypothesis (Section 1.1) is relaxed by removing the third part, i.e., the transverse normals do not remain perpendicular to the middle surface after deformation. Under these assumptions and restrictions (Section 2.2), the choices of shape functions (five-degree-of-freedom) are of the form:

$$\varphi_1(z) = z, \quad \varphi_2(z) = z, \quad \psi(z) = 0. \quad (3.1-10)$$

### 3.1.5 Shape functions in parabolic shear deformable beam theory subject to mechanical loading

The parabolic shear deformable beam theory [Bickford, 1982] [Reddy, 1984] to be developed is based on the same assumptions and restrictions (Sections 2.2), except that we relax the Kirchhoff's assumption (Section 1.1) on the straightness and normality of transverse normal after deformation. The shape functions (five-degree-of-freedom) are of the form:

$$\varphi_1(z) = z \left(1 - \frac{4z^2}{3h^2}\right), \quad \varphi_2(z) = z \left(1 - \frac{4z^2}{3h^2}\right), \quad \psi(z) = 0. \quad (3.1-11)$$

## 3.2 General three-degree-of-freedom beam theory (G3BT) for cross-ply laminated beams subject to mechanical loading

### 3.2.1 Formulation

The general three-degree-of-freedom beam theory (G3BT) begins with displacement approximation [Soldatos and Watson, 1997a]:

$$\begin{aligned} U(x, z) &= u_0(x) - zw_{0,x}(x) + \varphi_1(z)u_1(x), \\ W(x, z) &= w_0(x), \end{aligned} \quad (3.2-1)$$

and contains only three unknown degrees of freedom,  $u_0$ ,  $w_0$  and  $u_1$ , and involves one shape function,  $\varphi_1(z)$ .

The equations of equilibrium of the G3BT are therefore simplified as follows:

$$\begin{aligned} N_{x,x}^c &= 0, \\ M_{x,xx}^c &= q(x), \\ M_{x,x}^a - Q_x^a &= 0, \end{aligned} \tag{3.2-2}$$

where  $N_x^c$ ,  $M_x^c$ ,  $M_x^a$  and  $Q_x^a$  are the force and moment resultants as defined in equations (2.3-8) and (2.3-9).

The equilibrium equation can be converted into the following three Navier-type differential equations,

$$\begin{aligned} A_{11}^c u_{0,xx} - B_{11}^c w_{0,xxx} + B_{11}^a u_{1,xx} &= 0, \\ -B_{11}^c u_{0,xxx} + D_{11}^c w_{0,xxx} - D_{11}^a u_{1,xxx} &= q(x), \\ B_{11}^a u_{0,xx} - D_{11}^a w_{0,xxx} + D_{11}^{aa} u_{1,xx} - A_{55}^{aa} u_1 &= 0, \end{aligned} \tag{3.2-3}$$

for the three main unknown displacement functions:  $u_0$ ,  $w_0$  and  $u_1$ . Here, the appearing rigidities [Soldatos and Watson, 1997a] are given as follows:

$$\begin{aligned} (A_{11}^c, B_{11}^c, D_{11}^c, B_{11}^a, D_{11}^a, D_{11}^{aa}) &= \int_{-h/2}^{h/2} Q_{11}^{(r)}(1, z, z^2, \varphi, z\varphi, \varphi^2) dz, \\ A_{55}^{aa} &= \int_{-h/2}^{h/2} Q_{55}^{(r)}(\varphi')^2 dz. \end{aligned} \tag{3.2-4}$$

Equations (3.2-3) form an eighth-order of simultaneous ordinary differential equations. Regardless of the particular form of the shape functions employed, the eight constant coefficients of general solution of the ordinary differential equations can be obtained by applying edge boundary conditions. For simply supported, clamped and free edge, the following boundary conditions are as follows:

$$\begin{aligned}
 \text{Simply supported edge: } & N_x^c = w_0 = M_x^c = M_x^a = 0 \\
 \text{Clamped edge: } & u_0 = w_0 = w_{0,x} = u_1 = 0, \\
 \text{Free edge: } & N_x^c = M_x^c = M_{x,x}^c = M_x^a = 0.
 \end{aligned} \tag{3.2-5}$$

As may be easy to verify, the set of simply supported boundary conditions is satisfied exactly by a displacement choice of the following form,

$$(u_0, u_1) = (A, B) \cos(p_m x), \quad w_0 = C \sin(p_m x). \tag{3.2-6}$$

which is the set of particular integrals of the equilibrium equations. The unique solution of unknown constant coefficients  $A, B$  and  $C$  can be obtained through the equilibrium equations (Equation 3.2-3).

### 3.2.2 Determination of shape functions subject to mechanical loading

The shape function  $\varphi_1(z)$  of G3BT can be determined by making use of the first of the three-dimensional equations of equilibrium (Equation 2.2-3) only. For the cylindrical bending, this equation is simplified as follows [Soldatos and Watson, 1997a]:

$$\sigma_{x,x} + \tau_{xz,z} = 0. \quad (3.2-7)$$

Using strain-stress relation in connection with kinematic relation (Equation 2.2-2), displacement components (Equation 3.2-6) for simply supported edges, Equation (3.2-7) yields a second-order ordinary differential equation. The general solution of equation is given as follows in  $r$  th layer ( $r=1, 2, \dots, N$ ):

$$B_0 \varphi_1^{(r)}(z) = C_1^{(r)} e^{\alpha^{(r)} z} + C_2^{(r)} e^{-\alpha^{(r)} z} + C_0 p_m z - A_0, \quad (\alpha^{(r)})^2 = \frac{Q_{11}^{(r)}}{Q_{55}^{(r)}} p_m^2. \quad (3.2-8)$$

Here, the superscript  $^{(r)}$  is associated with the number of layers.  $C_i^{(r)}$  ( $i = 1, 2$ ) represent two arbitrary constants of integration in the  $r$  th layer.  $Q_{11}^{(r)}$  and  $Q_{55}^{(r)}$  denote the appropriate reduced elasticity stiffnesses [Jones, 1975].

For an  $N$ -layered beam, however, there are  $2N$  unknown constants ( $C_i^{(r)}$   $i = 1, 2; r = 1, 2, \dots, N$ ) to be determined. These will be determined by means of the  $2(N-1)$  continuity conditions (in-plane displacement,  $U$  and shear stress,  $\tau_{xz}$ ) employed on the  $N-1$  material interfaces of the laminated beam considered and the two zero shear traction (shear stress,  $\tau_{xz}$ ) boundary conditions specified on both top and bottom.

For a simply supported beam in cylindrical bending problem, values can initially be assigned to all these unknown constants ( $A_0, B_0$  and  $C_0$ ) in an almost arbitrary manner. In doing so, the only essential requirement is that non-zero values should be assigned to  $B_0$ . Thus, by pre-setting  $B_0 = 1$  and applying constraints of shape functions (Equations 2.3-2 and 2.3-3), their values ( $A_0, C_0$ ) can be determined uniquely.

### 3.3 General four-degrees-of-freedom beam theory (G4BT) for cross-ply laminated beams subjected to mechanical and thermal loadings

#### 3.3.1 Formulation

G4BT for cross-ply laminated beams subject to both mechanical and thermal loadings begins with the displacement field [Soldatos and Watson, 1997b, c],

$$\begin{aligned} U(x, z) &= u_0(x) - zw_{0,x} + \varphi(z) u_1(x), \\ W(x, z) &= w_0(x) + \psi(z) w_1(x), \end{aligned} \quad (3.3-1)$$

where,  $u_0$ ,  $w_0$ ,  $u_1$  and  $w_1$  are four unknown degrees of freedom,  $\varphi(z)$  and  $\psi(z)$  are two functions.

The three-dimensional thermoelastic anisotropic strain-stress relations are [Jones, 1999]:

$$\varepsilon_i = S_{ij} \sigma_j + \alpha_i \Delta T(x, z), \quad i, j = 1, 2, \dots, 6 \quad (3.3-2)$$

where, the total strains,  $\varepsilon_i$  is the sum of the mechanical strains,  $S_{ij} \sigma_j$ , and the free thermal strains,  $\alpha_i \Delta T$ .  $\Delta T(x, z)$  is the temperature change and  $\alpha_i$  is coefficient of thermal expansion. In addition, for an infinitesimal deformation, non-zero total strain components can be obtained by kinematic relations of three-dimensional elasticity (Equation 2.2-2) incorporated with the displacement approximation (Equation 3.3-1). For plane stress in an

orthotropic lamina in principle coordinates, the three-dimensional thermoelastic stress-strain relation [Jones, 1999] [Reddy, 1996] in  $r$  th layer is simplified as follows:

$$\begin{Bmatrix} \sigma_x^{(r)} \\ \sigma_z^{(r)} \\ \tau_{xz}^{(r)} \end{Bmatrix} = \begin{bmatrix} C_{11}^{(r)} & C_{13}^{(r)} & 0 \\ C_{13}^{(r)} & C_{33}^{(r)} & 0 \\ 0 & 0 & C_{55}^{(r)} \end{bmatrix} \begin{Bmatrix} \varepsilon_x^{(r)} - \alpha_x^{(r)} \Delta T \\ \varepsilon_z^{(r)} - \alpha_z^{(r)} \Delta T \\ \gamma_{xz}^{(r)} \end{Bmatrix} \quad (3.3-3)$$

Note that the coefficients of thermal expansion affect only extensional strains, not the shear strain in this case. Here the layer superscript  $(r)$  has been introduced in order to emphasise the dependency of the shape functions on the different elastic properties of each layer.

The four equilibrium equations of G4BT can be deduced from the six equilibrium equations of general six-degree-of-freedom plate theory (Equation 2.3-14) and written as follows,

$$\begin{aligned} N_{x,x}^c &= 0, \\ M_{x,xx}^c &= q(x), \\ M_{x,x}^a - Q_x^a &= 0, \\ P_{x,x}^a - N_z^a &= \psi(h/2)q(x), \end{aligned} \quad (3.3-4)$$

where the force and moment resultants are defined in equations (2.3-8) and (2.3-9).

It yields the following set of Navier-type differential equations:

$$\begin{aligned} A_{11}^c u_{0,xx} - B_{11}^a w_{0,xxx} + B_{11}^a u_{1,xx} + B_{13}^b w_{1,x} &= E_1^T, \\ B_{11}^c u_{0,xxx} - D_{11}^c w_{0,xxxx} + D_{11}^a u_{1,xxx} + D_{13}^b w_{1,xx} &= E_2^T, \\ B_{11}^a u_{0,xx} - D_{11}^a w_{0,xxx} + D_{11}^{aa} u_{1,xx} - A_{55}^{aa} u_1 + (D_{13}^{ab} - A_{55}^{ab}) w_{1,x} &= E_3^T, \\ -B_{13}^b u_{0,x} + D_{13}^b w_{0,xx} - (D_{13}^{ab} - A_{55}^{ab}) u_{1,x} + A_{55}^{bb} w_{1,xx} - D_{33}^{bb} w_1 &= \psi(h_{N+1})q(x) + E_4^T. \end{aligned} \quad (3.3-5)$$

The appearing rigidities and constants are given as follows:

$$\begin{aligned}
 (A_{11}^c, B_{11}^c, D_{11}^c, B_{11}^a, D_{11}^a, D_{11}^{aa}) &= \int_{-h/2}^{h/2} C_{11}^{(r)}(1, z, z^2, \varphi, z\varphi, \varphi^2) dz, \\
 (B_{13}^b, D_{13}^b, D_{13}^{ab}) &= \int_{-h/2}^{h/2} C_{13}^{(r)}(\psi', z\psi', \varphi\psi') dz, \\
 (A_{55}^{aa}, A_{55}^{ab}, A_{55}^{bb}) &= \int_{-h/2}^{h/2} C_{55}^{(r)}((\varphi')^2, \varphi'\psi, \psi^2) dz, \\
 D_{33}^{bb} &= \int_{-h/2}^{h/2} C_{33}^{(r)}(\psi')^2 dz, \\
 E_1^T &= \int_{-h/2}^{h/2} (\alpha_x^{(r)} C_{11}^{(r)} + \alpha_z^{(r)} C_{13}^{(r)}) (\Delta T)_{,x} dz, & E_2^T &= \int_{-h/2}^{h/2} (\alpha_x^{(r)} C_{11}^{(r)} + \alpha_z^{(r)} C_{13}^{(r)}) (\Delta T)_{,xx} z dz, \\
 E_3^T &= - \int_{-h/2}^{h/2} (\alpha_x^{(r)} C_{13}^{(r)} + \alpha_z^{(r)} C_{33}^{(r)}) \Delta T \psi' dz, & E_4^T &= - \int_{-h/2}^{h/2} (\alpha_x^{(r)} C_{13}^{(r)} + \alpha_z^{(r)} C_{33}^{(r)}) \Delta T \psi' dz,
 \end{aligned} \tag{3.3-6}$$

where a superscript  $T$  denotes the constants associated with thermal expansion, while  $\psi(h_{N+1})q(x)$  is contribution related to the mechanical loading only.

The equilibrium equations (3.3-5) form a tenth-order of four simultaneous ordinary differential equations and are accompanied by several sets of boundary conditions. All sets of boundary conditions applicable to the edges  $x = 0, L$  are given as follows:

$$\begin{aligned}
 \text{at simply supported edge: } & N_x^c = w = M_x^c = M_x^a = w_1 = 0, \\
 \text{at rigidly clamped edge: } & u_0 = w_0 = w_{0,x} = u_1 = w_1 = 0, \\
 \text{at free edge: } & N_x^c = M_{x,x}^c = M_x^c = M_x^a = P_x^a = 0.
 \end{aligned} \tag{3.3-7}$$

As may easily be verified, the simply support boundary conditions (3.3-7) are satisfied exactly by the following trigonometric displacement representation:

$$u_0 = A \cos(p_m x), \quad u_1 = B \cos(p_m x), \quad w_0 = C \sin(p_m x), \quad w_1 = D \sin(p_m x) \quad (3.3-8)$$

Moreover, they also satisfy the set of the differential equations (3.3-5), yielding the following set of linear algebraic equations:

$$\left[ \begin{array}{cccc} -p_m^2 A_{11}^c & p_m^3 B_{11}^c & -p_m^2 B_{11}^a & p_m B_{13}^b \\ & -p_m^4 D_{11}^c & p_m^3 D_{11}^a & -p_m^2 D_{13}^b \\ & & -p_m^2 D_{11}^{aa} - A_{55}^{aa} & p_m (D_{13}^{ab} - A_{55}^{ab}) \\ \text{Symmetric} & & & -p_m^2 A_{55}^{bb} - D_{33}^{bb} \end{array} \right] \begin{Bmatrix} A \\ C \\ B \\ D \end{Bmatrix} = \begin{Bmatrix} H_1^T \\ H_2^T \\ H_3^T \\ \psi(h/2)q_m + H_4^T \end{Bmatrix} \quad (3.3-9)$$

9)

here

$$H_1^T = \int_{-h/2}^{h/2} p_m (\alpha_x^{(r)} C_{11}^{(r)} + \alpha_z^{(r)} C_{13}^{(r)}) (T_0 + T_1 z) dz,$$

$$H_2^T = - \int_{-h/2}^{h/2} p_m^2 (\alpha_x^{(r)} C_{11}^{(r)} + \alpha_z^{(r)} C_{13}^{(r)}) (T_0 + T_1 z) z dz,$$

$$H_3^T = \int_{-h/2}^{h/2} p_m (\alpha_x^{(r)} C_{11}^{(r)} + \alpha_z^{(r)} C_{13}^{(r)}) (T_0 + T_1 z) \varphi dz, \quad (3.3-10)$$

$$H_4^T = - \int_{-h/2}^{h/2} (\alpha_x^{(r)} C_{13}^{(r)} + \alpha_z^{(r)} C_{33}^{(r)}) (T_0 + T_1 z) \psi' dz.$$

where the superscript  $(r)$  denotes the number of layers. Given a suitable set of shape functions, the coefficients  $A$ ,  $B$ ,  $C$  and  $D$  can be determined through the Equation (3.3-9) uniquely for simply supported beam.

### 3.3.2 Determination of shape functions subject to mechanical and thermal loadings

Shape functions  $\varphi_1(z)$  and  $\psi(z)$  in Equation (3.3-1) can be determined by making use of the three-dimensional equilibrium equations (Equation 2.2-3). The three-dimensional equilibrium equations of linear plane strain elasticity are given as follows [Soldatos and Watson, 1997b, c]:

$$\sigma_{x,x} + \tau_{xz,z} = 0, \quad \tau_{xz,x} + \sigma_{z,z} = 0. \quad (3.3-11)$$

Assume the beam is subjected to the combination of a mechanical loading of the form (Equation 3.1-5) and to a temperature field of the form (Equation 3.1-6). In connection with the three-dimensional thermoelastic stress-strain relation (Equation 3.3-6), displacement-strain relation (Equation 2.2-2) and the displacement components (Equation 3.3-8) for simply supported edge, the equilibrium Equations (3.3-11) yield the following 4<sup>th</sup>-order set of ordinary differential equations in  $r$ th layer:

$$\begin{aligned} C_{55}^{(r)} B \varphi'' - p_m^2 C_{11}^{(r)} B \varphi + p_m (C_{13}^{(r)} + C_{55}^{(r)}) D \psi' \\ = p_m^2 C_{11}^{(r)} (A - p_m z C) + p_m (C_{11}^{(r)} \alpha_x^{(r)} + C_{13}^{(r)} \alpha_z^{(r)}) (T_0 + T_1 z), \\ C_{33}^{(r)} D \psi'' - p_m^2 C_{55}^{(r)} D \psi - p_m (C_{13}^{(r)} + C_{55}^{(r)}) B \varphi' \\ = -p_m^2 C_{13}^{(r)} C + (C_{31}^{(r)} \alpha_x^{(r)} + C_{33}^{(r)} \alpha_z^{(r)}) T_1. \end{aligned} \quad (3.3-12)$$

It is of particular importance to note that the right-hand-sides of Equation (3.3-12) are entirely dependent upon the basic displacement field, mechanical and thermal loadings, while their left-hand-sides depend on the corresponding additional displacement field.

The general solution of Equation (3.3-12) can be written in the following form:

$$\begin{Bmatrix} B_0 \varphi^{(r)}(z) \\ D_0 \psi^{(r)}(z) \end{Bmatrix} = \begin{Bmatrix} \Phi^{(r)}(z) \\ \Psi^{(r)}(z) \end{Bmatrix} + \begin{Bmatrix} p_m \\ 0 \end{Bmatrix} C_0 z - \begin{Bmatrix} A_0 \\ C_0 \end{Bmatrix} + \begin{Bmatrix} f_1^{(r)} \\ f_2^{(r)} \end{Bmatrix} \quad (3.3-13)$$

where

$$\begin{aligned} f_1^{(r)} &= -(\alpha_x^{(r)} C_{11}^{(r)} + \alpha_z^{(r)} C_{13}^{(r)}) (T_0 + T_1 z) / (p_m C_{11}^{(r)}) \\ f_2^{(r)} &= [(C_{13}^{(r)} + C_{55}^{(r)}) (\alpha_x^{(r)} C_{11}^{(r)} + \alpha_z^{(r)} C_{13}^{(r)}) - C_{11}^{(r)} (\alpha_x^{(r)} C_{13}^{(r)} + \alpha_z^{(r)} C_{33}^{(r)})] \\ &\quad T_1 / (p_m^2 C_{11}^{(r)} C_{55}^{(r)}) \end{aligned} \quad (3.3-14)$$

The term that involves the functions  $\Phi$  and  $\Psi$  in the right-hand-side of the equation represent the complementary solution of Equation (3.3-12), while the other terms represent the particular integrals in the  $r$ th layer of a simply supported laminate ( $r = 1, 2, \dots, N$ ). In more detail,  $\Phi$  and  $\Psi$  can be given in the following form:

$$\begin{aligned} \Phi^{(r)}(z) &= (C_{13}^{(r)} + C_{55}^{(r)}) \sum_{i=1}^4 k_i^{(r)} \lambda_i^{(r)} e^{p_m \lambda_i^{(r)} z}, \\ \Psi^{(r)}(z) &= \sum_{i=1}^4 k_i^{(r)} (C_{11}^{(r)} - \lambda_i^{(r)2} C_{55}^{(r)}) e^{p_m \lambda_i^{(r)} z}, \end{aligned} \quad (3.3-15)$$

where  $\lambda_i^{(r)}$  are the four roots of:

$$C_{33}^{(r)}C_{55}^{(r)}\lambda^4 - [C_{11}^{(r)}C_{33}^{(r)} - (C_{13}^{(r)})^2 - 2C_{13}^{(r)}C_{55}^{(r)}]\lambda^2 + C_{11}^{(r)}C_{55}^{(r)} = 0, \quad (3.3-16)$$

and  $k_i^{(r)}$  ( $r = 1, 2, \dots, N$ ;  $i = 1, 2, 3, 4$ ) are  $4N$  unknown constants. It is worth noticing that  $\Phi$  and  $\Psi$  are exponential functions of the transverse co-ordinate,  $z$ , with the exponents being dependent on the material and the geometrical properties of the beam considered. The  $4N$  unknown constants,  $k_i^{(r)}$ , will be determined from an equal number of interface continuity and lateral plane boundary conditions briefly outlined next.

The continuity of displacements ( $U$  and  $W$ ) at all material interfaces  $z = h_r$  ( $r = 1, 2, \dots, N - 1$ ) in a simply supported beam implies,

$$\begin{aligned} \Phi^{(r)}(h_r) - \Phi^{(r+1)}(h_r) &= [\alpha_x^{(r)}C_{13}^{(r)} - \alpha_z^{(r)}C_{13}^{(r)}](T_0 + T_1 h_r)/(p_m C_{11}^{(r)}) \\ &\quad - [\alpha_x^{(r+1)}C_{13}^{(r+1)} - \alpha_z^{(r+1)}C_{13}^{(r+1)}](T_0 + T_1 h_r)/(p_m C_{11}^{(r+1)}), \\ \Psi^{(r)}(h_r) - \Psi^{(r+1)}(h_r) &= -[(C_{13}^{(r)} + C_{55}^{(r)})(\alpha_x^{(r)}C_{11}^{(r)} + \alpha_z^{(r)}C_{13}^{(r)}) \\ &\quad - C_{11}^{(r)}(\alpha_x^{(r)}C_{13}^{(r)} + \alpha_z^{(r)}C_{33}^{(r)})]T_1 / (p_m^2 C_{11}^{(r)} C_{55}^{(r)}) \\ &\quad + [(C_{13}^{(r+1)} + C_{55}^{(r+1)})(\alpha_x^{(r+1)}C_{11}^{(r+1)} + \alpha_z^{(r+1)}C_{13}^{(r+1)}) \\ &\quad - C_{11}^{(r+1)}(\alpha_x^{(r+1)}C_{13}^{(r+1)} + \alpha_z^{(r+1)}C_{33}^{(r+1)})]T_1 / (p_m^2 C_{11}^{(r+1)} C_{55}^{(r+1)}) \end{aligned} \quad (3.3-17)$$

Moreover, continuity of the inter-laminar stresses,  $\sigma_z$  and  $\tau_{xz}$ , at those material interfaces of a simply supported beam implies,

$$\begin{aligned} &- p_m C_{13}^{(r-1)}\Phi^{(r-1)}(h_r) + C_{33}^{(r-1)}\Psi^{(r-1)}(h_r) + p_m C_{13}^{(r)}\Phi^{(r)}(h_r) - C_{33}^{(r)}\Psi^{(r)}(h_r) \\ &= [\alpha_z^{(r-1)}(C_{33}^{(r-1)} - C_{13}^{(r-1)2} / C_{11}^{(r-1)}) / C_{11}^{(r-1)} - \alpha_z^{(r)}(C_{33}^{(r)} - C_{13}^{(r)2} / C_{11}^{(r)})](T_0 + T_1 h_r), \\ &C_{55}^{(r-1)}(\Phi^{(r-1)'}(h_r) + p_m \Psi^{(r-1)}(h_r)) - C_{55}^{(r)}(\Phi^{(r)'}(h_r) + p_m \Psi^{(r)}(h_r)) \\ &= [\alpha_z^{(r-1)}(C_{33}^{(r-1)} - C_{13}^{(r-1)2} / C_{11}^{(r-1)}) / C_{11}^{(r-1)} - \alpha_z^{(r)}(C_{33}^{(r)} - C_{13}^{(r)2} / C_{11}^{(r)})]T_1 / p_m. \end{aligned} \quad (3.3-18)$$

Finally, the zero stress boundary conditions ( $\sigma_z = 0, \tau_{xz} = 0$ ) imposed on lateral surfaces require,

$$\begin{aligned} -p_m C_{13}^{(I)} \Phi^{(I)}(h_0) + C_{33}^{(I)} \Psi^{(I)}(h_0) &= (C_{33}^{(I)} - C_{13}^{(I)2} / C_{11}^{(I)}) \alpha_z^{(I)} (T_0 + T_1 h_0) \\ C_{55}^{(I)} (\Phi^{(I)'}(h_0) + p_m \Psi^{(I)}(h_0)) &= (C_{33}^{(I)} - C_{13}^{(I)2} / C_{11}^{(I)}) \alpha_z^{(I)} T_1 / p_m \end{aligned} \quad (3.3-19)$$

$$\begin{aligned} -p_m C_{13}^{(N)} \Phi^{(N)}(h_N) + C_{33}^{(N)} \Psi^{(N)}(h_N) &= (C_{33}^{(N)} - C_{13}^{(N)2} / C_{11}^{(N)}) \alpha_z^{(N)} (T_0 + T_1 h_N) \\ C_{55}^{(N)} (\Phi^{(N)'}(h_N) + p_m \Psi^{(N)}(h_N)) &= (C_{33}^{(N)} - C_{13}^{(N)2} / C_{11}^{(N)}) \alpha_z^{(N)} T_1 / p_m \end{aligned} \quad (3.3-20)$$

where  $h_0$  and  $h_N$  represent the value of the transverse coordinate at the bottom and the top lateral planes of the beam, respectively.

Given the constraints (Equation 2.3-3) on the shape functions (Equation 3.3-13), we further obtain four algebraic equations, the solution of which provides the following unique values  $A_0, B_0, C_0$  and  $D_0$ :

$$\begin{aligned} A_0 &= (C_{13}^{(ca)} + C_{55}^{(ca)}) \sum_{i=1}^4 k_i^{(ca)} \lambda_i^{(ca)} - T_0 (\alpha_x^{(ca)} C_{11}^{(ca)} + \alpha_z^{(ca)} C_{13}^{(ca)}) / (p_m C_{11}^{(ca)}) \\ B_0 &= p_m \sum_{i=1}^4 k_i^{(ca)} \left[ C_{11}^{(ca)} + (\lambda_i^{(ca)})^2 C_{13}^{(ca)} \right] - (C_{33}^{(ca)} - C_{13}^{(ca)2} / C_{11}^{(ca)}) \alpha_z^{(ca)} T_1 / (p_m C_{55}^{(ca)}), \\ C_0 &= \sum_{i=1}^4 k_i^{(ca)} \left[ C_{11}^{(ca)} - (\lambda_i^{(ca)})^2 C_{55}^{(ca)} \right] + [(C_{13}^{(ca)} + C_{55}^{(ca)}) (\alpha_x^{(ca)} C_{11}^{(ca)} + \alpha_z^{(ca)} C_{13}^{(ca)})] \\ &\quad - C_{11}^{(ca)} (\alpha_x^{(ca)} C_{13}^{(ca)} + \alpha_z^{(ca)} C_{33}^{(ca)}) T_1 / (p_m^2 C_{11}^{(ca)} C_{55}^{(ca)}), \\ D_0 &= p_m \sum_{i=1}^4 k_i^{(ca)} \lambda_i^{(ca)} \left[ C_{11}^{(ca)} - (\lambda_i^{(ca)})^2 C_{55}^{(ca)} \right] \end{aligned} \quad (3.3-21)$$

Those quantities indicated by a superscript  $(ca)$  are related to the layer that contains the central axis of the beam considered.

### 3.4 General five-degree-of-freedom beam theory (G5BT) for angle-ply laminated beams subject to mechanical loading

#### 3.4.1 Formulation

Assuming that the beam (or plate in cylindrical bending) is angle-ply laminated, general five-degree-of-freedom beam theory can be formulated starting with a displacement approximation of the form [Soldatos and Watson, 1997a] [Shu and Soldatos, 2000]:

$$\begin{aligned} U(x, z) &= u_0(x) - z w_{0,x}(x) + \varphi_1(z) u_1(x), \\ V(x, z) &= v_0(x) + \varphi_2(z) v_1(x), \\ W(x, z) &= w_0(x). \end{aligned} \quad (3.4-1)$$

where,  $u_0$ ,  $v_0$ ,  $w_0$ ,  $u_1$  and  $v_1$  are five unknown degrees of freedom, and  $\varphi_1(z)$  and  $\varphi_2(z)$  are two shape functions.

The equations of equilibrium of the present G5BT are simplified as follows:

$$\begin{aligned} N_{x,x}^c &= 0, \\ N_{xy,x}^c &= 0, \\ M_{x,xx}^c &= q(x), \\ M_{x,x}^a - Q_x^a &= 0, \\ M_{yx,x}^a - Q_y^a &= 0, \end{aligned} \quad (3.4-2)$$

where the force and moment resultants,  $N_x^c$ ,  $N_{xy}^c$ ,  $M_x^a$ ,  $M_{yx}^a$ ,  $Q_x^a$  and  $Q_y^a$ , are defined in equation (2.3-8) and (2.3-9).

It can be converted into the following five Navier-type differential equations in terms of the five unknown functions,

$$\begin{aligned}
A_{11}u_{0,xx} + A_{16}v_{0,xx} + B_{111}u_{1,xx} + B_{162}v_{1,xx} - B_{11}w_{0,xxx} &= 0, \\
A_{16}u_{0,xx} + A_{66}v_{0,xx} + B_{161}u_{1,xx} + B_{662}v_{1,xx} - B_{16}w_{0,xxx} &= 0, \\
B_{11}u_{0,xxx} + B_{16}v_{0,xxx} + D_{111}u_{1,xxx} + D_{162}v_{1,xxx} - D_{11}w_{0,xxx} &= -q(x), \\
B_{111}u_{0,xx} + B_{161}v_{0,xx} + D_{1111}u_{1,xx} + D_{1612}v_{1,xx} - A_{5511}u_1 - A_{4512}v_1 - D_{111}w_{0,xxx} &= 0, \\
B_{162}u_{0,xx} + B_{662}v_{0,xx} + D_{1612}u_{1,xx} + D_{6622}v_{1,xx} - A_{4512}u_1 - A_{4422}v_1 - D_{162}w_{0,xxx} &= 0.
\end{aligned} \tag{3.4-3}$$

where the appearing rigidities are quoted from the following definitions [Soldatos and Timarci, 1993] [Timarci and Soldatos, 1995]:

$$\begin{aligned}
A_{ij} &= \int_{-h/2}^{h/2} Q_{ij}^{(k)} dz, \quad A_{ijlm} = \int_{-h/2}^{h/2} Q_{ij}^{(k)} \varphi'_l \varphi'_m dz, \quad B_{ij} = \int_{-h/2}^{h/2} Q_{ij}^{(k)} z dz, \quad B_{ijl} = \int_{-h/2}^{h/2} Q_{ij}^{(k)} \varphi_l dz, \\
D_{ij} &= \int_{-h/2}^{h/2} Q_{ij}^{(k)} z^2 dz, \quad D_{ijl} = \int_{-h/2}^{h/2} Q_{ij}^{(k)} \varphi_l z dz, \quad D_{ijlm} = \int_{-h/2}^{h/2} Q_{ij}^{(k)} \varphi_l \varphi_m dz,
\end{aligned} \tag{3.4-4}$$

by assigning appropriate indices. Here,  $Q_{ij}$  ( $i, j = 1, 2, \dots, 6$ ) denote the appropriate reduced elastic stiffnesses (Jones, 1975).

Equations (3.4-3) form a twelfth-order of five simultaneous ordinary differential equations that, for a given appropriate set of the shape functions involved, can be solved for the five unknown displacement functions. Regardless of the particular form of the shape functions employed, the twelve constant coefficients of the general solution of that set of ordinary differential equations can be obtained by applying the same number of edge

boundary conditions. For a simply supported, a clamped and a free edge, these boundary conditions are as follows ( $x = 0$  or  $x = L$ ):

$$\begin{aligned}
 \text{Simply supported edge: } & N_x^c = N_{xy}^c = w_0 = M_x^c = M_x^a = M_{yx}^a = 0 \\
 \text{Clamped edge: } & u_0 = v_0 = w_0 = w_{,x} = u_1 = v_1 = 0, \\
 \text{Free edge: } & N_x^c = N_{xy}^c = M_x^c = M_{x,x}^c = M_x^a = M_{yx}^a = 0.
 \end{aligned} \tag{3.4-5}$$

Finally, note that the sets of edge boundary conditions described by equation (3.4-5) are the one-dimensional analogues of the following "point by point" sets of plane strain boundary conditions ( $x = 0, L$ ):

$$\begin{aligned}
 \text{Simply supported edge: } & \sigma_x = W = 0, \\
 \text{Rigidly clamped edge: } & U = W = 0, \\
 \text{Free edge: } & \sigma_x = \tau_{xz} = 0.
 \end{aligned} \tag{3.4-6}$$

As may easily be verified, the set of simply supported boundary conditions is satisfied exactly by a displacement choice of the form,

$$(u_0, u_1, v_0, v_1) = (A, B, C, D) \cos(p_m x), \quad w_0 = E \sin(p_m x). \tag{3.4-7}$$

which is the set of particular integrals of the Equilibrium equations (Equation 3.4-3). For any given set of shape functions  $\varphi_1(z)$  and  $\varphi_2(z)$ , the integrations (Equation 3.4-4) can be performed either analytically or numerically. The unique solution of unknown constant coefficients  $A, B, C, D$  and  $E$  can be obtained through the equilibrium equations (3.4-3).

### 3.4.2 Determination of shape functions subject to mechanical loading

The shape functions,  $\varphi_1(z)$  and  $\varphi_2(z)$ , can be determined by making use of the first and second of the three-dimensional equations of equilibrium. For the cylindrical bending of angle-ply laminated beam, these equations are simplified as follows [Shu and Soldatos, 2000]:

$$\sigma_{x,x} + \tau_{xz,x} = 0, \quad \tau_{xy,x} + \tau_{yz,x} = 0. \quad (3.4-8)$$

Using Hooke's law in connection with kinematic relation (Equation 2.2-2) and the displacement components (Equation 3.4-7) for simply supported edge, Equation (3.4-8) yields the following fourth-order of simultaneous ordinary differential equations,

$$\begin{aligned} Q_{35}^{(r)}\Phi_{1,zx}^{(r)} + Q_{45}^{(r)}\Phi_{2,zx}^{(r)} - Q_{11}^{(r)}p_m^2\Phi_1^{(r)} - Q_{16}^{(r)}p_m^2\Phi_2^{(r)} &= Q_{11}^{(r)}p_m^2(A - zEp_m) + Q_{16}^{(r)}Cp_m^2, \\ Q_{45}^{(r)}\Phi_{1,zx}^{(r)} + Q_{44}^{(r)}\Phi_{2,zx}^{(r)} - Q_{16}^{(r)}p_m^2\Phi_1^{(r)} - Q_{66}^{(r)}p_m^2\Phi_2^{(r)} &= Q_{16}^{(r)}p_m^2(A - zEp_m) + Q_{66}^{(r)}Cp_m^2, \end{aligned} \quad (3.4-9)$$

where,

$$\Phi_1^{(r)}(z) = B_0\varphi_1^{(r)}(z), \quad \Phi_2^{(r)}(z) = D_0\varphi_2^{(r)}(z). \quad (3.4-10)$$

Here, the superscript  $^{(r)}$  is associated with the shape functions in order to make it clear that, in general, their distribution changes from layer to layer.  $Q_{ij}^{(r)}$  ( $i, j = 1, 2, \dots, 6$ ;  $r = 1, 2, \dots, N$ ) denote the appropriate reduced elastic stiffnesses (Jones, 1975).

The general solution of equations (3.4-9) is given as follows:

$$\begin{aligned}\Phi_1^{(r)}(z) &= \sum_{i=1}^4 C_i^{(r)} e^{\alpha_i^{(r)} z} + E_0 p_m z - A_0, \\ \Phi_2^{(r)}(z) &= \sum_{i=1}^4 \frac{Q_{55}^{(r)} (\alpha_i^{(r)})^2 - Q_{11}^{(r)} p_m^2}{Q_{16}^{(r)} p_m^2 - Q_{45}^{(r)} (\alpha_i^{(r)})^2} C_i^{(r)} e^{\alpha_i^{(r)} z} - C_0,\end{aligned}\tag{3.4-11}$$

where  $C_i^{(r)}$  ( $i = 1, 2, 3, 4$ ) represent four arbitrary constants of integration in the  $k$ th layer. The appearing constants  $\alpha_i^{(r)}$  are the four roots of the following quartic algebraic equation:

$$\begin{aligned} [Q_{44}^{(r)} Q_{55}^{(k)} - (Q_{45}^{(r)})^2] \alpha^4 - (Q_{11}^{(r)} Q_{44}^{(r)} + Q_{66}^{(r)} Q_{55}^{(r)} - 2Q_{16}^{(r)} Q_{45}^{(r)}) p_m^2 \alpha^2 \\ + [Q_{11}^{(r)} Q_{66}^{(r)} - (Q_{16}^{(r)})^2] p_m^4 = 0,\end{aligned}\tag{3.4-12}$$

and, in general, differ from layer to layer.

For an  $N$  layered beam, however, there are still  $4N$  additional unknown constants,  $C_i^{(r)}$  ( $i = 1, 2, 3, 4; r = 1, 2, \dots, N$ ), to be determined. They can be determined by means of the  $4(N-1)$  in-plane displacement and shear stress continuity conditions ( $U(x, z)$ ,  $V(x, z)$ ,  $\tau_{xz}$ ,  $\tau_{yz}$ ) employed on the  $N-1$  material interfaces considered and the four zero shear traction boundary conditions ( $\tau_{xz}$ ,  $\tau_{yz}$ ) specified on top and bottom lateral planes. Thus,  $4N$  unknowns ( $C_i^{(k)}$ ) can be determined by a set of  $4N$  linear algebraic equations.

In a close relation to the corresponding results obtained in [Soldatos and Watson, 1997a], the right-hand-sides of Equations (3.4-11) are entirely dependent upon the displacement field of the classical plate theory, whereas the left-hand-sides depend on the

corresponding additional field that incorporates the effects of transverse shear deformation. This is further clarified by the fact that, with the form of Equation (3.4-9) and (3.4-11), their equivalent elasticity Equations (3.4-8) are satisfied regardless of the values of all the five unknown constants ( $A_0$ ,  $B_0$ ,  $C_0$ ,  $D_0$  and  $E_0$ ). As a result, for the cylindrical bending of simply supported, angle-ply beam, values can initially be assigned to all these unknown constants in an almost arbitrary manner. Thus, by pre-setting  $B_0 = 1$  and using the shape function constraints (Equation 2.3-2 and 2.3-3), the Equation (3.4-11) provides the unique solution of  $A_0$ ,  $C_0$ ,  $D_0$  and  $E_0$ . Here,  $B_0$  is chosen to be the non-zero proportionality factor that, since its value leaves the final numerical results unaffected, can be left undetermined or set equal to unity without loss of generality [Soldatos and Watson, 1987a] [Shu and Soldatos, 2000].

## **Chapter 4**

# **A predictor-corrector method for accurate stress analysis of composite beams and plates**

### **4.1 Introduction**

It is well known that conventional beam and plate theories yield poor results when dealing with stress predictions in highly reinforced laminated components. In more detail, the classical plate theory disregards the transverse stresses. The uniform shear deformable plate theory assumed the transverse shear stress distributed as a constant in each layer through the plate thickness. The parabolic shear deformable plate theory considered the transverse shear stress on the top and bottom plane of the plate, but it do not take the inter-laminar interface shear stress continuity into account. Due to the shear deformable plate theories use the plane stress-reduced stiffnesses, they are not able to predict the transverse normal stress in predictor phase. In this chapter, a predictor-corrector method that can improve the accuracy of transverse stress analysis results has been used for comparing the accuracy and assessing the performance of composite plate/beam theories.

In more detail, working on a predictor-corrector basis the in-plane stresses that are initially predicted by means of a certain conventional or generalized beam or plate theory are substituted into the differential equations of three-dimensional elasticity, which in a corrector phase are integrated through the plate thickness. The resulting transverse shear and transverse normal stress distributions are expected to be improvements and are actually found to be more accurate stress predictions than their initially predicted counterparts. This

can only be and is verified however through appropriate comparisons with corresponding results based on the few existing exact elasticity solutions.

#### 4.2 Determination of stresses in the predictor phase

The beam theories employed in this study are all based on displacement approximations that are particular cases of the generalised displacement field:

$$\begin{aligned}
 U(x, z) &= u_0(x) - zw_{0,x}(x) + \varphi_1(z)u_1(x), \\
 V(x, z) &= v_0(x) + \varphi_2(z)v_1(x), \\
 W(x, z) &= w_0(x) + \psi(z)w_1(x),
 \end{aligned} \tag{4.2-1}$$

detailed in the preceding chapters. The displacement field can be obtained through the general solution of equilibrium equations (Equations 3.2-3, 3.3-5, 3.4-3) of corresponding plate/beam theories. The uniform shear deformable theory (USDT) [Timoshenko, 1921] (Section 3.1 and 3.2), parabolic shear deformable theory (PSDT) [Bickford, 1984] (Section 3.1 and 3.2), general 3-degree-of-freedom beam theory (G3BT) [Soldatos and Watson, 1997a] (Section 3.2) and general 4-degree-of-freedom beam theory (G4BT) [Soldatos and Watson, 1997b, c] (Section 3.3) are employed for the analysis of cross-ply composite laminates, while general 5-degree-of-freedom beam theory (G5BT) [Shu and Soldatos, 2000] (Section 3.4) is used for the analysis of angle-ply composite laminates subject to mechanical loading. Further, a newly derived general 4-degree-of-freedom

theory (G4BT) (Section 3.3) for the analysis of cross-ply composite laminates subject to thermal loading is employed in this study.

As described in Chapter 2 and can be easily verified, most conventional plate/beam theories (including the uniform shear deformable theory and parabolic shear deformable theory) are particular cases of the general five-degree-of-freedom plate theory. Also, following Chapter 3 the uniform shear deformable beam theory and parabolic shear deformable beam theory can be considered as the specific cases of the general five-degree-of-freedom beam theory for a cross-ply plate of cylindrical bending.

Stresses are obtained through the generalized Hooke's law (Equation 3.1-1). In dealing with individual beam theory, the appropriate reduced constitutive relations are employed [Jones, 1975] (Equation 3.1-4) in G3BT [Soldatos and Watson, 1997a], the USDT [Timoshenko, 1921] and the PSDT [Bickford, 1982]. The three-dimensional constitutive equations used in G4BT [Soldatos and Watson, 1997b, c] are those of plane strain elasticity, namely [Jones, 1975] (Equation 3.1-2). The transformed reduced constitutive relations [Jones, 1975] (Equation 3.1-3) are employed in G5BT [Shu and Soldatos, 2000]. In the application of the USDT predictor phase, a shear correction factor is used to improve the values of the shear stresses. The determination of accurate correction factor was studied by several investigators (see, for example, references [Timoshenko, 1921], [Copper, 1966], [Chow, 1971], [Whitney, 1973] and [Raman, 1996]) but in this thesis its most commonly used value, namely  $5/6$ , is adopted.

### 4.3 Corrector phase

In the plane strain state considered, all physical quantities are independent of the  $y$  co-ordinate parameter. Accordingly, the equilibrium equations of three-dimensional elasticity are simplified to:

$$\begin{aligned}\frac{\partial \sigma_x}{\partial x} + \frac{\partial \tau_{xz}}{\partial z} &= 0, \\ \frac{\partial \tau_{xz}}{\partial x} + \frac{\partial \sigma_z}{\partial z} &= 0.\end{aligned}\tag{4.3-1}$$

The bending stress,  $\sigma_x$ , is calculated in the predictor phase by substituting the displacement field obtained through a chosen beam theory, into the strain-displacement relations and then using the appropriate constitutive equation. Upon integrating three-dimensional equilibrium equation (4.3-1) with respect to  $z$ , the corrected shear stress in the  $r$ th layer can be obtained as follows:

$$\tau_{xz}^{(r)}(x, z) = - \int \frac{\partial \sigma_x^{(r)}(x, z)}{\partial x} dz + c_0^{(r)}(x), \quad (r = 1, 2, \dots, N)\tag{4.3-2}$$

where  $c_0^{(r)}(x)$  represent  $N$  arbitrary functions of  $x$  ( $r = 1, 2, \dots, N$ ). These can be determined by using the following lateral surface shear stress boundary conditions together with the appropriate interface shear stress continuity conditions applied at material interfaces,  $h_r$ :

$$\begin{aligned}
\tau_{xz}^{(1)}(x, h_0) &= 0, \\
\tau_{xz}^{(N)}(x, h_N) &= 0, \\
\tau_{xz}^{(r+1)}(x, h_r) &= \tau_{xz}^{(r)}(x, h_r). \quad (r = 1, 2, \dots, N-1)
\end{aligned} \tag{4.3-3}$$

Here,  $h_0 = -h/2$  and  $h_N = h/2$  represent the transverse co-ordinate parameters of the lateral planes of the beam. This forms an apparently over-determined problem, in which the  $N$  unknown functions  $c_0^{(r)}(x)$  should satisfy the  $N+1$  constraints (4.3-3). In the numerical calculations, the  $N-1$  constraints (4.3-3c) are combined with either (4.3-3a) or (4.3-3b), which then makes the shear stress distribution to automatically satisfy the remaining lateral surface boundary condition, namely (4.3-3b) or (4.3-3a), respectively. Under these considerations and combining Equation (4.3-3c) with Equation (4.3-3a), the  $N$  functions  $c_0^{(r)}(x)$  ( $r = 1, 2, \dots, N$ ) can be determined in the following form:

$$\begin{aligned}
c_0^{(1)}(x) &= \left[ \int_{z=h_0} \frac{\partial \sigma_x^{(1)}(x, z)}{\partial x} dz \right], \\
c_0^{(r+1)}(x) &= \left[ \int_{z=h_r} \frac{\partial \sigma_x^{(r+1)}(x, z)}{\partial x} dz - \int_{z=h_r} \frac{\partial \sigma_x^{(r)}(x, z)}{\partial x} dz \right] + c_0^{(r)}(x). \tag{4.3-4} \\
&\quad (r = 1, 2, \dots, N-1)
\end{aligned}$$

Upon subtracting the partial derivative of equation (4.3-1b) with respect to  $z$  from the partial derivative of equation (4.3-1a) with respect to  $x$  and, then, integrating the result twice with respect to  $z$ , the corrected transverse normal stress is next obtained in the following form:

$$\sigma_z^{(r)}(x) = \int \left( \int \frac{\partial^2 \sigma_x^{(r)}(x, z)}{\partial x^2} dz \right) dz + c_1^{(r)}(x) z + c_2^{(r)}(x). \quad (4.3-5)$$

$(r = 1, 2, \dots, N)$

where  $c_1^{(r)}$  and  $c_2^{(r)}$  are arbitrary functions of  $x$ . These can be obtained by using the known lateral transverse normal stress boundary conditions together with the appropriate continuity conditions of transverse normal stress and its derivative at the beam material interfaces, namely,

$$\begin{aligned} \sigma_z^{(1)}(x, h_0) &= 0, \\ \sigma_z^{(N)}(x, h_N) &= q(x), \\ \sigma_z^{(r+1)}(x, h_r) &= \sigma_z^{(r)}(x, h_r), \\ \frac{\partial \sigma_z^{(r+1)}(x, z)}{\partial z} \Big|_{z=h_r} &= \frac{\partial \sigma_z^{(r)}(x, z)}{\partial z} \Big|_{z=h_r}. \end{aligned} \quad (4.3-6)$$

$(r = 1, 2, \dots, N-1)$

These yield the following  $2N$  linear algebraic equations,

$$\begin{aligned} c_1^{(1)}(x) h_0 + c_2^{(1)}(x) &= \left[ - \int \left( \int \frac{\partial^2 \sigma_x^{(1)}(x, z)}{\partial x^2} dz \right) dz \right]_{z=h_0}, \\ c_1^{(N)}(x) h_N + c_2^{(N)}(x) &= \left[ - \int \left( \int \frac{\partial^2 \sigma_x^{(N)}(x, z)}{\partial x^2} dz \right) dz \right]_{z=h_N}, \\ c_1^{(r+1)}(x) h_r + c_2^{(r+1)}(x) - c_1^{(r)}(x) h_r - c_2^{(r)}(x) &= \\ &= \left[ - \int \left( \int \frac{\partial^2 \sigma_x^{(r+1)}(x, z)}{\partial x^2} dz \right) dz + \int \left( \int \frac{\partial^2 \sigma_x^{(r)}(x, z)}{\partial x^2} dz \right) dz \right]_{z=h_r}, \end{aligned} \quad (4.3-7)$$

$$c_1^{(r+1)}(x) - c_1^{(r)}(x) = \left[ - \int \frac{\partial^2 \sigma_x^{(r+1)}(x, z)}{\partial x^2} dz + \int \frac{\partial^2 \sigma_x^{(r)}(x, z)}{\partial x^2} dz \right]_{z=h_r},$$

$$(r = 1, 2, \dots, N - 1)$$

which are solved simultaneously for the determination of the same number of unknown functions  $c_1^{(r)}$  and  $c_2^{(r)}$  ( $r = 1, 2, \dots, N$ ).

## **Chapter 5**

### **Application of the predictor-corrector method for cross-ply composite laminates subject to mechanical loading**

#### **5.1 Introduction**

This chapter assesses the stress analysis performance of the most commonly used conventional shear deformable beam theories as well as the advanced beam theories presented in references [Soldatos and Watson, 1997a, b, c], by employing the predictor-corrector method detailed in the preceding section. The assessment deals with the accuracy of the distribution of interlaminar (transverse shear and transverse normal) stresses through the entire beam thickness. As far as simply supported laminated beams are concerned, it compares the corresponding stress analysis results obtained with their exact elasticity counterparts [Pagano, 1969, 1970].

Based on the conclusions of this type of initial assessment, the application of the predictor-corrector method on general three-degree-of-freedom beam theory and general four-degree-of-freedom beam theory are made for other sets of boundary conditions. Comparisons are also performed, between the general three-degree-of-freedom beam theory and the general four-degree-of-freedom beam theory results, for other sets of edge boundary conditions for which explicit 3D elasticity results are unavailable or very difficult to obtain.

For single-layered beams having both their edges clamped, some preliminary comparisons with certain exact elasticity results [Vel and Batra, 2000] are also presented

(see also [Soldatos and Liu, 2001]). However, those dealt only with the values of displacements and stresses at particular points along the beam span and not with corresponding detailed distributions through the beam thickness.

## **5.2 Assessment of certain refined models for cross-ply laminated simply supported beams**

A two-layered anti-symmetric cross-ply simply supported laminated beam, with the material interface placed at  $z/h = 0.2$  and fibres in the bottom layer aligned along the  $x$ -axis ( $0^\circ/90^\circ$ ), is now considered. As mentioned in references [Soldatos and Watson, 1997b, c], the particular lay-up employed has been selected in an attempt to magnify the effects of the possible discontinuity that the inter-laminar stresses predictions may exhibit in the predictor phase and, therefore, to quantitatively estimate the extent to which these can affect the accuracy of the results obtained. The laminated composite beam considered is subject to a sinusoidal loading distribution that has the following form (Equation 3.2-1):

$$q(x) = q_m \sin(p_m x), \quad p_m = m\pi/L, \quad (m = 1, 2, \dots) \quad (5.2-1)$$

and is applied downwards on the top lateral plane of the beam. For simplicity,  $m$  is taken equal to 1 in this study. Hence,  $q(x)$  might be thought as the one of the terms of the Fourier sine-series expansion of a general mechanical loading.

The orthotropic material of the laminates considered in the following applications has the following elastic properties:

$$E_L / E_T = 40, \quad G_{LT} / E_T = 0.5, \quad G_{TT} / E_T = 0.2, \quad \nu_{LT} = \nu_{TT} = 0.25, \quad (5.2-2)$$

where the subscripts  $_L$  and  $_T$  denote properties associated with the longitudinal and transverse fibre directions respectively.  $E_L / E_T = 40$  is chosen in almost all applications except cases showing stress variations with varying the stiffness ratio (Figures 5.2-2 and 5.2-5). Similarly, the aspect ratio  $L/h = 10$  is chosen for most applications except cases showing stress variations with varying aspect ratios of the laminated beam (Figures 5.2-3 and 5.2-6). The percentage error denoted in Figures 5.2-1 to 5.2-6 for simply supported beams is defined as follows:

$$Er\% = \frac{(\sigma_{ij}^{(e)} - \sigma_{ij}^{(a)})}{\sigma_{ij}^{(e)}} * 100, \quad (i = x, z; j = z) \quad (5.2-3)$$

where  $\sigma_{ij}^{(e)}$  represents exact stresses calculated by means of Pagano's exact elasticity solution (ES) [Pagano, 1969], and  $\sigma_{ij}^{(a)}$  represents approximate stresses obtained by means of the corresponding approximate beam model employed.

For a notation convenience, the following abbreviations have been used in Figures:

(i) USDTC and PSDTC indicate results obtained by means of the corrector phase of the USDT [Timoshenko, 1921] and the PSDT [Bickford, 1982], respectively, (ii) G3TP and G3TC indicate results obtained by means of the predictor and the corrector phase of the G3BT [Soldatos and Watson, 1997a] (see also Chapter 3 and Chapter 4), respectively, and (iii) G4TP and G4TC indicate results obtained by means of the predictor and corrector phases of the G4BT [Soldatos and Watson, 1997b, c] (see also Chapter 3 and Chapter 4), respectively. For simply supported beams, the shear stresses obtained by means of the

predictor phases of USDT and PSDT are very inaccurate. Hence, the corresponding percentage errors are so large that do not fit and therefore are not shown in Figures 5.2-1 to 5.2-6. The shear stress distribution obtained by means of the corrector phase of G3BT is essentially identical to its predictor phase counterpart given that corresponding results agree to more than six significant figures. This shows that the corrector phase is not needed for shear stress results evaluated via the G3BT. As was pointed out in references [Soldatos and Watson, 1997b, c] G4BT yields the exact elasticity results [Pagano, 1969] for simply supported plates, so the corrector phase is not needed in this case neither for transverse shear nor for transverse normal stress predictions.

Specific co-ordinate points where maximum transverse stresses occur along the beam span and/or across the beam thickness have been chosen for a better illustration of some of the results. Accordingly, the points  $(x = 0, z = -0.1h)$  and  $(x = L/2, z = -0.1h)$  are chosen to illustrate the variation of the maximum shear stress and transverse normal stress values, respectively, for the simply supported beam results shown (Tables 5.2-1 and 5.2-2 and Figures 5.2-1 to 5.2-6).

Table 5.2-1 gives the transverse shear stress values across the thickness of the beam obtained by the various theories and the corresponding percentage errors are given in Figure 5.2-1. In the predictor phase, the USDT yields a very inaccurate constant value of shear stress across the thickness of each layer. Hence, neither the zero shear stress boundary conditions on the beam top and bottom lateral planes nor the inter-laminar shear stress continuity at the interface are satisfied. On the other hand, the shear stress distribution of the predictor phase of PSDT satisfies the top and bottom zero shear stress boundary conditions but it is still inaccurate and does not satisfy the inter-laminar continuity condition. Contrary to this, the shear stress distributions of the USDTC, PSDTC and G3TP satisfy both the top and bottom zero shear stress boundary conditions and the

Table 5.2-1. Comparison of shear stress distributions,  $\tau_{xz}(0, z)/q_1$ , for a two-layered simply supported beam

$z/h$	<i>USDT</i>	<i>USDT</i>	<i>PSDT</i>	<i>PSDT</i>	<i>G3BT</i>	<i>G4BT, ES*</i>
	Predictor	Corrector	Predictor	Corrector	Predictor & Corrector	
0.5	-2.1724	0	0	0	0	0
0.4	-2.1724	-0.1552	-0.7677	-0.1593	-0.1813	-0.1881
0.3	-2.1724	-0.2843	-1.3648	-0.2876	-0.3272	-0.3410
0.2	-2.1724	-0.3873	-1.7913	-0.3880	-0.4385	-0.4593
0.2	-5.4309	-0.3873	-4.4782	-0.3880	-0.4385	-0.4593
0.1	-5.4309	-3.4634	-5.1180	-3.3684	-3.5412	-3.5483
0	-5.4309	-5.4957	-5.3312	-5.3650	-5.4657	-5.4633
-0.1	-5.4309	-6.4842	-5.1180	-6.3946	-6.3653	-6.3565
-0.2	-5.4309	-6.4289	-4.4782	-6.4404	-6.3116	-6.2991
-0.3	-5.4309	-5.3298	-3.4120	-5.4517	-5.3002	-5.2873
-0.4	-5.4309	-3.1868	-1.9192	-3.3442	-3.2508	-3.2414
-0.5	-5.4309	0	0	0	0	0

\* ES-Pagano's elasticity solution [Pagano, 1969]

Table 5.2-2 Comparison of transverse normal stress distributions,  $\sigma_z(L/2, z)/q_1$ , for a two-layered simply supported beam

$z/h$	<i>USDT</i> Corrector	<i>PSDT</i> Corrector	<i>G3BT</i> Corrector	<i>G4BT, ES*</i>
0.5	-1	-1	-1	-1
0.4	-0.9975	-0.9974	-0.9971	-0.9970
0.3	-0.9905	-0.9903	-0.9890	-0.9885
0.2	-0.9799	-0.9796	-0.9769	-0.9759
0.2	-0.9799	-0.9796	-0.9769	-0.9759
0.1	-0.9167	-0.9180	-0.9110	-0.9096
0	-0.7732	-0.7783	-0.7667	-0.7652
-0.1	-0.5823	-0.5910	-0.5783	-0.5770
-0.2	-0.3767	-0.3868	-0.3767	-0.3757
-0.3	-0.1893	-0.1972	-0.1917	-0.1912
-0.4	-0.0528	-0.0560	-0.0545	-0.0543
-0.5	0	0	0	0

\* ES-Pagano's elasticity solution [Pagano, 1969]

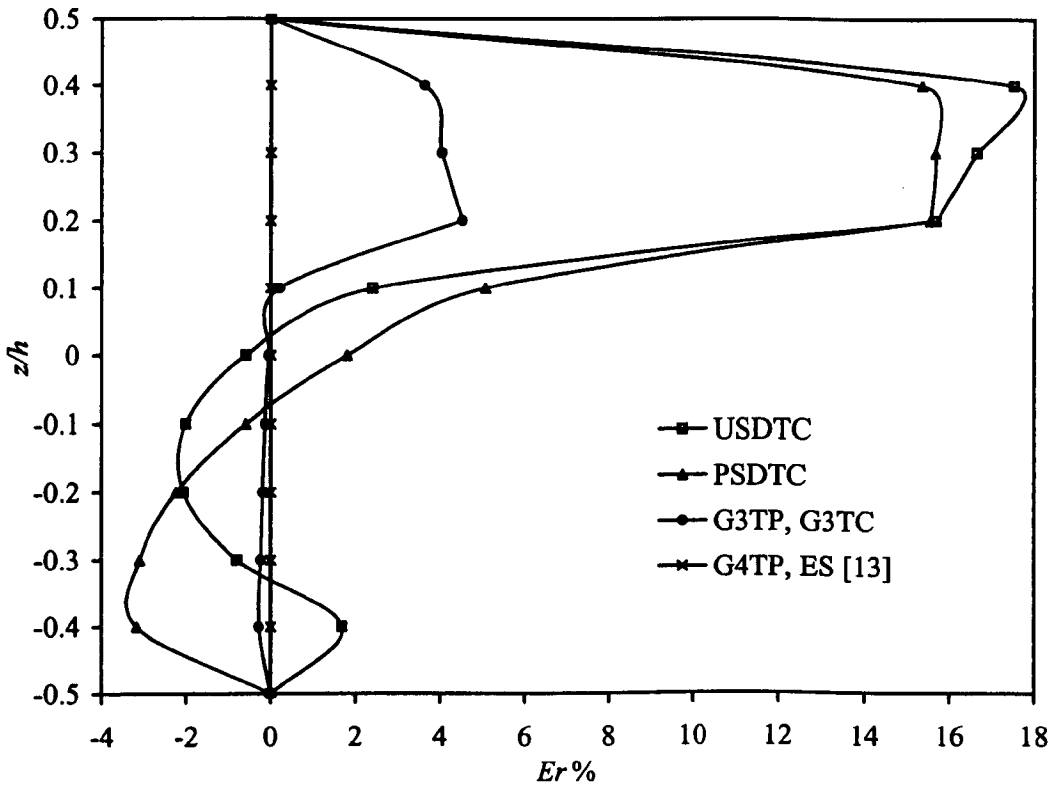


Fig 5.2-1. Percentage error of shear stress,  $\tau_{xz}(0, z)/q_1$ , for a simply supported beam

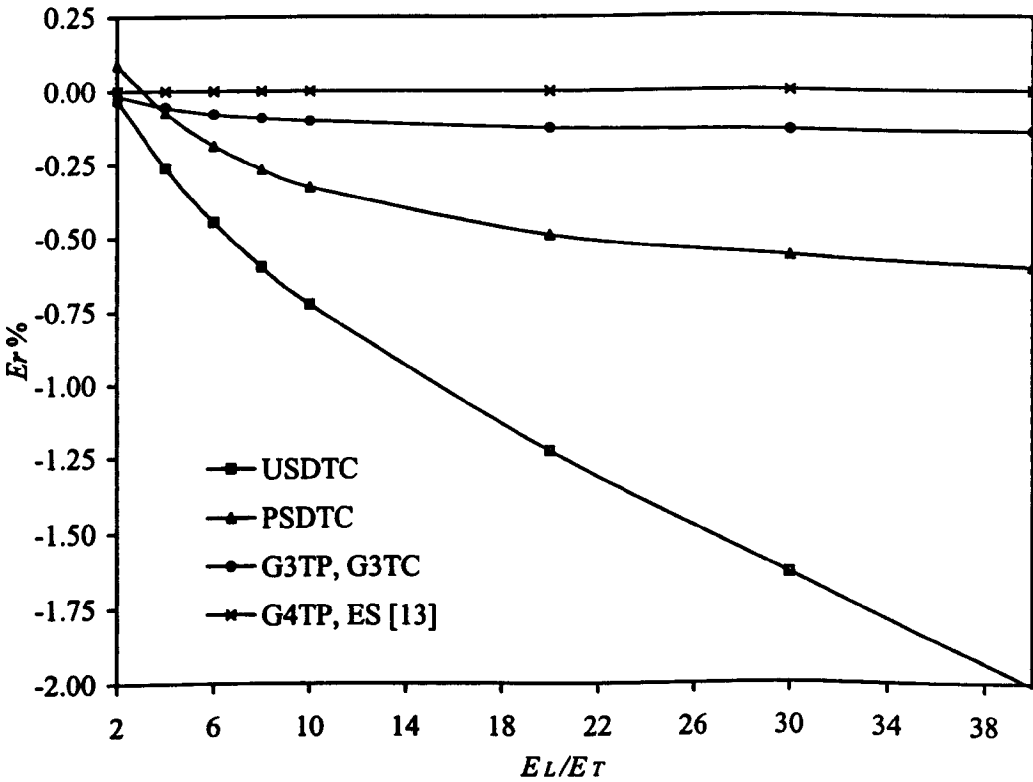


Fig 5.2-2. Percentage error of shear stress,  $\tau_{xz}(0, -0.1h)/q_1$ , for a simply supported beam

interface continuity condition. However, they have larger percentage errors in the domain of  $0.1h < z < 0.5h$  than in the domain of  $-0.5h < z < 0.1h$ . At the material interface  $z/h = 0.2$ , these errors are about 16%, 16% and 5% respectively, thus showing clearly that the corrector phase of G3BT is more accurate than the corrector phase of either USDT or PSDT.

Figure 5.2-2 illustrates the variation of percentage error in the maximum shear stress values,  $\tau_{xz}(0, -0.1h)$ , with increasing stiffness ratio,  $E_L/E_T$ . Apart the G4BT that yields the exact elasticity values, the percentage errors on the shear stress predictions of all remaining models increase with increasing  $E_L/E_T$  taking on maximum values at  $E_L/E_T = 40$ . Figure 5.2-2 shows clearly the excellent performance and effectiveness of G3BT, the magnitude of the relative error never exceeding 0.2%. Figure 5.2-3 illustrates the variation of corresponding percentage errors with increasing length-to-thickness ratio,  $L/h$ . As expected these errors decrease for all models with increasing  $L/h$ . However, of the models USDT, PSDT and G3BT it again exhibits the most reliable performance, even from its predictor phase.

Table 5.2-2 presents corresponding transverse normal stress distribution values across the thickness of a simply supported beam and the corresponding percentage errors are illustrated in Figure 5.2-4. Due to their limitations, none of the USDT, PSDT or the G3BT can yield estimates of the transverse normal stress distributions during its predictor phase. However, the maximum errors of the transverse normal stress value obtained via the corrector phase of the USDT, the PSDT and the G3BT are approximately 3%, -3% and -0.3%, respectively, appearing at about  $x = 0, z = -0.4h$  (bottom layer). These errors clearly indicate the effectiveness of both the predictor-corrector method and the shear deformable theories employed in predicting transverse normal stresses. They show that

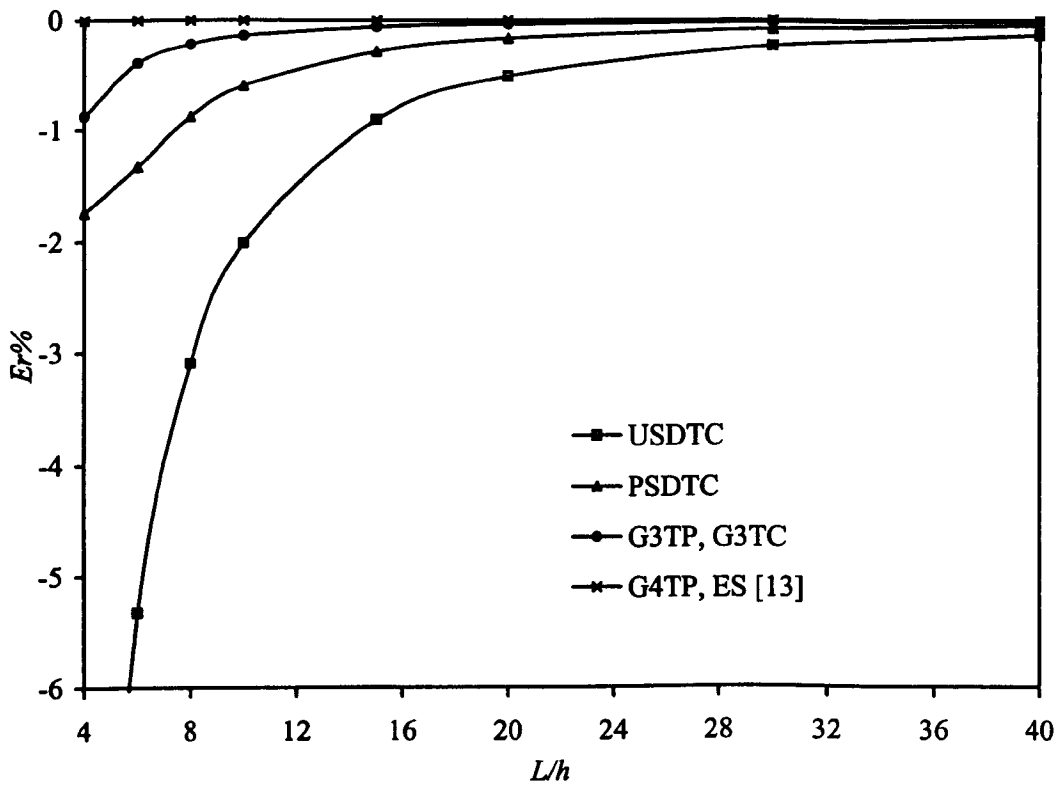


Fig 5.2-3. Percentage error of shear stress,  $\tau_{xz}(0, -0.1h)/q_1$ , for a simply supported beam

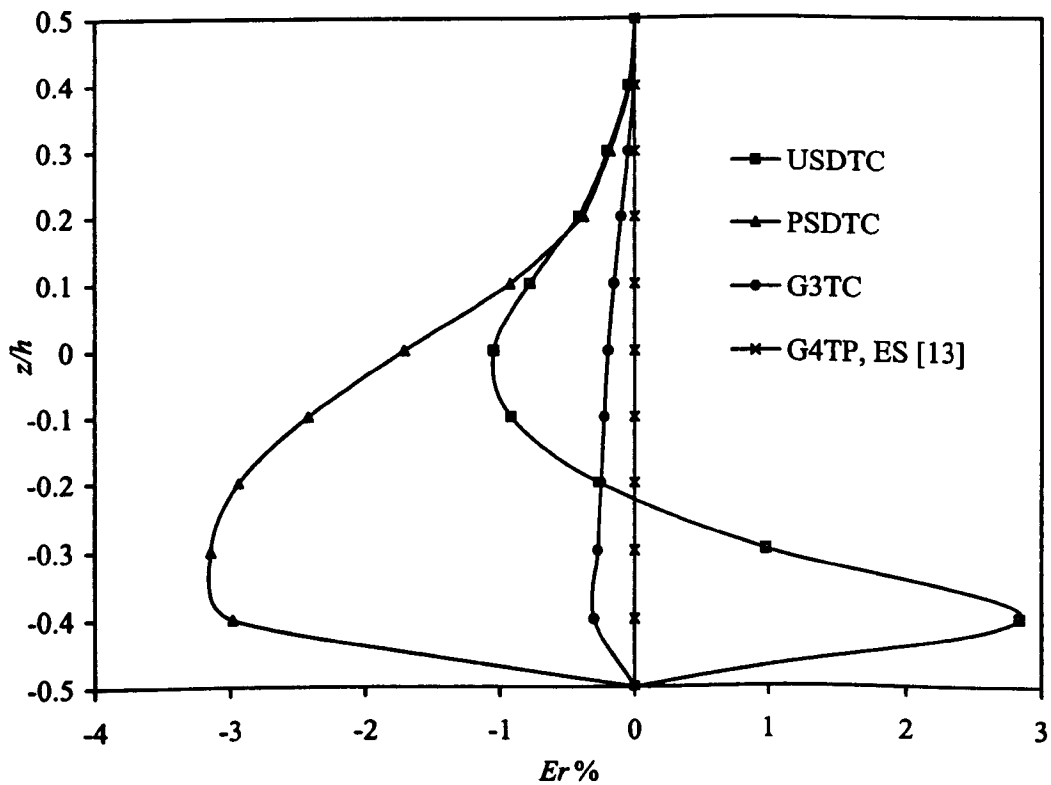


Fig 5.2-4. Percentage error of transverse normal stress,  $\sigma_z(L/2, z)/q_1$ , for a simply supported beam

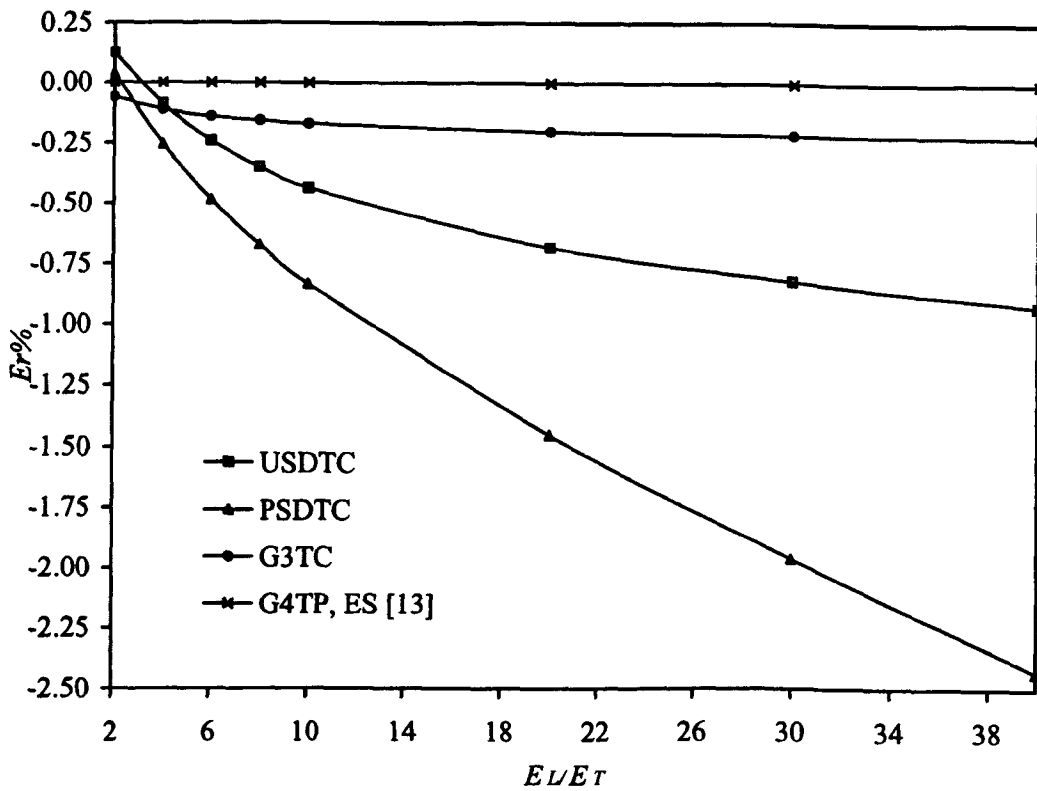


Fig 5.2-5. Percentage error of transverse normal stress,  $\sigma_z(L/2, -0.1h)/q_1$ , for a simply supported beam

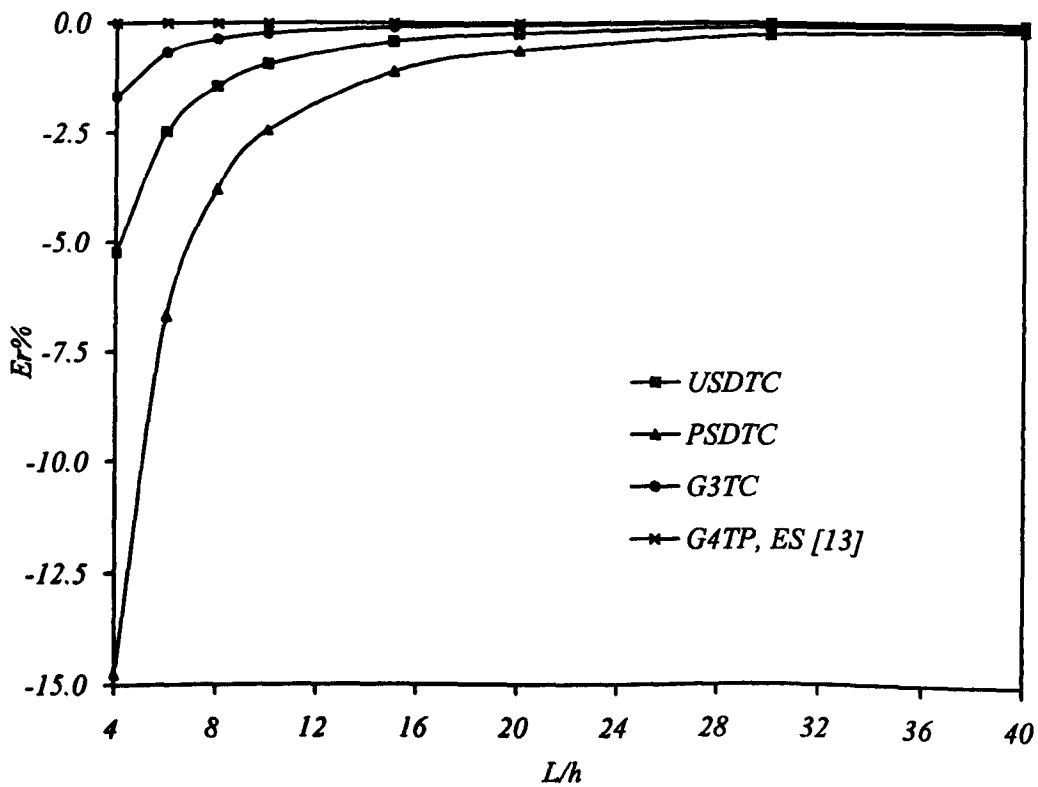


Fig 5.2-6. Percentage error of transverse normal stress,  $\sigma_z(L/2, -0.1h)/q_1$ , for a simply supported beam

G3BT is the best among the shear deformable theories employed and yields the most accurate numerical results.

Figure 5.2-5 illustrates the variation of corresponding percentage errors in transverse normal stress predictions with increasing the stiffness ratio,  $E_L / E_T$ . These can be seen to increase with increasing stiffness ratio though the magnitude of their maximum values (at  $E_L / E_T = 40$ ) do not exceed 1%, 2.5% and 0.3% for the USDTC, the PSDTC and the G3TC, respectively. Figure 5.2-6 shows the variation in percentage errors with increasing length-to-thickness ratio,  $L / h$ . As expected, these errors decrease with increasing  $L/h$ . The maximum error, at  $L/h = 4$ , is less than -2% for the G3TC whereas it is as large as -6% and -15% for the USDTC and the PSDTC respectively. Hence, those results given in figures 6 and 7 illustrate once again the high efficiency of the G3BT.

### **5.3 Application on general three-degree-of-freedom and four-degree-of-freedom beam theory for different sets of boundary conditions**

Following the considerations of Section 5.2, the outlined predictor-corrector method is now applied to the accurate determination of stress distributions in composite beams subjected to different sets of boundary conditions (clamped-clamped and cantilevered beams), but only in connection with the G4BT and G3BT, namely the most accurate theories among the ones already employed and tested. Certain relevant preliminary results dealing with beams having both their edges clamped have already been published in reference [Soldatos and Liu, 2001]. They are also compared against corresponding exact elasticity results [Vel and Batra, 2000] and found to be very accurate. However, these preliminary results will be listed in Section 5.4. Hence, the stress analysis results shown in

Tables 5.3-1, 5.3-2 and Figures 5.3-1 to 5.3-4 for clamped-clamped and clamped-free (cantilevered) beams are entirely new in the literature.

For clamped-clamped and clamped-free beams, the cross-section  $x = L/4$  is chosen to show the transverse shear stress variation, while the cross-section  $x = L/2$  illustrates transverse normal stress variation across the thickness (Tables 5.3-1 and 5.3-2). The points  $(x = L/4, z = -0.1h)$  and  $(x = L/2, z = -0.1h)$  are used to illustrate the transverse shear and transverse normal stress predictions, respectively, when increasing the length-to-thickness ratio (Figures 5.3-1, 5.3-3 and Figures 5.3-2, 5.3-4).

Table 5.3-1 presents corresponding transverse shear and normal stress values obtained by means of both the G3BT and G4BT for clamped-clamped beams. The shear stress of the G3BT predictor phase satisfies the lateral surfaces zero shear stress boundary conditions and the interface continuity. The shear stress predictor phase of G4BT yields non-zero values on the top and bottom lateral surfaces and discontinuity at the interface, which are negligible. The shear stress distributions obtained through the predictor phase of the G3BT are in very good agreement with the improved shear stress distribution obtained through the corrector phases of both G3BT and G4BT. It is of interest to note that the difference in corresponding maximum shear stresses, at about  $z = -0.1h$ , remains much smaller than 1% in either the predictor or the corrector phase of the two theories. As already mentioned the G3BT cannot yield transverse normal stresses in its predictor phase, whereas the transverse normal stress distribution obtained through the predictor phase of the G4BT is quite unrealistic and therefore inaccurate (it satisfies neither the lateral surface boundary condition nor the continuity at material interface). Contrary to this, the corrector phase of both G3BT and G4BT improve their transverse normal stress distributions and are both being in excellent agreement.

Table 5.3-1. Shear stress,  $\tau_{xz}(L/4, z)$ , and transverse normal stress,  $\sigma_z(L/2, z)$ , for a two-layered clamped-clamped beam

$z/h$	Shear stress				Transverse normal stress		
	<i>G3BT</i>	<i>G3BT</i>	<i>G4BT</i>	<i>G4BT</i>	<i>G3BT</i>	<i>G4BT</i>	<i>G4BT</i>
	Predictor	Corrector	Predictor	Corrector	Corrector	Predictor	Corrector
0.5	0.0000	0.0000	0.0000	0.0000	-1.0000	-0.4265	-1.0000
0.4	-0.1282	-0.1286	-0.1330	-0.1333	-0.9971	-0.4182	-0.9970
0.3	-0.2314	-0.2320	-0.2411	-0.2415	-0.9890	-0.4107	-0.9885
0.2	-0.3100	-0.3108	-0.3248	-0.3253	-0.9769	-0.4038	-0.9759
0.2	-0.3100	-0.3108	-0.3248	-0.3253	-0.9769	-0.3799	-0.9759
0.1	-2.5036	-2.5052	-2.5089	-2.5098	-0.9110	-0.3565	-0.9096
0	-3.8642	-3.8644	-3.8628	-3.8629	-0.7667	-0.3184	-0.7650
-0.1	-4.5003	-4.4992	-4.4943	-4.4936	-0.5783	-0.2720	-0.5770
-0.2	-4.4623	-4.4612	-4.4537	-4.4531	-0.3767	-0.2231	-0.3757
-0.3	-3.7472	-3.7474	-3.7382	-3.7384	-0.1917	-0.1776	-0.1912
-0.4	-2.2983	-2.2996	-2.2916	-2.2926	-0.0545	-0.1411	-0.0543
-0.5	0.0000	0.0000	0.0002	0.0000	0.0000	-0.1205	0.0000

Table 5.3-2. Shear stress,  $\tau_{xz}(L/4, z)$ , and transverse normal stress,  $\sigma_z(L/2, z)$ , for a two-layered clamped-free beam

$z/h$	Shear stress				Transverse normal stress		
	<i>G3BT</i>	<i>G3BT</i>	<i>G4BT</i>	<i>G4BT</i>	<i>G3BT</i>	<i>G4BT</i>	<i>G4BT</i>
	Predictor	Corrector	Predictor	Corrector	Corrector	Predictor	Corrector
0.5	0.0000	0.0000	-0.0004	0.0000	-1.0000	0.4152	-1.0000
0.4	-0.1827	-0.1552	-0.1891	-0.1614	-0.9971	0.4310	-0.9970
0.3	-0.3297	-0.2843	-0.3427	-0.2969	-0.9890	0.4372	-0.9885
0.2	-0.4418	-0.3873	-0.4619	-0.4064	-0.9769	0.4357	-0.9759
0.2	-0.4418	-0.3873	-0.4608	-0.4064	-0.9769	0.4946	-0.9759
0.1	-3.5676	-3.4634	-3.5720	-3.4695	-0.9110	0.4550	-0.9096
0	-5.5065	-5.4957	-5.5016	-5.4928	-0.7667	0.3373	-0.7652
-0.1	-6.4129	-6.4842	-6.4026	-6.4756	-0.5783	0.1756	-0.5770
-0.2	-6.3587	-6.4289	-6.3466	-6.4175	-0.3767	0.0008	-0.3757
-0.3	-5.3398	-5.3298	-5.3297	-5.3185	-0.1917	-0.1576	-0.1912
-0.4	-3.2750	-3.1868	-3.2718	-3.1791	-0.0545	-0.2685	-0.0543
-0.5	0.0000	0.0000	-0.0109	0.0000	0.0000	-0.2973	0.0000

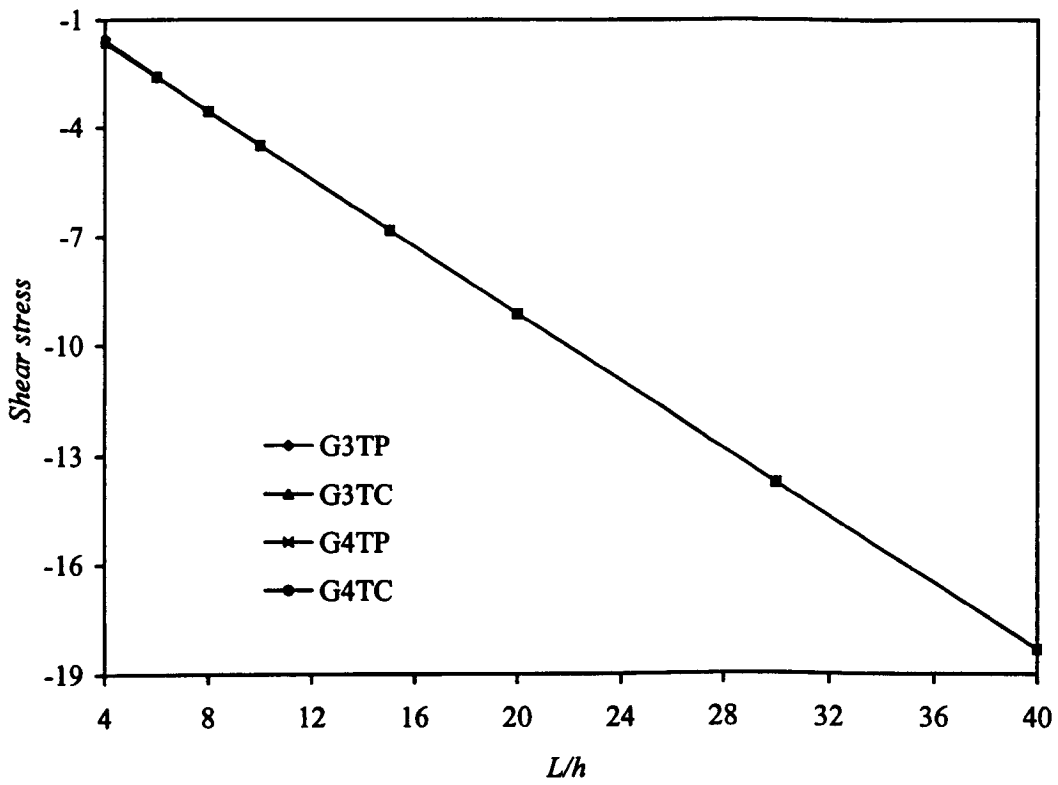


Fig 5.3-1. Shear stress,  $\tau_{xz}(L/4, -0.1h)/q_1$ , for a clamped-clamped composite beam

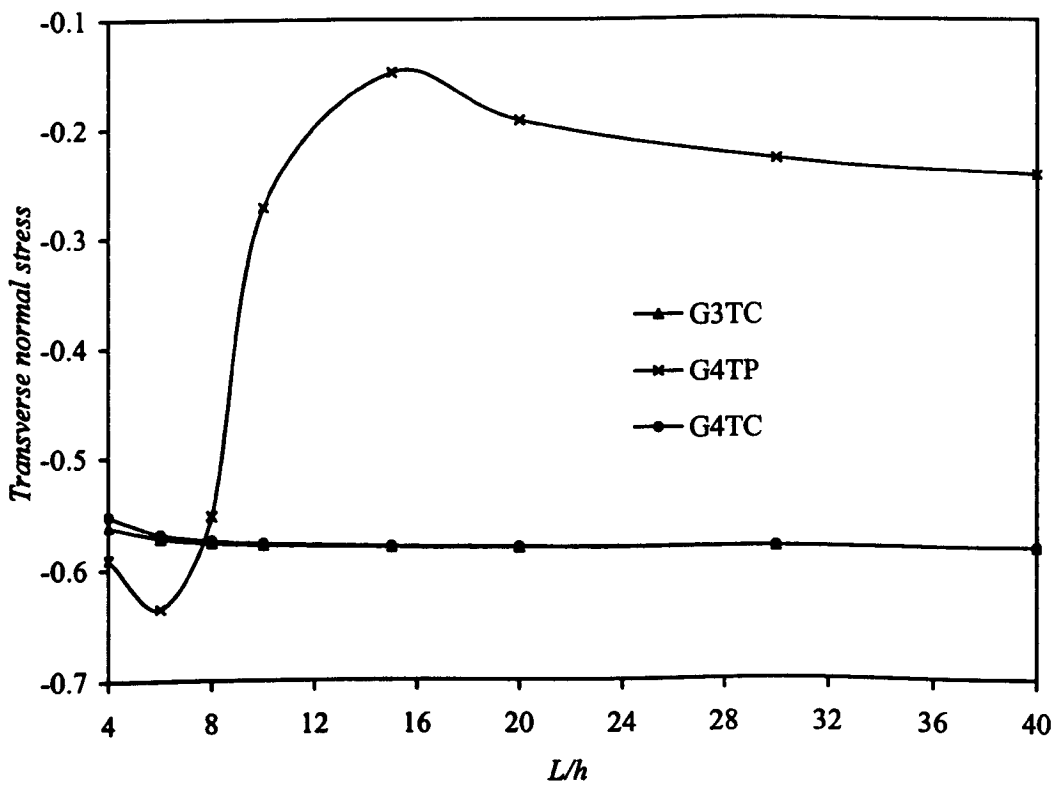


Fig 5.3-2. Transverse normal stress,  $\sigma_z(L/2, -0.1h)/q_1$ , for a clamped-clamped composite beam

Figures 5.3-1 and 5.3-2 illustrate the variations in certain transverse shear and transverse normal stress values, respectively, for clamped-clamped beams. These were obtained by means of predictor and corrector phases for both G3BT and G4BT with increasing length-to-thickness ratio,  $L/h$ . Figure 5.3-1 shows that the shear stress values based on the G3BT and the G4BT predictor and corrector phases are in good agreement and vary almost linearly with increasing length-to-thickness ratio. In a similar manner, Figure 5.3-2 illustrates the excellent agreement of the transverse normal stress values obtained through the corrector phases of both G3BT and G4BT. Note, the thinner the composite beam, the better the agreement of transverse normal stresses obtained through the corrector phase of both theories. Given that the G3BT and G4BT are approximate in the present case of stress predictions in clamped beams, the remarkable agreement between numerical results obtained through the corrector phase of the two theories appears to favour the G3BT, which uses a smaller number of degrees of freedom.

Table 5.3-2 presents corresponding transverse shear and normal stress values obtained by means of both the G3BT and the G4BT for clamped-free beams. The shear stress of the G3BT predictor phase satisfies the lateral surfaces zero shear stress boundary conditions and the interface continuity, while the G4BT shear stress predictor phase yields negligible non-zero values on the lateral surfaces and a slight discontinuity at the interface. The distributions of shear stress predictor phases of the two theories are in very good agreement, and so are distributions of the shear stress corrector phases. It is interesting to note that the difference between maximum shear stresses, at about  $z = -0.1h$ , remains smaller than 1% in either the predictor or the corrector phases of the two theories. The corrector phase of both G3BT and G4BT improve greatly their transverse normal stress distributions and both being in excellent agreement.

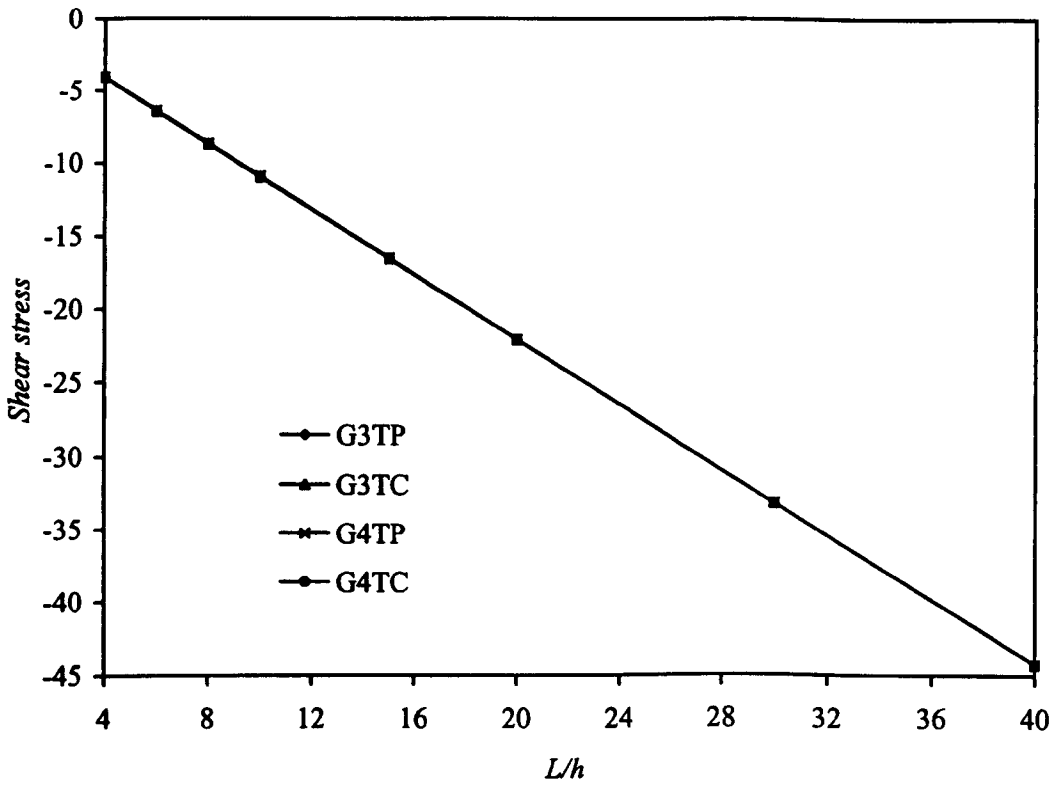


Fig 5.3-3. Shear stress,  $\tau_x(L/4, -0.1h)/q_1$ , for a clamped-free composite beam

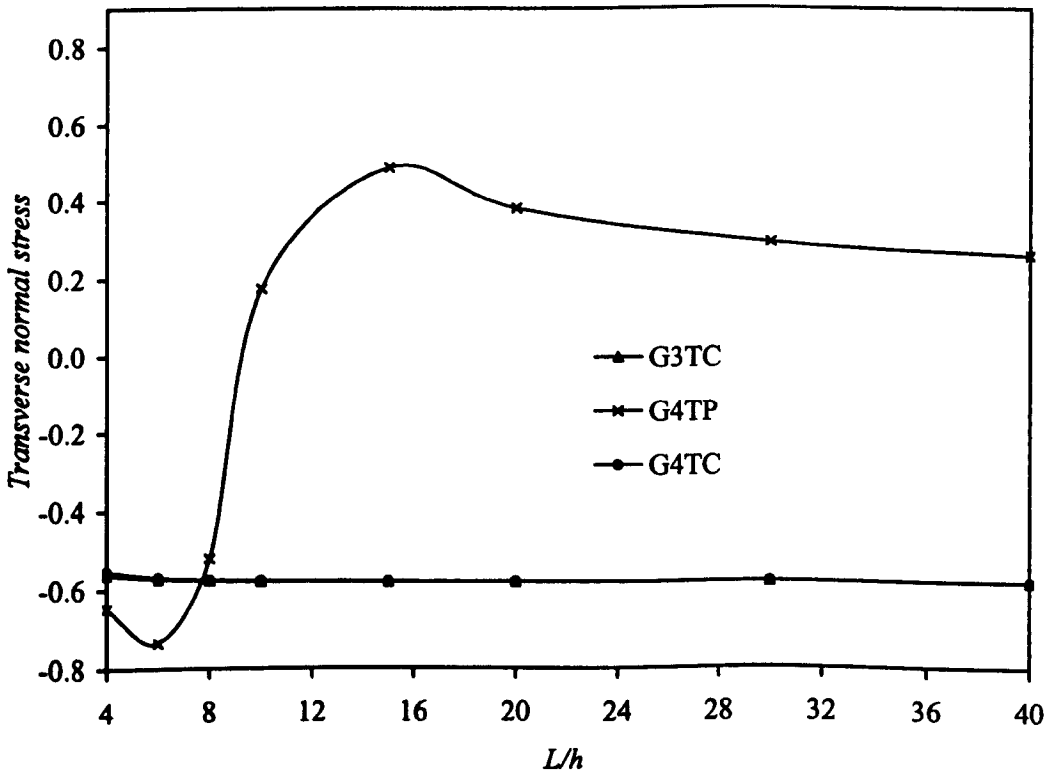


Fig 5.3-4. Transverse normal stress,  $\sigma_x(L/2, -0.1h)/q_1$ , for a clamped-free composite beam

Figures 5.3-3 and 5.3-4 illustrate the variation of certain transverse shear and transverse normal stress values, respectively, for clamped-free beams. These were obtained by means of predictor and corrector phases of both the G3BT and G4BT with increasing length-to-thickness ratio,  $L/h$ . Figure 5.3-3 shows that the shear stress values based on the G3BT and the G4BT predictor and corrector phases are in good agreement and vary almost linearly with increasing length-to-thickness ratio. In a similar manner, Figure 5.3-4 illustrates the excellent agreement of the transverse normal stress values obtained through the corrector phases of both G3BT and G4BT. The thinner the composite beam, the better the agreement of the transverse normal stresses obtained through the corrector phase of both theories. With both G3BT and G4BT being approximate for stress predictions in cantilever beams, the remarkable agreement between corresponding numerical results obtained through the corrector phase of the two theories appears to be in favour of the G3BT, which uses a smaller number of degrees of freedom.

#### **5.4 On the generalised plane strain deformations of thick anisotropic composite laminated plates**

Vel and Batra (2000) presented an analytical elasticity solution based on the Eshelby-Stroh formalism, as well as corresponding numerical results for the plane strain problem of a clamped-clamped anisotropic laminated plate subjected to a certain kind of sinusoidal lateral loading. This new development comes as a welcome addition to the well-known and considerably simpler Pagano's (1969) elasticity solution that deals with plates having both their edges simply supported.

The comparisons shown in Table 5.4-1 are for homogeneous orthotropic plates having the following material properties:

$$E_L / E_T = 25, \quad G_{LT} / E_T = 0.5, \quad G_{TT} / E_T = 0.2, \quad \nu_{LT} = \nu_{TT} = 0.25. \quad (5.4-1)$$

It should be noted that these material properties differ considerably from the ones used in [Soldatos and Watson, 1997] and, therefore, the numerical results denoted in Table 5.4-1 as 'present results' are new. Moreover, all the results presented in Table 5.4-1 are tabulated by means of the non-dimensional quantities employed in [Soldatos and Watson, 1997]. These have been found preferable to those employed in [Vel and Batra, 2000], because they show in a more clear manner the difference in order of magnitude, between the bending stress,  $\sigma_{11}$ , and the transverse stresses,  $\sigma_{13}$  or  $\sigma_{33}$ .

As far as transverse displacements and bending stresses are concerned, the numerical results provided in this study can be based only on its predictor phase. Compared with corresponding results due to Vel and Batra (2000), there appears to be excellent agreement between corresponding displacement bending stress values, particularly for  $L/h > 6$ . Given that two-dimensional plate theories are generally known to be inadequate for the accurate prediction of through thickness displacement and stress distributions, while their applicability in other types of problems (e. g. vibrations, buckling) is not unconditionally trusted for  $L/h > 6.5$  (approximate span limit of moderately thick plates), this agreement between the corresponding transverse displacement and particularly bending stress results as a very successful result of this approximate stress analysis methods is regarded.

This conclusion is further verified by the comparisons shown in Table 5.4-1 between corresponding transverse shear stress predictions. The fact that for relatively thin plates

Table 5.4-1 Comparison of corresponding numerical results for increasing values of length to thickness ratio

L/h	$\sigma_{11}(L/2, h)/q_0$			$E_1 W(L/2, h/2)/Lq_0$			$E_1 W(L/2, h)/Lq_0 - E_1 W(L/2, 0)/Lq_0$		
	Vel et al	G3BT	G4BT	Vel et al	G3BT	G4BT	Vel et al	G3BT	G4BT
		Predictor	Predictor		Predictor	Predictor		Predictor	Predictor
4	-7.8192	-7.7165	-8.4211	-0.9565	-0.8735	-0.8605	-0.1156	0	-0.1206
6	-12.7152	-12.5377	-12.9456	-1.6010	-1.5040	-1.4967	-0.0777	0	-0.0829
8	-19.1168	-18.8957	-19.1296	-2.4003	-2.2970	-2.2922	-0.0584	0	-0.0603
10	-27.1600	-26.9355	-27.0400	-3.4020	-3.2960	-3.2930	-0.0467	0	-0.0403
15	-54.8325	-54.6401	-54.6750	-7.1246	-7.0162	-7.0133	-0.0312	0	-0.0116
20	-93.5200	-93.3323	-93.4000	-13.2160	-13.1110	-13.1040	-0.0234	0	-0.0069
30	-203.9400	-203.8108	-203.9400	-35.6940	-35.5857	-35.5860	-0.0156	0	-0.0050
40	-358.5600	-358.4554	-358.5600	-77.1200	-77.0473	-77.0560	-0.0117	0	0.0039
60	-800.2800	-800.2789	-800.2800	-242.3520	-242.2477	-242.1360	-0.0078	0	-0.0027

L/h	$\sigma_{13}(L/4, h/2)/q_0$					$\sigma_{33}(L/2, h/2)/q_0$				
	Vel et al	G3BT		G4BT		Vel et al	G3BT		G4BT	
		Predictor	Corrector	Predictor	Corrector		Corrector	Predictor	Corrector	
4	-1.1060	-1.2181	-1.1876	1.2142	-1.1781	-0.490	-0.500	-0.513	-0.493	
6	-1.8066	-1.9249	-1.9172	-1.9242	-1.9164	-0.497	-0.500	-0.531	-0.498	
8	-2.5280	-2.6214	-2.6199	-2.6216	-2.6200	-0.499	-0.500	-0.515	-0.499	
10	-3.2460	-3.3107	-3.3105	-3.3110	-3.3110	-0.500	-0.500	-0.431	-0.500	
15	-4.9995	-5.0192	-5.0192	-5.0190	-5.0190	-0.500	-0.500	-0.185	-0.500	
20	-6.7120	-6.7181	-6.7181	-6.7180	-6.7180	-0.500	-0.500	-0.148	-0.500	
30	-10.1040	-10.1055	-10.1055	-10.1070	-10.1070	-0.500	-0.500	-0.159	-0.500	
40	-13.4880	-13.4847	-13.4847	-13.4880	-13.4880	-0.500	-0.500	-0.168	-0.500	
60	-20.2440	-20.2455	-20.2455	-20.2440	-20.2440	-0.500	-0.500	-0.175	-0.500	

$(L/h > 8)$  the corrector phase cannot improve any further the value of the initial prediction is a consequence of the evident fact that, for thin plates, the initially predicted stress values are already very accurate. Apart the case of the thickest plate considered ( $L/h = 4$ ), the differences between the present and the exact approach predictions are within acceptable engineering limits. Moreover, the trend of the corrector phase is to move the initially predicted transverse shear stress values towards their exact elasticity counterparts [Vel and Batra, 2000].

In contrast to the outlined observations (G4BT) both the initially predicted value of the transverse normal stress,  $\sigma_{33}$ , and the difference of the transverse displacement from the top to the bottom lateral plane appear to be relatively inaccurate, and surprisingly the inaccuracy increases with decreasing plate thickness. It should be noted however that although the exact value of  $\sigma_{33}$  remains essentially constant with decreasing plate thickness, the corresponding values of  $W$ ,  $\sigma_{11}$  and  $\tau_{13}$  increase. Hence with  $\sigma_{33}$  being essentially two to four orders of magnitude smaller than either  $W$  or  $\sigma_{11}$ , small errors in the prediction of the later quantities are substantially magnified during the prediction of the quantities measured in the last two columns of Table 5.4-1. Under these considerations, it is of particular importance to further notice that the inaccuracy detected in the initial prediction of  $\sigma_{33}$  has essentially disappeared in the corrector phase, which yields almost the exact transverse normal stress value, regardless of the value of the aspect ratio  $L/h$ . Moreover, with  $W$  remaining practically constant throughout the thickness of a thin plate, a slight inaccuracy in measuring the difference that values of  $W$  take on the lateral plate planes is not a considerable disadvantage to the approximate stress analysis method developed in [Soldatos and Watson, 1997b, c]. The zero difference of transverse displacement yielded by general three-degree-of-freedom beam theory on the top and

bottom lateral surfaces is due to the Kirchhoff hypothesis applied, and the transverse normal stress corrector phase of G3BT keeps the same value, 0.5, which is the accurate result for a thinner plate ( $L/h > 8$ ).

Finally, apart from the plate cross-sections, which are in the vicinity of the plate edges, all the stress distributions plotted in [Vel and Batra, 2000] look very similar to those obtained on the basis of our analysis. Solving however only one-dimensional (ordinary) differential equations, the order of which differs from the order of the partial differential equations solved by Vel and Batra (2000), our analysis treats the edge boundary conditions in a different, through thickness averaged, manner.

## 5.5. Conclusions

The assessment performed in this study has clearly verified the fact that the shear stress distributions obtained through the predictor phase of conventional theories (USDT [Timoshenko, 1921] and PSDT [Bickford, 1982]) are very inaccurate. Contrary to this, the predictor phase of the generalized G3BT [Soldatos and Watson, 1997a] gives practically identical shear stress results with its corrector counterpart, at least as far as simply supported beams are concerned. Hence the predictor phase of G3BT [Soldatos and Watson, 1997a] is already much more accurate than even the corrector phase of either USDT or PSDT. In dealing however with simply supported beams only, the generalized G4BT [Soldatos and Watson, 1997b, c] yields straight away the exact elasticity stress distributions and, therefore, it does not need the application of corrector phase. Unlike the shear deformable theories (USDT, PSDT or G3BT), the G4BT also yields predictions of transverse normal stress distributions, regardless of the edge boundary conditions

employed. For simply supported beams, however, such G4BT normal stress predictions are again identical to their exact elasticity counterparts.

For beams with more complicated edge boundary conditions the stress distributions obtained through the predictor phase of either G3BT or G4BT may be not as accurate as their simply supported counterparts. In their corrector phases, however, both G3BT and G4BT improve considerably their initial predictions and produce almost identical transverse shear and transverse normal stress distributions, at least for the particular material arrangement considered in this paper. This remarkable agreement of the corresponding numerical results obtained through the corrector phase of the two generalized theories appears to be in favour of G3BT, which uses a smaller number of degrees of freedom.

As compared with corresponding results due to Vel and Batra (2000), there is a very good agreement of corresponding displacement values and an excellent agreement of corresponding bending stress values, which were provided based on predictor phase of both G3BT and G4BT. These conclusions are further verified by the comparisons shown in Table 5.4-1 of corresponding transverse shear stress predictions. For relatively thin plates ( $L/h \geq 10$ ) the corrector phase does not improve at all the value of the initial prediction, is the evident fact that, for thin plates, the initially predicted shear stress values are already very accurate. Apart from the case of the thickest plate ( $L/h = 4$ ) the differences between the exact approach prediction and the predictions of the present approach do not exceed the trend of engineering acceptable error (5%). Moreover, the value of the corrector phase is to move the initially predicted transverse shear stress values towards their exact values [Vel and Batra, 2000]. Apart from plate cross-sections in the vicinity of the plate edges, all the stress distributions plotted in [Vel and Batra, 2000] look very similar to those obtained on the basis of the present analysis.

## Chapter 6

### Application of the predictor-corrector method for angle-ply composite laminates subject to mechanical loading

#### 6.1 Introduction

In this chapter the predictor-corrector method described in Chapter 4 is applied to improve the performance of transverse shear and normal stresses for angle-ply composite laminates subject to mechanical loading. General five-degree-of-freedom beam theory (G5BT, Chapter 3) is employed for this application. Formulation derivations and shape functions of G5BT were illustrated in Chapter 3. Arbitrary  $N$ -layered angle-ply laminated composite plates are considered, with  $\alpha_i$  denoting the angle that the fibres make in  $i$ th layer with  $x$ -axis.

#### 6.2 General considerations

Consider a straight elastic beam as described in chapter 3 (Figure 3.2-1) with external transverse load,  $q$ , as considered in Chapter 5 (Equation 5.2-1) taking the following general form (Equation 3.2-1),

$$q(x) = q_m \sin(p_m x), \quad p_m = m\pi / L, \quad m = 1, 2, \dots \quad (6.2-1)$$

which acts normally and downwards on its top lateral plane,  $z = h/2$ . The integer value  $m$  that characterises the particular harmonic employed in the Fourier sine-series expansion of any loading distribution applied on the top lateral plane (Equation 6.2-1) is chosen as 1. For the static analysis in plain strain state all these quantities are independent of the  $y$  parameter and, therefore, all their partial derivatives with respect to  $y$  are zero.

The orthotropic material used in all of the applications has the following elastic properties:

$$E_L / E_T = 25, \quad G_{LT} / E_T = 0.5, \quad G_{TT} / E_T = 0.2, \quad \nu_{LT} = \nu_{TT} = 0.25, \quad (6.2-2)$$

except of cases dealing with varying stiffness ratio,  $E_L / E_T$ . The plate thickness is mainly determined by the ratio  $L/h = 10$  except of cases dealing with varying aspect ratio,  $L/h$ . This ( $L/h = 10$ ) characterises a moderate thick plate, and in conjunction with the high value of the stiffness ratio  $E_L/E_T$ , is considered to be an adequate test of the reliability of both the theoretical model and the method. Some cases of thin and thick, stiff and soft, small and large angled-ply beams have however also been examined to find the limitation of the general five-degree-of-freedom beam theory tested. All the numerical results shown in what follows are presented by means of the following non-dimensional parameters:

$$\bar{\tau}_{xz} = \tau_{xz} h / q_m L, \quad \bar{\sigma}_z = \sigma_z / q_m. \quad (6.2-3)$$

In this chapter, the shear stress  $\tau_{xz}$  percentage error (in the corresponding paragraph described for tables 6.3-3 and 6.3-4) between predictor and corrector phases is defined as follows:

$$\left| \frac{\tau_{xz}^{(P)} - \tau_{xz}^{(C)}}{\tau_{xz}^{(P)}} \right| * 100, \quad (6.2-4)$$

where  $\tau_{xz}^{(P)}$  and  $\tau_{xz}^{(C)}$  represent shear stress in predictor phase and corrector phase, respectively. For notation convenience, the general five-degree-of-freedom beam theory is written as G5BT.

### 6.3 Numerical results and discussion

When deriving the shape functions of G5BT predictor phase, for simply supported arbitrary layered laminates [Shu and Soldatos, 2000], the shear stress,  $\tau_{xz}$ , is required to be zero at the top and bottom lateral surfaces and continuity at the inter-laminar material interfaces. As a consequence, for a simply supported beam, when one changes the number of layers, angles of fibre alignment, span or stiffness ratio, the shear stress  $\tau_{xz}$  of predictor phase is always required to satisfy the applied conditions, i.e., the top and bottom lateral surface zero shear stress and interface continuity. Its corrector phase is almost always identical to its predictor phase given its high accuracy. Hence the shear stress  $\tau_{xz}$  corrector phase is not needed. For simply supported homogenous beam, the accuracy of G5BT predictor phase was assessed by comparing the exact elasticity solution [Pagano, 1970] [Ren, 1986], and tabulated by Shu and Soldatos, [2000]. So, corrections of the transverse shear and normal stresses for simply supported beams will not be presented in this chapter. Only the clamped-clamped and clamped-free beams are chosen as cases to show the results of the predictor-corrector method applied to the G5BT. In addition, given the fact that the

five-degree-of-freedom beam theory uses the properly reduced stiffness, it is not able to predict the transverse normal stress  $\sigma_z$  in predictor phase, but only through the corrector phase.

In this chapter, three-layered laminates with the thickness ratios of  $h_1 / h_2 / h_3 / h = 0.3/0.4/0.3/1.0$  and the angles of  $\alpha_1 = -\alpha$ ,  $\alpha_2 = \alpha$  and  $\alpha_3 = -\alpha$  counted from the bottom layer to the top layer have been selected to attempt to magnify the effects of possible discontinuity of the inter-laminar stresses. Here,  $h_1, h_2, h_3$  and  $h$  are the thickness of bottom layer, middle layer, top layer and the beam thickness,  $\alpha_1, \alpha_2$  and  $\alpha_3$  present angles that bottom layer fibres, middle layer fibres and top layer fibres make with  $x$  axis, respectively. It could be mentioned that, in the special case of two-layered antisymmetric lay-up with equal thickness and the angles of  $-\alpha/\alpha$  which was employed in [Shu and Soldatos, 2000] for both clamped-clamped and clamped-free beams, the transverse shear stress  $\tau_{xz}$  satisfies both top, bottom lateral plane zero shear stress boundary conditions, and inter-laminar interface transverse shear stress continuity. The transverse shear stress corrector phase and predictor phase, in such specific lay-up, are in very good agreement except at the vicinity of clamped and free edges. Hence this particular choice can not show clearly the improvement of transverse shear stress in corrector phase.

Table 6.3-1 presents numerical values of normalised transverse normal and shear stresses at the selected points, which were evenly distributed through the beam length and thickness ( $\alpha = 30^\circ$ ). It should be noted that, due to the symmetries of the problem, the shear stress  $\bar{\tau}_{xz}$  and transverse normal stress  $\bar{\sigma}_z$  at  $x/L$  and  $1-x/L$  have identical through-thickness distributions. Moreover, due to the fact that the shear deformable beam theories completely ignore the effects of transverse normal deformation, the through-thickness transverse shear stress predictions,  $\bar{\tau}_{xz}$ , are also symmetric with respect to the plate middle

Table 6.3-1. Transverse shear and normal stress predictions for three-layered clamped-clamped beam ( $\alpha = 30^\circ$ )

	$z/h$	$x/L=0.0$	0.1	0.2	0.3	0.4	0.5
$\bar{\tau}_{xz}$ Predictor	0.5	0	0	0	0	0	0
	0.4	0	-0.1534	-0.1408	-0.1042	-0.0551	0
	0.3	0	-0.2621	-0.2406	-0.1780	-0.0941	0
	0.2	0	-0.3300	-0.3028	-0.2240	-0.1185	0
	0.2	0	-0.3800	-0.3206	-0.2298	-0.1202	0
	0.1	0	-0.4404	-0.3762	-0.2710	-0.1420	0
	0	0	-0.4603	-0.3946	-0.2846	-0.1492	0
$\bar{\tau}_{xz}$ Corrector	0.5	0	0	0	0	0	0
	0.4	-1.1370	-0.1998	-0.1468	-0.1059	-0.0556	0
	0.3	-0.9642	-0.2949	-0.2433	-0.1786	-0.0943	0
	0.2	0.0624	-0.3077	-0.2955	-0.2216	-0.1178	0
	0.2	0.0624	-0.3077	-0.2955	-0.2216	-0.1178	0
	0.1	0.4131	-0.4350	-0.3782	-0.2717	-0.1422	0
	0	0.5576	-0.4760	-0.4053	-0.2882	-0.1503	0
$\bar{\sigma}_z$ Corrector	0.5	0.0000	-0.3090	-0.5878	-0.8090	-0.9511	-1.0000
	0.4	2.1412	-0.2362	-0.5675	-0.7846	-0.9227	-0.9702
	0.3	5.3610	-0.1272	-0.5215	-0.7224	-0.8490	-0.8926
	0.2	6.1687	-0.1041	-0.4681	-0.6373	-0.7457	-0.7834
	0.2	6.1687	-0.1041	-0.4681	-0.6373	-0.7457	-0.7834
	0.1	3.8279	-0.1369	-0.3942	-0.5300	-0.6188	-0.6498
	0	0.0000	-0.1545	-0.2939	-0.4045	-0.4755	-0.5000
	-0.1	-3.8279	-0.1721	-0.1936	-0.2790	-0.3323	-0.3502
	-0.2	-6.1687	-0.2049	-0.1196	-0.1717	-0.2053	-0.2166
	-0.2	-6.1687	-0.2049	-0.1196	-0.1717	-0.2053	-0.2166
	-0.3	-5.3610	-0.1818	-0.0663	-0.0867	-0.1020	-0.1074
-0.4	-2.1412	-0.0728	-0.0202	-0.0244	-0.0284	-0.0298	
-0.5	0	0	0	0	0	0	

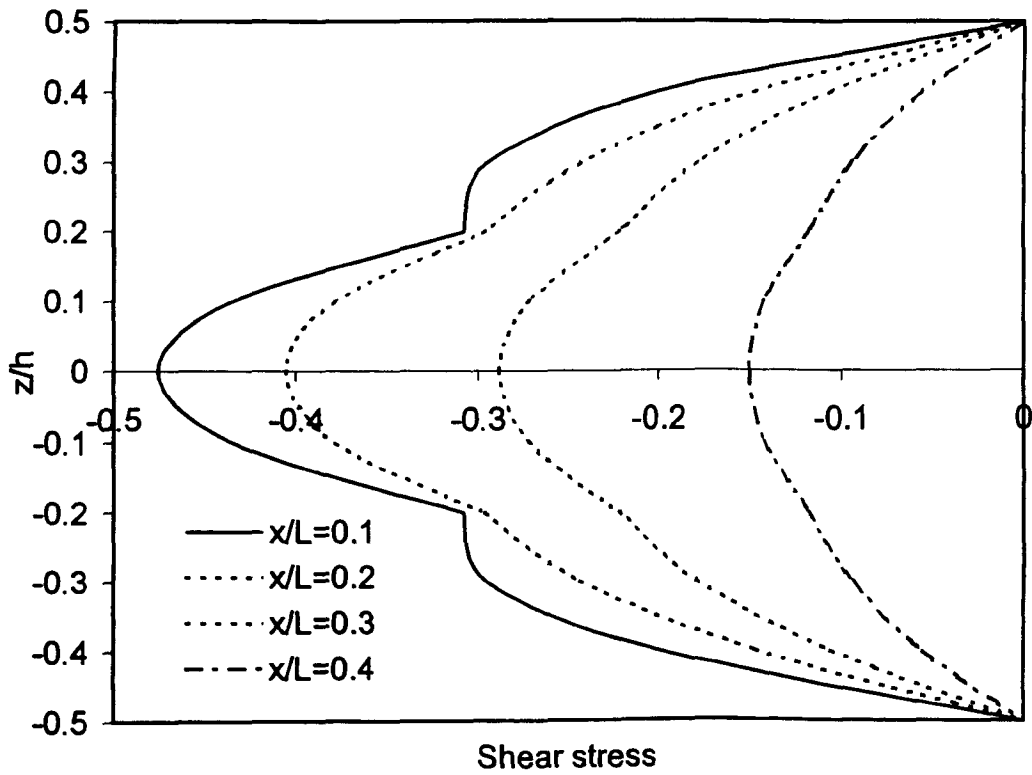


Figure 6.3-1. Normalized shear stress distributions,  $\bar{\tau}_{xz}$ , in corrector phase for a CC beam

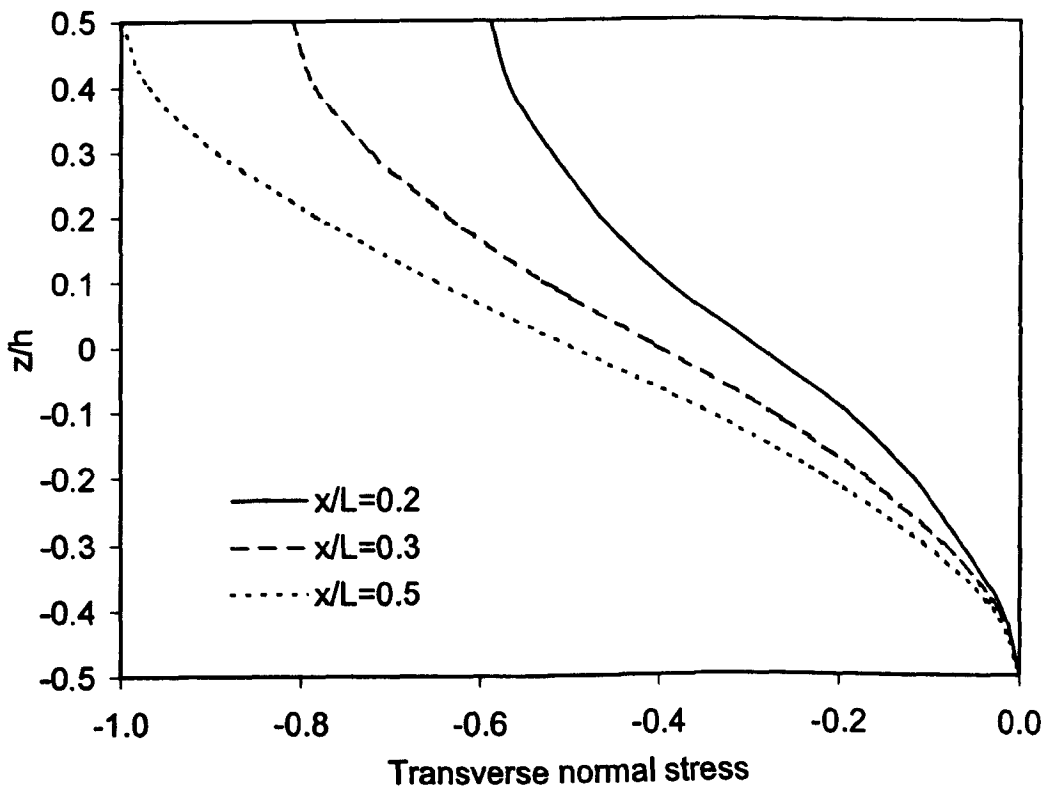


Figure 6.3-2. Normalized transverse normal stress distributions,  $\bar{\sigma}_z$ , in corrector phase for a CC beam

plane. Hence, the numerical results for  $\bar{\tau}_{xz}$  are only presented for the left and top quarter of the beam and the numerical results for  $\bar{\sigma}_z$  are only presented for the left half of the clamped-clamped beam. In corrector phase, the observations may be detailed with regard to the corresponding through-thickness distributions of the shear stress  $\bar{\tau}_{xz}$  (Figure 6.3-1) and transverse normal stress (Figure 6.3-2). At the middle cross-section of the beam,  $x = L/2$ , it yields the point by point zero shear stress and large variations of the transverse shear and normal stresses at the clamped edge (these edge stress distributions are not plotted in figures). As has also been pointed out in [Soldatos and Watson, 1997a, b] and [Shu and Soldatos, 2000], although the magnitude of the  $\bar{\tau}_{xz}$  distribution is naturally increasing when approaching the clamped edge, the predictor phase erroneously predicts that  $\bar{\tau}_{xz}$  suddenly becomes zero at that clamped edge (Table 6.3-1). This slight drawback, which is corrected and clearly illustrated by the results of the corrector phase of transverse shear stress  $\bar{\tau}_{xz}$ , is apparently due to the limitations of the G5BT. As was initially detailed in [Soldatos and Watson, 1997a] and verified afterwards [Soldatos and Watson, 1997b, c] [Shu and Soldatos, 2000], an apparent way to improve this drawback, which might be considered as a more accurate theory, is to replace G5BT with a theory that also accounts for transverse normal deformation effects. Such a change of the beam theory which, for the cylindrical bending problem of angle-ply laminated beam, would involve the appropriate determination of at least three inter-related shape functions, is beyond the scope of the present study.

Table 6.3-2 presents numerical values of normalised transverse shear and normal stress distributions for a three-layered clamped-free beam ( $\alpha = 30^\circ$ ). The shear stress  $\bar{\tau}_{xz}$  distributions occur again in symmetric form with respect to the beam middle plane and, hence, the corresponding numerical results are only presented for the top half of the beam.

Table 6.3-2. Transverse shear and normal stress predictions for three-layered clamped-free beam ( $\alpha = 30^\circ$ )

	$z/h$	$x/L=0.0$	0.2	0.4	0.6	0.8	1.0
$\bar{\tau}_{xz}$ Predictor	0.5	0	0	0	0	0	0
	0.4	0	-0.3200	-0.2387	-0.1285	-0.0387	-0.0044
	0.3	0	-0.5465	-0.4076	-0.2194	-0.0660	-0.0074
	0.2	0	-0.6880	-0.5129	-0.2761	-0.0831	-0.0093
	0.2	0	-0.7131	-0.5050	-0.2645	-0.0712	0.0026
	0.1	0	-0.8396	-0.5995	-0.3155	-0.0866	0.0008
	0	0	-0.8812	-0.6306	-0.3322	-0.0916	0.0002
	$\bar{\tau}_{xz}$ Corrector	0.5	0	0	0	0	0
0.4		-2.2740	-0.3201	-0.2276	-0.1164	-0.0265	0.0078
0.3		-1.9284	-0.5434	-0.3992	-0.2106	-0.0572	0.0014
0.2		0.1247	-0.6781	-0.5167	-0.2813	-0.0885	-0.0147
0.2		0.1247	-0.6781	-0.5167	-0.2813	-0.0885	-0.0147
0.1		0.8262	-0.8453	-0.6017	-0.3172	-0.0883	-0.0009
0		1.1151	-0.9005	-0.6299	-0.3293	-0.0885	0.0034
$\bar{\sigma}_z$ Corrector		0.5	0.0000	-0.5878	-0.9511	-0.9511	-0.5878
	0.4	4.2997	-0.5646	-0.9226	-0.9228	-0.5703	0
	0.3	10.7629	-0.5184	-0.8491	-0.8489	-0.5246	0
	0.2	12.3765	-0.4774	-0.7471	-0.7445	-0.4599	0
	0.2	12.3765	-0.4774	-0.7471	-0.7445	-0.4599	0
	0.1	7.6748	-0.4084	-0.6205	-0.6173	-0.3813	0
	0	0.0000	-0.2939	-0.4755	-0.4755	-0.2939	0
	-0.1	-7.6748	-0.1794	-0.3306	-0.3338	-0.2065	0
	-0.2	-12.3765	-0.1104	-0.2039	-0.2066	-0.1278	0
	-0.2	-12.3765	-0.1104	-0.2039	-0.2066	-0.1278	0
	-0.3	-10.7629	-0.0694	-0.1019	-0.1022	-0.0631	0
	-0.4	-4.2997	-0.0231	-0.0285	-0.0283	-0.0175	0
	-0.5	0	0	0	0	0	0

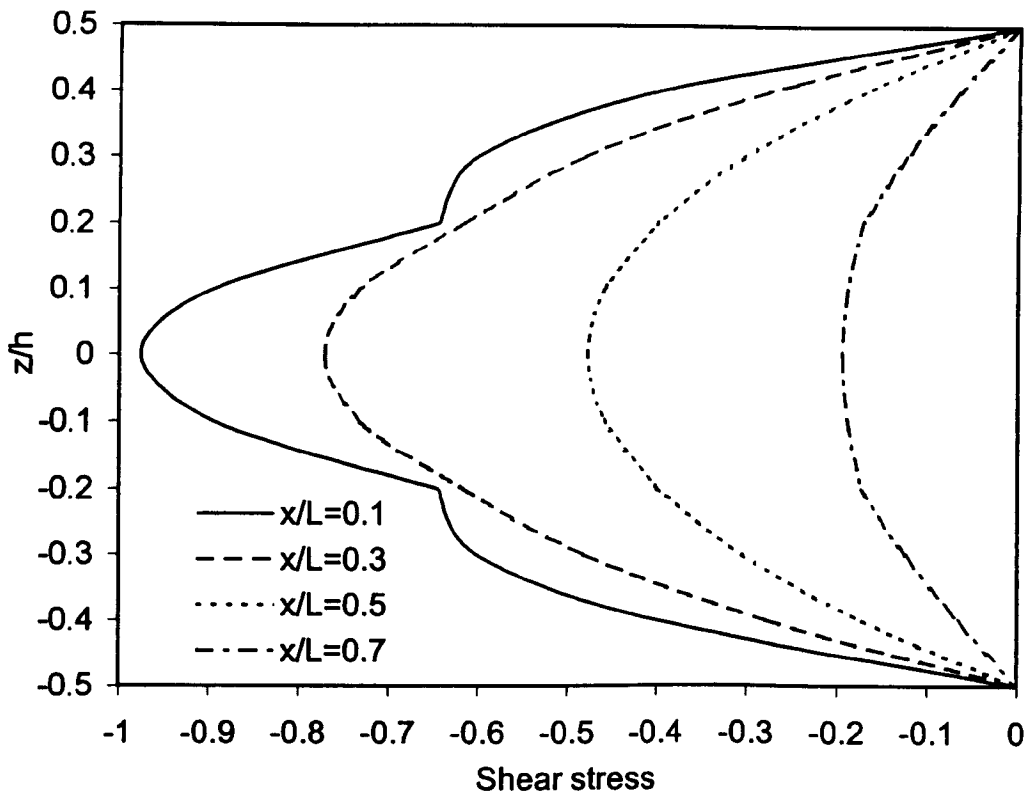


Figure 6.3-3. Normalized shear stress distributions,  $\bar{\tau}_{xz}$ , in corrector phase for a CF beam

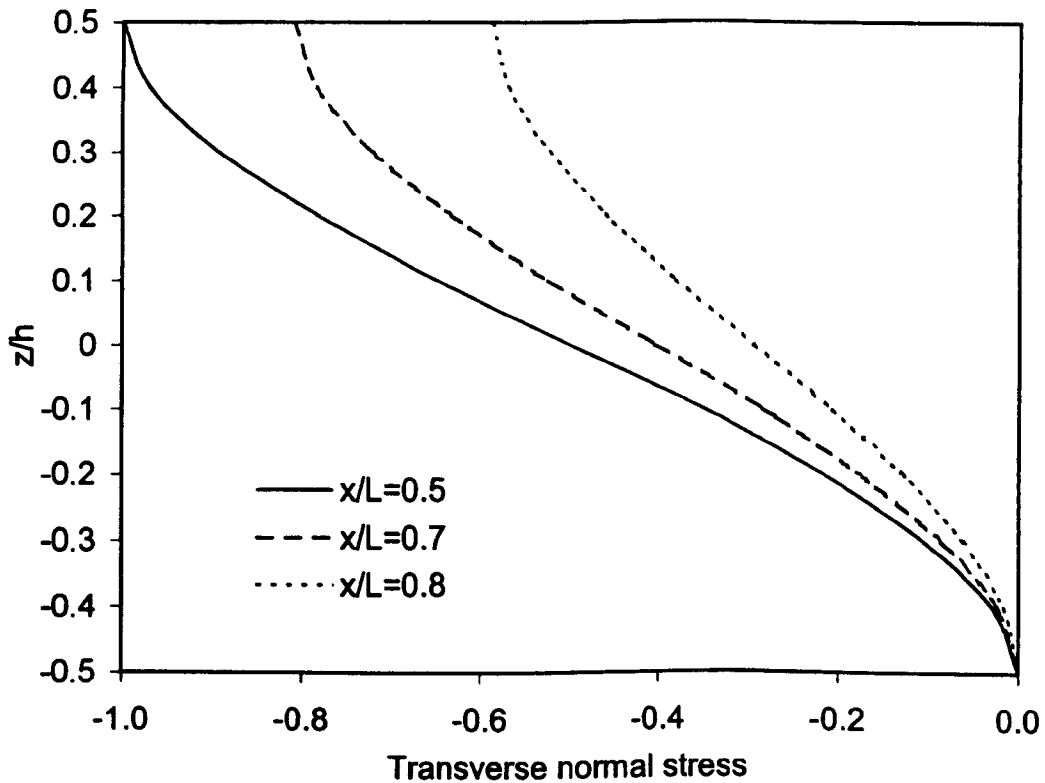


Figure 6.3-4. Normalized transverse normal stress distributions,  $\bar{\sigma}_y$ , in corrector phase for a CF beam

In this case, the associated complete through-thickness distributions of transverse shear and normal stresses obtained in the corrector phase are shown graphically in figures 6.3-3 and 6.3-4, respectively, using selected  $x$ -coordinate values across the beam length. Shear stresses vary rapidly at the vicinity of the free edge of an angle-ply laminated clamped-free beam in both predictor and corrector phases. They become negligible at  $x/L = 1.0$ , to approximately meet the boundary conditions. In more detail, the transverse shear and normal stresses predicted in corrector phase are very large on the clamped edge ( $x = 0$ ), on which its value is almost 2 times the value that it takes at the edge of the corresponding, less flexible, clamped-clamped beam (see Tables 6.3-1 and 6.3-2).

Table 6.3-3 presents the variation of shear stress  $\bar{\tau}_{xz}$  in both predictor and corrector phases with varying angles, span and stiffness ratios for clamped-clamped beam. It is noted that, at the points,  $z = 0$ , of selected corresponding cross-sections, the transverse shear stress distributions are close to maximum values (Table 6.3-1). The point  $(0.25L, 0)$  on the middle lateral plane is selected to investigate variations of the shear stress  $\bar{\tau}_{xz}$  with varying angles, span and stiffness ratios. For the purpose of observing the influence of the interface shear stress discontinuity onto the maximum shear stress corrector phase, the point,  $(x = 0.25L, z = 0.2h)$ , which is allocated at the interface of the corresponding cross-sections is selected to show the results. For varying angles, span and stiffness ratios, Table 6.3-3 shows that at the point  $(0.25L, 0)$ , the correction percentage of the shear stress is always less than about 3%. In more detail, when one keeps  $L/h = 10$ ,  $E_L/E_T = 25$ , and then changes the angles  $\alpha$  of fibres, the correction percentage of the shear stress is always less than about 2%. At  $\alpha = 75^\circ$ , the shear stress predictions of predictor and corrector phases are practically identical. At  $\alpha = 30^\circ$ ,  $E_L/E_T = 25$  and  $L/h = 8$ , the correction

Table 6.3-3 Normalised transverse shear parameters,  $\bar{\tau}_{xz}(0.25L, z)$ , of three-layered clamped-clamped beam

$\alpha$	$L/h$	$E_I/E_T$	Predictor	Corrector	Predictor	Predictor	Corrector
			$z=0$	$z=0$	$z=0.2h+0^+$	$z=0.2h+0^-$	$z=0.2h$
15°	10	25	-0.3349	-0.3370	-0.2780	-0.2793	-0.2760
30°			-0.3434	-0.3497	-0.2677	-0.2779	-0.2635
45°			-0.3464	-0.3523	-0.2639	-0.2809	-0.2640
60°			-0.3421	-0.3437	-0.2723	-0.2839	-0.2756
75°			-0.3372	-0.3372	-0.2829	-0.2834	-0.2831
30°	4	25	-0.3451	-0.3536	-0.2175	-0.2516	-0.1994
	8		-0.3462	-0.3565	-0.2590	-0.2760	-0.2519
	15		-0.3397	-0.3414	-0.2773	-0.2800	-0.2767
	25		-0.3381	-0.3382	-0.2817	-0.2819	-0.2817
	50		-0.3377	-0.3377	-0.2831	-0.2831	-0.2831
30°	10	5	-0.3376	-0.3378	-0.2813	-0.2825	-0.2814
		10	-0.3389	-0.3403	-0.2778	-0.2812	-0.2773
		20	-0.3419	-0.3465	-0.2710	-0.2790	-0.2682
		30	-0.3447	-0.3528	-0.2646	-0.2769	-0.2590
		40	-0.3472	-0.3583	-0.2587	-0.2748	-0.2502

Table 6.3-4 Normalised transverse shear parameters,  $\bar{\tau}_{xz}(0.75L, z)$ , of three-layered clamped-free beam

$\alpha$	$L/h$	$E_I/E_T$	Predictor	Corrector	Predictor	Predictor	Corrector
			$z=0$	$z=0$	$z=0.2h+0^+$	$z=0.2h+0^-$	$z=0.2h$
15°	10	25	-0.1406	-0.1431	-0.1189	-0.1168	-0.1225
30°			-0.1407	-0.1375	-0.1225	-0.1106	-0.1278
45°			-0.1396	-0.1354	-0.1272	-0.1077	-0.1270
60°			-0.1385	-0.1380	-0.1261	-0.1112	-0.1215
75°			-0.1396	-0.1404	-0.1184	-0.1170	-0.1179
30°	4	25	-0.1454	-0.1461	-0.1288	-0.0850	-0.1536
	8		-0.1411	-0.1369	-0.1245	-0.1069	-0.1327
	15		-0.1402	-0.1386	-0.1199	-0.1144	-0.1223
	25		-0.1400	-0.1394	-0.1184	-0.1163	-0.1193
	50		-0.1399	-0.1397	-0.1177	-0.1172	-0.1179
30°	10	5	-0.1396	-0.1402	-0.1195	-0.1162	-0.1190
		10	-0.1398	-0.1395	-0.1207	-0.1146	-0.1213
		20	-0.1404	-0.1381	-0.1220	-0.1119	-0.1257
		30	-0.1410	-0.1369	-0.1229	-0.1093	-0.1299
		40	-0.1416	-0.1359	-0.1235	-0.1068	-0.1337

percentage becomes as big as about 2.5%, but when the beam gets thinner, the agreement of shear stress predictor and corrector phases gets better. When the beam is as thin as  $L/h = 50$ , the shear stress predictions of predictor and corrector phases are practically identical. At  $L/h = 10$ ,  $\alpha = 30^\circ$  and  $E_L/E_T = 40$ , the correction percentage is about 3%, then as the stiffness ratio becomes smaller, the agreement of shear stress predictor and corrector phases improves. Similar observations can be obtained at the point,  $(x=0.25L, z = 0.2h)$ , which is located at the interface of the same cross section. In Table 6.3-3,  $z = 0.2h + 0^+$  denotes the bottom lateral surface of the upper layer, while  $z = 0.2h + 0^-$  denotes at the top lateral surface of the lower layer at the material inter-laminar interface. Table 6.3-3 shows also clearly that, at the material interface, the shear stress corrected is not certainly to be evaluated between those two values originally predicted at the bottom of the upper layer and the top of lower layer. Fixing the span ratio at 10, stiffness ratio at 25 and changing the material fibre aligning orientation, the correction percentage at the interface is always less than 6%. The thinner the beam, the better the agreement of the shear stress predictor and corrector phases at the material interface. For  $L/h = 50$  ( $\alpha = 30^\circ, E_L/E_T = 25$ ), the shear stress predictor and corrector phases are almost identical. The smaller the stiffness ratio, the better the agreement of the shear stress predictor and corrector phases at material interface. For  $E_L/E_T = 5$  ( $\alpha = 30^\circ, L/h = 10$ ), the differences between them are negligibly small. However, at the  $z = 0$ , the fact that the shear stress correction percentage is larger at the interface does not significantly affect the good agreement of maximum shear stress predictor and corrector phases. Such as when  $\alpha = 30^\circ$ ,  $E_L/E_T = 25$  and  $L/h = 4$ , at  $z = 0.2h$ , the correction percentage of shear stress is about 20% at the material interface; at the  $z = 0$ , the maximum shear stress correction percentage is about 2.5%.

Table 6.3-4 presents analogous results for corresponding clamped-free beams. At the points,  $z = 0$ , of selected corresponding cross-sections, the transverse shear stress distributions near maximum values (Table 6.3-2). In order to show the influence from the free edge, the points  $(0.75L, 0)$  and  $(0.75L, 0.2h)$ , which are located near the free edge side, are chosen to illustrate variations of the shear stress  $\bar{\tau}_{xz}$  with varying angles, span and stiffness ratio. Given these variations, Table 6.3-4 shows that at the point  $(0.75L, 0)$ , the correction percentage of the shear stress is always less than about 4%. In more detail, when one fixes  $L/h = 10$  and  $E_L/E_T = 25$ , and then changes the angles  $\alpha$  of fibres orientation, the correction percentage of the shear stress is always less than about 3%. Once more, Table 6.3-4 shows that, in the same cross-section, the big shear stress correction percentage at the interface does not significantly affect the good agreement of maximum shear stress predictor and corrector phases. For example, when  $\alpha = 30^\circ$ ,  $E_L/E_T = 25$  and  $L/h = 4$ , at  $z = 0.2h$ , the correction percentage of shear stress is as large as 80% at the material interface; at  $z = 0$ , the maximum shear stress correction percentage is as small as 0.5%.

#### 6.4 Conclusions

For simply supported beam, the  $\tau_{xz}$  corrector phase is always practically identical to its predictor phase. Hence the  $\tau_{xz}$  corrector phase for simply supported composite beam is not needed. In addition, given the fact that the five-degree-of-freedom beam theory uses the properly reduced stiffness, it is not able to predict the transverse normal stress  $\sigma_z$  in predictor phase, but only through the corrector phase. G5BT predictor phase yields exactly the point-by-point zero but non-realistic shear stress distribution at the clamped edge. For both the clamped-clamped and clamped-free beams, the shear stress  $\tau_{xz}$  predictor phase

satisfies both the top and bottom lateral plane boundary conditions, but there is a discontinuity at the material interface. Thus, both transverse shear and normal stresses predictions needs to improve.

When varying angles, span and stiffness ratio at the selected points, the correction percentage of the maximum shear stress always remain less than about 3% and 4% for the clamped-clamped beam and clamped-free beam, respectively. The larger shear stress correction percentage at the interface does not significantly affect the good agreement between maximum shear stress predictor and corrector phases predicted at beam middle plane,  $z = 0$ . As expected, the agreements of predictor and corrector phases at both the material interface and middle plane get better when the beam gets thinner or as the stiffness ratio becomes smaller. In general, the agreement of shear stress corrector and predictor phases is better in clamped-clamped than in clamped-free beams.

## **Chapter 7**

### **Application of general four-degree-of-freedom beam theory (G4BT) for cross-ply laminated composite beams subjected to thermal loading**

#### **7.1 Introduction**

A method for accurate strain-stress analysis in composite laminates subject to thermal loading is proposed (Sections 3.4) (Section 3.6-5). The general four-degree-of-freedom beam theory (G4T) [Soldatos and Watson, 1997] is employed in developing this model that it is accompanied with an appropriate set of through-thickness shape functions. A predictor-corrector method (Chapter 4) is used for the improvement of transverse shear and normal stresses and further verification of the reliability of the new proposed method.

The method produces an excellent choice of both shape functions involved, and it leads to the exact elasticity solution presented by Murakami [1993] subject to thermal loading for simply supported infinite strips. By means of those shape functions, exact through-thickness displacement and stress distributions are "extracted" from the well-known elasticity solution and are appropriately "fitted" into the corresponding distributions assumed for the development of general four-degree-of-freedom beam theory.

#### **7.2 General considerations**

Consider an elastic beam (Figure 3.2-1) in plane strain state. Assume next that the

thermal deformation of the beam is due to the non-uniform temperature field (Equation 3.2-2):

$$\Delta T(x, z) = (T_0 + T_1 z) \sin(p_m x), \quad p_m = m\pi / L, \quad (m = 1, 2, \dots). \quad (7.2-1)$$

This can be understood as being a simple harmonic in a Fourier sine-series expansion of any relevant temperature field satisfying Fourier's Heat Conduction Law [Reddy, 1997]. The integer value that characterises the particular harmonic employed in the Fourier sine-series expansion of any thermal expansion applied is taken as  $m = 1$  (Equation 7.2-1).

The orthotropic material in all of the applications considered has the following elastic properties:

$$E_L / E_T = 25, \quad G_{TT} / E_T = 0.5, \quad \nu_{LT} = 0.5, \quad \nu_{TT} = 0.25 \quad (7.2-2)$$

and the coefficients of thermal expansions

$$\alpha_L / \alpha_T = 0.1 \quad (7.2-3)$$

where the subscripts  $_L$  and  $_T$  denote properties associated with the longitudinal and the transverse fibre direction, respectively. The large differences in material properties and coefficients of conductivity along longitudinal and transverse fibre directions have been chosen in an attempt to magnify their effects in laminates and to quantitatively estimate the extent to which it can affect the accuracy of the results obtained.

For the purpose of showing clearly the corresponding results that are induced by either constant part,  $T_0 \sin(m\pi x/L)$ , or linear variation,  $T_1 z \sin(m\pi x/L)$ , along  $z$ , numerical values will be illustrated, individually. All the numerical results shown are presented in terms of the following non-dimensional parameters:

(a) For numerical results induced by  $\Delta T(x, z) = T_0 \sin(p_m x)$  (Equation 7.2-1),

$$\begin{aligned} \bar{U} &= \frac{U}{\alpha_L T_0 L}, & \bar{W} &= \frac{W}{\alpha_L T_0 L}, \\ \bar{\sigma}_x &= \frac{\sigma_x}{E_T \alpha_L T_0}, & \bar{\sigma}_z &= \frac{\sigma_z}{E_T \alpha_L T_0}, & \bar{\tau}_{xz} &= \frac{\tau_{xz}}{E_T \alpha_L T_0}, \end{aligned} \quad (7.2-4)$$

(b) For numerical results induced by  $\Delta T(x, z) = T_1 z \sin(p_m x)$  (Equation 7.2-1),

$$\begin{aligned} \bar{U} &= \frac{10 U}{\alpha_L T_1 L^2}, & \bar{W} &= \frac{10 W}{\alpha_L T_1 L^2}, \\ \bar{\sigma}_x &= \frac{10 \sigma_x}{E_T \alpha_L T_1 L}, & \bar{\sigma}_z &= \frac{10 \sigma_z}{E_T \alpha_L T_1 L}, & \bar{\tau}_{xz} &= \frac{10 \tau_{xz}}{E_T \alpha_L T_1 L} \end{aligned} \quad (7.2-5)$$

### 7.3 Numerical results and discussion

A two-layered anti-symmetric cross-ply laminated beam, with equal-thickness and fibres in the bottom layer aligned along the  $x$ -axis ( $0^\circ/90^\circ$ ), is now considered. The beam thickness considered in all cases is determined by the ratio  $L/h = 10$ .

Tables 7.3-1 and 7.3-2 present numerical values of normalized displacement and stress distributions caused by uniform temperature variation for simply supported beam. Corresponding figures of in-plane displacement, in-plane bending stress and transverse

Table 7.3-1 Normalised displacements given  $T_0 \sin p_1 x$  for simply supported beam

		$x/L$					
$z/h$		0.0	0.1	0.2	0.3	0.4	0.5
$\bar{U}$	0.5	-2.3229	-2.2092	-1.8793	-1.3654	-0.7178	0
	0.4	-2.0642	-1.9632	-1.6700	-1.2133	-0.6379	0
	0.3	-1.8005	-1.7124	-1.4566	-1.0583	-0.5564	0
	0.2	-1.5304	-1.4555	-1.2382	-0.8996	-0.4729	0
	0.1	-1.2528	-1.1915	-1.0136	-0.7364	-0.3871	0
	0	-0.9664	-0.9191	-0.7818	-0.5680	-0.2986	0
	0	-0.9664	-0.9191	-0.7818	-0.5680	-0.2986	0
	-0.1	-0.7249	-0.6895	-0.5865	-0.4261	-0.2240	0
	-0.2	-0.5068	-0.4820	-0.4100	-0.2979	-0.1566	0
	-0.3	-0.3011	-0.2864	-0.2436	-0.1770	-0.0931	0
	-0.4	-0.0978	-0.0930	-0.0791	-0.0575	-0.0302	0
	-0.5	0.1133	0.1077	0.0916	0.0666	0.0350	0
$\bar{W}$	0.5	0	2.5236	4.8001	6.6068	7.7667	8.1664
	0.4	0	2.4805	4.7183	6.4942	7.6343	8.0272
	0.3	0	2.4369	4.6352	6.3798	7.4999	7.8859
	0.2	0	2.3925	4.5508	6.2637	7.3634	7.7423
	0.1	0	2.3474	4.4651	6.1456	7.2246	7.5964
	0	0	2.3016	4.3778	6.0256	7.0835	7.4480
	0	0	2.3016	4.3778	6.0256	7.0835	7.4480
	-0.1	0	2.2720	4.3216	5.9481	6.9925	7.3523
	-0.2	0	2.2417	4.2640	5.8689	6.8993	7.2544
	-0.3	0	2.2109	4.2054	5.7882	6.8045	7.1546
	-0.4	0	2.1796	4.1458	5.7062	6.7080	7.0532
	-0.5	0	2.1477	4.0851	5.6226	6.6098	6.9500

Table 7.3-2 Normalised stresses given  $T_0 \sin p_1 x$  for simply supported beam

		$x/L$					
$z/h$		0.0	0.1	0.2	0.3	0.4	0.5
$\bar{\sigma}_x$	0.5	0	-1.6116	-3.0655	-4.2193	-4.9601	-5.2154
	0.4	0	-1.8632	-3.5440	-4.8779	-5.7343	-6.0294
	0.3	0	-2.1192	-4.0310	-5.5481	-6.5222	-6.8579
	0.2	0	-2.3808	-4.5286	-6.2330	-7.3274	-7.7045
	0.1	0	-2.6492	-5.0391	-6.9357	-8.1534	-8.5730
	0	0	-2.9255	-5.5647	-7.6591	-9.0038	-9.4672
	0	0	15.7760	30.0078	41.3022	48.5537	51.0524
	-0.1	0	9.9031	18.8368	25.9267	30.4786	32.0471
	-0.2	0	4.5934	8.7371	12.0256	14.1369	14.8644
	-0.3	0	-0.4138	-0.7870	-1.0833	-1.2735	-1.3390
	-0.4	0	-5.3641	-10.2032	-14.0435	-16.5091	-17.3587
	-0.5	0	-10.5007	-19.9736	-27.4913	-32.3180	-33.9811
$\bar{\tau}_{xz}$	0.5	0	0	0	0	0	0
	0.4	-0.1766	-0.1680	-0.1429	-0.1038	-0.0546	0
	0.3	-0.3790	-0.3604	-0.3066	-0.2228	-0.1171	0
	0.2	-0.6077	-0.5779	-0.4916	-0.3572	-0.1878	0
	0.1	-0.8633	-0.8211	-0.6984	-0.5074	-0.2668	0
	0	-1.1466	-1.0905	-0.9276	-0.6740	-0.3543	0
	0	-1.1466	-1.0905	-0.9276	-0.6740	-0.3543	0
	-0.1	0.1528	0.1453	0.1236	0.0898	0.0472	0
	-0.2	0.8860	0.8427	0.7168	0.5208	0.2738	0
	-0.3	1.0970	1.0433	0.8875	0.6448	0.3390	0
	-0.4	0.8038	0.7645	0.6503	0.4725	0.2484	0
	-0.5	0	0	0	0	0	0
$\bar{\sigma}_z$	0.5	0	0	0	0	0	0
	0.4	0	0.0008	0.0016	0.0022	0.0026	0.0027
	0.3	0	0.0035	0.0067	0.0092	0.0108	0.0114
	0.2	0	0.0083	0.0157	0.0217	0.0255	0.0268
	0.1	0	0.0154	0.0293	0.0403	0.0474	0.0498
	0	0	0.0251	0.0478	0.0658	0.0773	0.0813
	0	0	0.0251	0.0478	0.0658	0.0773	0.0813
	-0.1	0	0.0295	0.0561	0.0772	0.0907	0.0954
	-0.2	0	0.0240	0.0456	0.0628	0.0738	0.0776
	-0.3	0	0.0140	0.0265	0.0365	0.0430	0.0452
	-0.4	0	0.0043	0.0082	0.0113	0.0133	0.0140
	-0.5	0	0	0	0	0	0

Table 7.3-3 Normalised displacements given  $T_1 z \sin p_1 x$  for simply supported beam

		$x/L$					
$z/h$		0.0	0.1	0.2	0.3	0.4	0.5
$\bar{U}$	0.5	-0.7315	-0.6957	-0.5918	-0.4300	-0.2260	0
	0.4	-0.6256	-0.5950	-0.5061	-0.3677	-0.1933	0
	0.3	-0.5168	-0.4915	-0.4181	-0.3038	-0.1597	0
	0.2	-0.4060	-0.3861	-0.3284	-0.2386	-0.1255	0
	0.1	-0.2941	-0.2797	-0.2380	-0.1729	-0.0909	0
	0	-0.1822	-0.1733	-0.1474	-0.1071	-0.0563	0
	0	-0.1822	-0.1733	-0.1474	-0.1071	-0.0563	0
	-0.1	-0.0823	-0.0783	-0.0666	-0.0484	-0.0254	0
	-0.2	0.0122	0.0116	0.0099	0.0072	0.0038	0
	-0.3	0.1048	0.0997	0.0848	0.0616	0.0324	0
	-0.4	0.1989	0.1891	0.1609	0.1169	0.0615	0
	-0.5	0.2977	0.2831	0.2408	0.1750	0.0920	0
$\bar{W}$	0.5	0	1.0235	1.9467	2.6794	3.1499	3.3120
	0.4	0	1.0033	1.9085	2.6268	3.0880	3.2469
	0.3	0	0.9878	1.8789	2.5861	3.0401	3.1966
	0.2	0	0.9768	1.8580	2.5573	3.0063	3.1610
	0.1	0	0.9703	1.8457	2.5404	2.9864	3.1401
	0	0	0.9684	1.8421	2.5354	2.9805	3.1339
	0	0	0.9684	1.8421	2.5354	2.9805	3.1339
	-0.1	0	0.9703	1.8457	2.5404	2.9864	3.1401
	-0.2	0	0.9751	1.8548	2.5529	3.0012	3.1556
	-0.3	0	0.9829	1.8695	2.5732	3.0250	3.1806
	-0.4	0	0.9935	1.8898	2.6011	3.0578	3.2151
	-0.5	0	1.0071	1.9157	2.6367	3.0996	3.2591

Table 7.3-4 Normalised stresses given  $T_1 z \sin p_1 x$  for simply supported beam

		$x/L$					
$z/h$		0.0	0.1	0.2	0.3	0.4	0.5
$\bar{\sigma}_x$	0.5	0	-1.2243	-2.3287	-3.2052	-3.7680	-3.9619
	0.4	0	-0.9399	-1.7879	-2.4608	-2.8928	-3.0417
	0.3	0	-0.6582	-1.2520	-1.7233	-2.0258	-2.1301
	0.2	0	-0.3783	-0.7196	-0.9904	-1.1643	-1.2242
	0.1	0	-0.0993	-0.1889	-0.2600	-0.3056	-0.3213
	0	0	0.1797	0.3417	0.4704	0.5529	0.5814
	0	0	4.4357	8.4372	11.6128	13.6516	14.3542
	-0.1	0	2.7803	5.2885	7.2789	8.5569	8.9973
	-0.2	0	1.2539	2.3850	3.2827	3.8590	4.0576
	-0.3	0	-0.2262	-0.4303	-0.5923	-0.6963	-0.7321
	-0.4	0	-1.7404	-3.3104	-4.5563	-5.3563	-5.6319
	-0.5	0	-3.3705	-6.4111	-8.8241	-10.3734	-10.9072
$\bar{\tau}_{xz}$	0.5	0	0	0	0	0	0
	0.4	-0.1100	-0.1046	-0.0890	-0.0646	-0.0340	0
	0.3	-0.1912	-0.1818	-0.1547	-0.1124	-0.0591	0
	0.2	-0.2439	-0.2319	-0.1973	-0.1434	-0.0754	0
	0.1	-0.2682	-0.2550	-0.2169	-0.1576	-0.0829	0
	0	-0.2641	-0.2511	-0.2136	-0.1552	-0.0816	0
	0	-0.2641	-0.2511	-0.2136	-0.1552	-0.0816	0
	-0.1	0.1013	0.0963	0.0819	0.0595	0.0313	0
	-0.2	0.3056	0.2906	0.2472	0.1796	0.0944	0
	-0.3	0.3578	0.3403	0.2895	0.2103	0.1106	0
	-0.4	0.2585	0.2458	0.2091	0.1519	0.0799	0
	-0.5	0	0	0	0	0	0
$\bar{\sigma}_z$	0.5	0	0	0	0	0	0
	0.4	0	0.0006	0.0011	0.0015	0.0017	0.0018
	0.3	0	0.0020	0.0039	0.0053	0.0063	0.0066
	0.2	0	0.0042	0.0079	0.0109	0.0129	0.0135
	0.1	0	0.0067	0.0127	0.0175	0.0206	0.0216
	0	0	0.0093	0.0177	0.0243	0.0286	0.0301
	0	0	0.0093	0.0177	0.0243	0.0286	0.0301
	-0.1	0	0.0099	0.0189	0.0260	0.0306	0.0322
	-0.2	0	0.0078	0.0149	0.0205	0.0241	0.0254
	-0.3	0	0.0045	0.0086	0.0118	0.0139	0.0146
	-0.4	0	0.0014	0.0026	0.0036	0.0043	0.0045
	-0.5	0	0	0	0	0	0

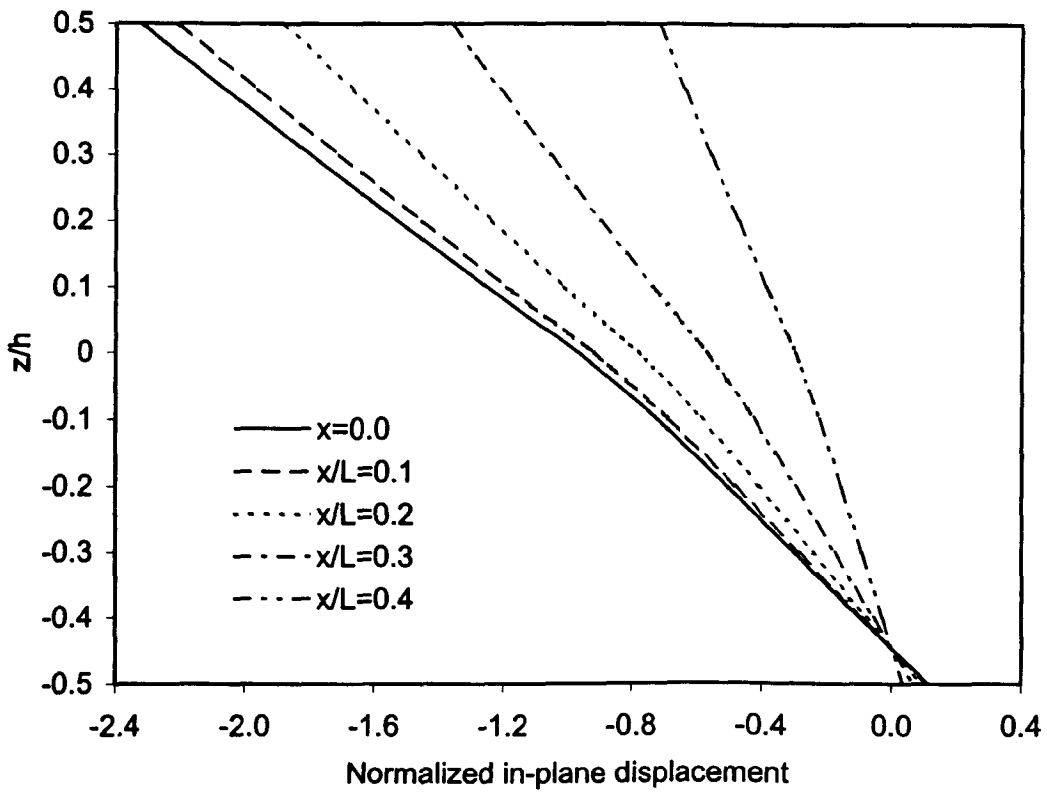


Figure 7.3-1 In-plane displacement distributions for a simply supported beam induced by  $T_0 \sin(p_1 x)$

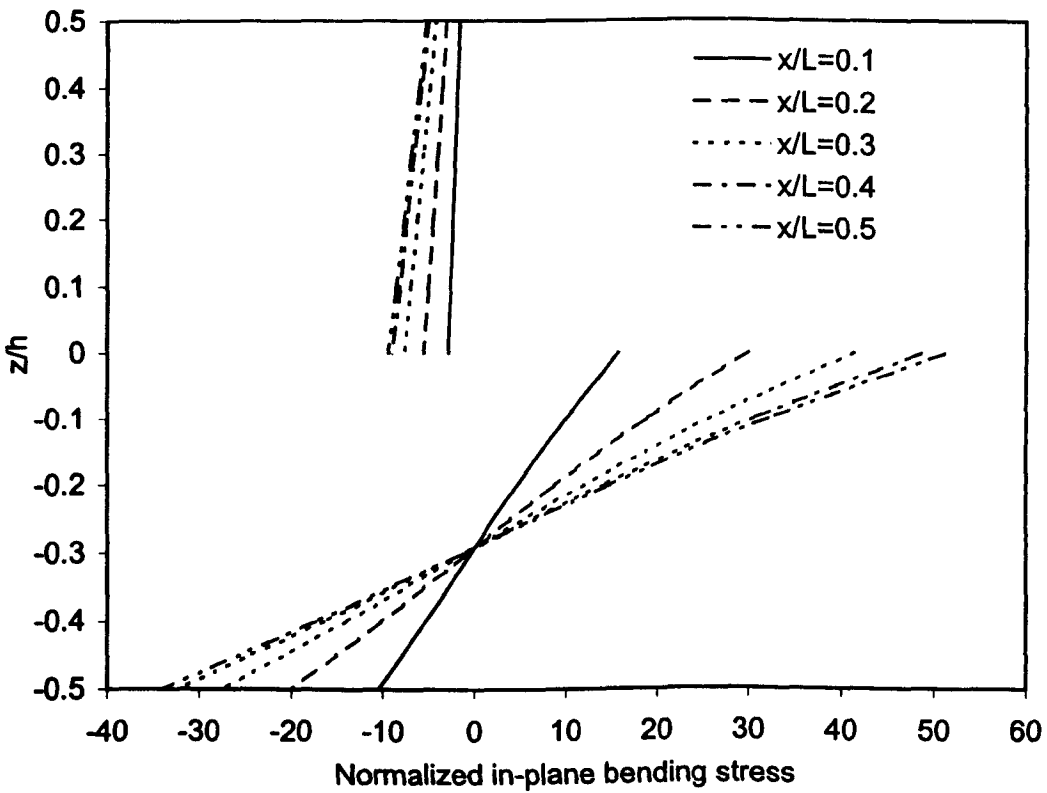


Figure 7.3-2 In-plane bending stress distributions for a simply supported beam induced by  $T_0 \sin(p_1 x)$

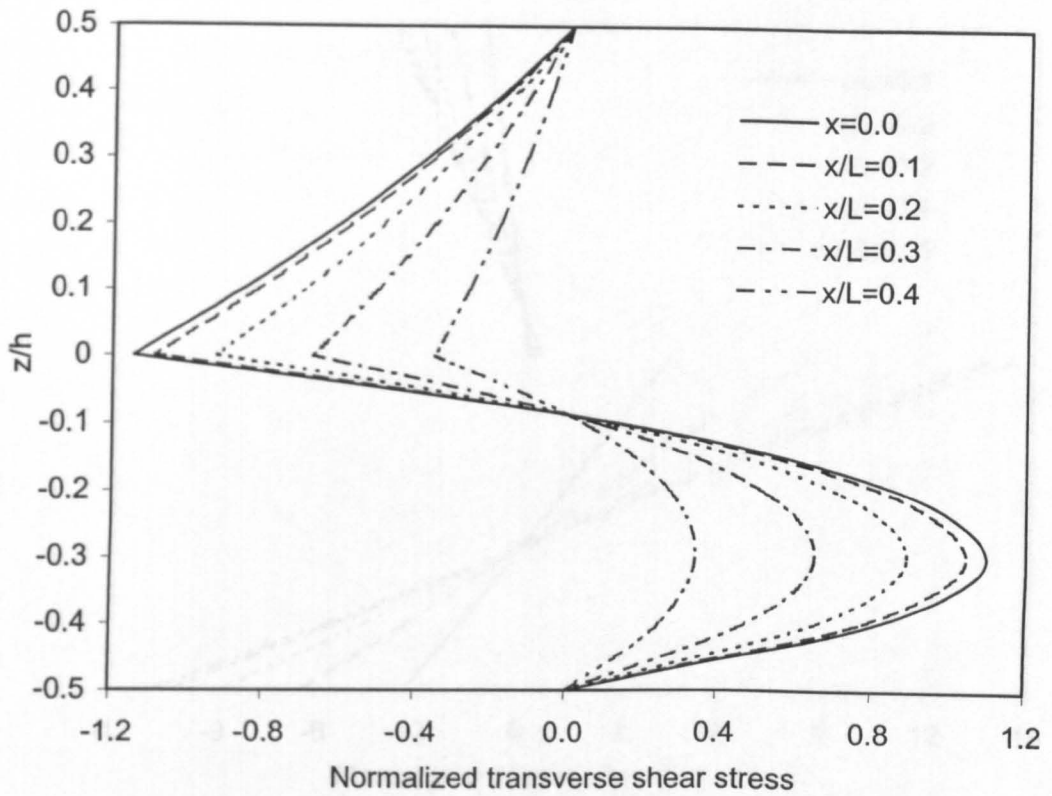


Figure 7.3-3 Transverse shear stress distributions for a simply supported beam induced by  $T_0 \sin(p_1 x)$

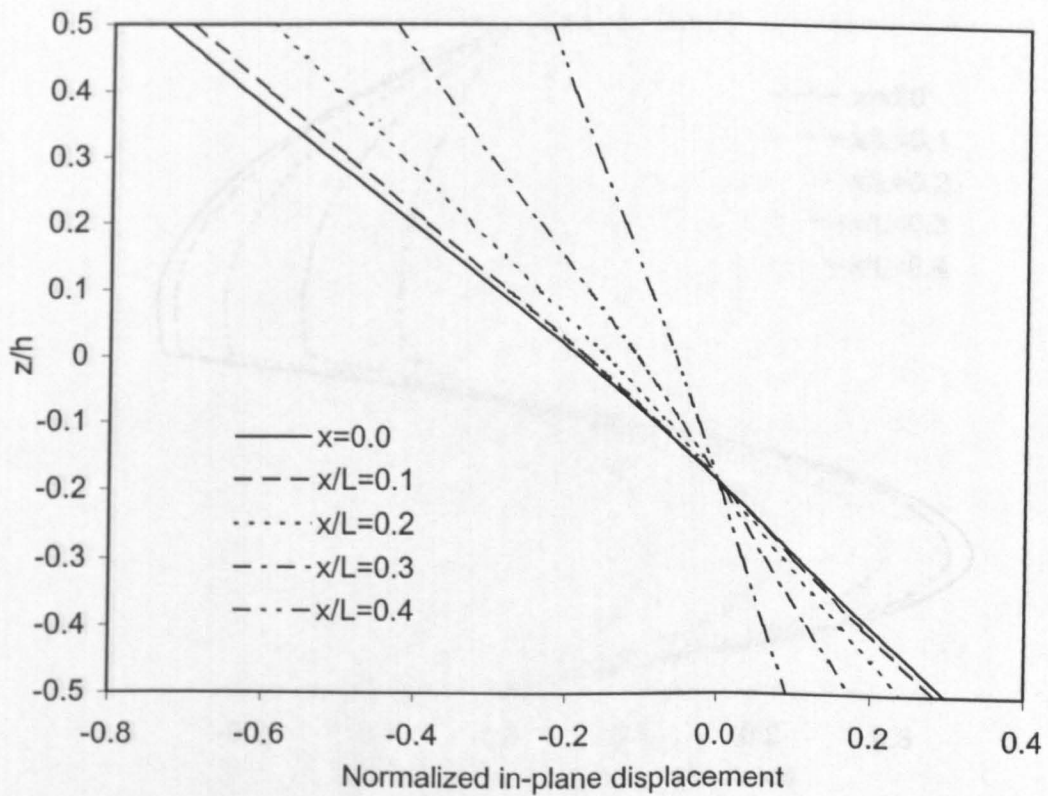


Figure 7.3-4 In-plane displacement distributions for a simply supported beam induced by  $T_1 z \sin(p_1 x)$

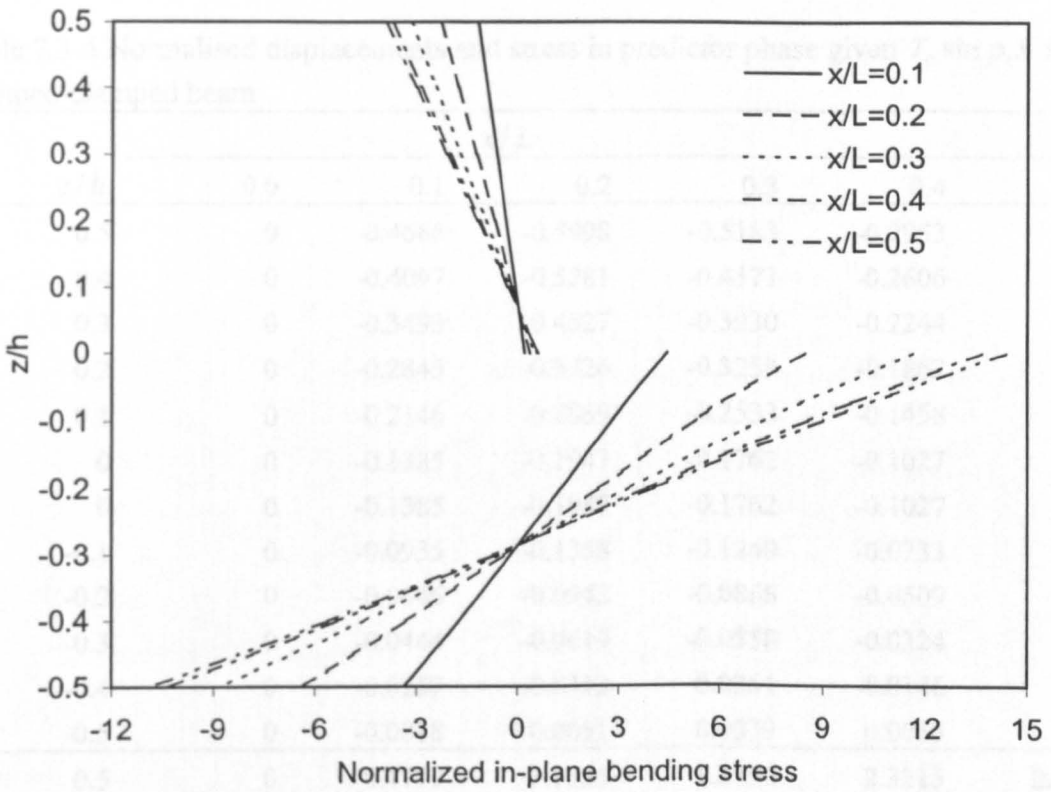


Figure 7.3-5 In-plane bending stress distributions for a simply supported beam induced by  $T_1 z \sin(p_1 x)$

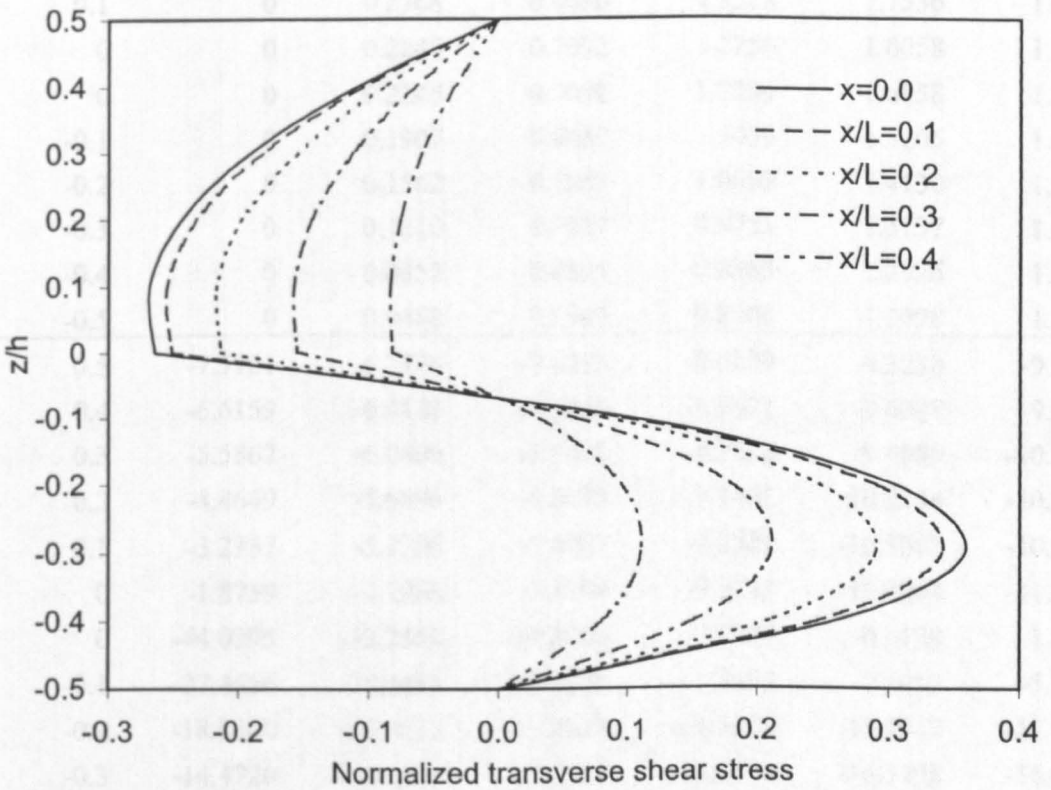


Figure 7.3-6 Transverse shear stress distributions for a simply supported beam induced by  $T_1 z \sin(p_1 x)$

Table 7.3-5 Normalised displacements and stress in predictor phase given  $T_0 \sin p_1 x$  for clamped-clamped beam

		$x/L$					
$z/h$		0.0	0.1	0.2	0.3	0.4	0.5
$\bar{U}$	0.5	0	-0.4666	-0.5998	-0.5183	-0.2953	0
	0.4	0	-0.4097	-0.5281	-0.4571	-0.2606	0
	0.3	0	-0.3493	-0.4527	-0.3930	-0.2244	0
	0.2	0	-0.2845	-0.3726	-0.3253	-0.1862	0
	0.1	0	-0.2146	-0.2869	-0.2533	-0.1458	0
	0	0	-0.1385	-0.1947	-0.1762	-0.1027	0
	0	0	-0.1385	-0.1947	-0.1762	-0.1027	0
	-0.1	0	-0.0935	-0.1358	-0.1249	-0.0733	0
	-0.2	0	-0.0646	-0.0942	-0.0868	-0.0509	0
	-0.3	0	-0.0444	-0.0619	-0.0558	-0.0324	0
	-0.4	0	-0.0257	-0.0312	-0.0261	-0.0146	0
	-0.5	0	-0.0018	0.0051	0.0079	0.0055	0
$\bar{W}$	0.5	0	0.4779	1.1635	1.8390	2.3213	2.4952
	0.4	0	0.4288	1.0755	1.7201	2.1826	2.3497
	0.3	0	0.3789	0.9861	1.5995	2.0419	2.2021
	0.2	0	0.3283	0.8953	1.4769	1.8989	2.0521
	0.1	0	0.2768	0.8030	1.3523	1.7536	1.8996
	0	0	0.2245	0.7092	1.2256	1.6058	1.7445
	0	0	0.2245	0.7092	1.2256	1.6058	1.7445
	-0.1	0	0.1907	0.6487	1.1439	1.5105	1.6445
	-0.2	0	0.1562	0.5868	1.0603	1.4130	1.5422
	-0.3	0	0.1210	0.5237	0.9751	1.3137	1.4380
	-0.4	0	0.0852	0.4595	0.8885	1.2126	1.3320
	-0.5	0	0.0488	0.3943	0.8004	1.1098	1.2242
$\bar{\sigma}_x$	0.5	-7.5721	-6.7726	-7.6253	-8.6229	-9.3238	-9.5712
	0.4	-6.6159	-6.4141	-7.5856	-8.7871	-9.6097	-9.8982
	0.3	-5.5862	-6.0409	-7.5492	-8.9616	-9.9089	-10.2393
	0.2	-4.4649	-5.6496	-7.5173	-9.1491	-10.2248	-10.5982
	0.1	-3.2337	-5.2366	-7.4907	-9.3521	-10.5608	-10.9786
	0	-1.8739	-4.7983	-7.4704	-9.5735	-10.9204	-11.3842
	0	-44.0295	-32.2558	-18.8806	-7.8085	-0.6139	1.8736
	-0.1	-27.4556	-25.3658	-18.3255	-11.7275	-7.3013	-5.7575
	-0.2	-18.8300	-19.9612	-17.2328	-14.3120	-12.2947	-11.5856
	-0.3	-14.4720	-15.3539	-15.8510	-16.1794	-16.3778	-16.4449
	-0.4	-10.9093	-10.8948	-14.4145	-17.9120	-20.2900	-21.1224
	-0.5	-4.7087	-5.9419	-13.1551	-20.0858	-24.7623	-26.3960

Table 7.3-6 Normalised stresses given  $T_0 \sin p_1 x$  for clamped-clamped beam

	$z/h$	$x/L$					
		0.0	0.1	0.2	0.3	0.4	0.5
$\bar{\tau}_{xz}$ Predictor	0.5	0.8404	0.1199	0.0310	0.0080	0.0020	0
	0.4	0.6776	-0.0255	-0.1059	-0.0942	-0.0522	0
	0.3	0.5123	-0.1890	-0.2621	-0.2112	-0.1143	0
	0.2	0.3443	-0.3711	-0.4379	-0.3433	-0.1844	0
	0.1	0.1736	-0.5722	-0.6337	-0.4907	-0.2627	0
	0	0.0000	-0.7928	-0.8502	-0.6539	-0.3494	0
	0	0.0000	-0.7928	-0.8502	-0.6539	-0.3494	0
	-0.1	-0.2798	0.0657	0.1030	0.0845	0.0459	0
	-0.2	-0.5662	0.5319	0.6361	0.4999	0.2687	0
	-0.3	-0.8579	0.6361	0.7817	0.6174	0.3323	0
	-0.4	-1.1545	0.3911	0.5534	0.4474	0.2423	0
	-0.5	-1.4565	-0.2078	-0.0538	-0.0139	-0.0034	0
	$\bar{\tau}_{xz}$ Corrector	0.5	0	0	0	0	0
0.4		0.2805	-0.0666	-0.1165	-0.0970	-0.0529	0
0.3		0.4707	-0.1757	-0.2586	-0.2103	-0.1141	0
0.2		0.5587	-0.3307	-0.4274	-0.3405	-0.1837	0
0.1		0.5299	-0.5355	-0.6243	-0.4882	-0.2621	0
0		0.3669	-0.7951	-0.8509	-0.6541	-0.3495	0
0		0.3669	-0.7951	-0.8509	-0.6541	-0.3495	0
-0.1		0.1812	0.1614	0.1278	0.0909	0.0475	0
-0.2		-0.5819	0.5399	0.6382	0.5004	0.2688	0
-0.3		-1.0291	0.5931	0.7705	0.6145	0.3316	0
-0.4		-0.7902	0.4258	0.5623	0.4497	0.2428	0
-0.5		0	0	0	0	0	0
$\bar{\sigma}_z$ Predictor		0.5	-1.9167	-0.7012	-0.5369	-0.4944	-0.4836
	0.4	-1.6747	-0.5368	-0.3948	-0.3578	-0.3480	-0.3461
	0.3	-1.4140	-0.3653	-0.2476	-0.2155	-0.2063	-0.2043
	0.2	-1.1302	-0.1852	-0.0942	-0.0668	-0.0575	-0.0551
	0.1	-0.8185	0.0050	0.0661	0.0892	0.0993	0.1024
	0	-0.4743	0.2069	0.2343	0.2533	0.2651	0.2691
	0	-0.5871	-0.1754	-0.1554	-0.1382	-0.1269	-0.1229
	-0.1	-0.3661	0.0108	0.0212	0.0379	0.0503	0.0548
	-0.2	-0.2511	0.1574	0.1694	0.1839	0.1942	0.1979
	-0.3	-0.1930	0.2836	0.3039	0.3157	0.3226	0.3249
	-0.4	-0.1455	0.4074	0.4384	0.4484	0.4521	0.4532
	-0.5	-0.0628	0.5466	0.5865	0.5967	0.5993	0.5998
	$\bar{\sigma}_z$ Corrector	0.5	0	0	0	0	0
0.4		-0.0488	-0.0062	-0.0002	0.0017	0.0024	0.0026
0.3		-0.1914	-0.0231	-0.0002	0.0074	0.0103	0.0111
0.2		-0.4205	-0.0478	0.0012	0.0179	0.0244	0.0263
0.1		-0.7269	-0.0770	0.0054	0.0341	0.0457	0.0490
0		-1.0992	-0.1070	0.0136	0.0569	0.0749	0.0801
0		-1.0992	-0.1070	0.0136	0.0569	0.0749	0.0801
-0.1		-1.2945	-0.1259	0.0159	0.0667	0.0878	0.0940
-0.2		-1.0969	-0.1109	0.0108	0.0537	0.0713	0.0764
-0.3		-0.6522	-0.0673	0.0055	0.0311	0.0414	0.0444
-0.4		-0.2007	-0.0205	0.0018	0.0096	0.0128	0.0138
-0.5		0	0	0	0	0	0

Table 7.3-7 Normalised displacements and stress in predictor phase given  $T_1 z \sin p_1 x$  for clamped-clamped beam

		$x/L$					
$z/h$		0.0	0.1	0.2	0.3	0.4	0.5
$\bar{U}$	0.5	0	-0.1405	-0.1823	-0.1584	-0.0905	0
	0.4	0	-0.1201	-0.1559	-0.1354	-0.0774	0
	0.3	0	-0.0977	-0.1272	-0.1108	-0.0633	0
	0.2	0	-0.0738	-0.0971	-0.0850	-0.0487	0
	0.1	0	-0.0492	-0.0662	-0.0586	-0.0338	0
	0	0	-0.0245	-0.0352	-0.0321	-0.0188	0
	0	0	-0.0245	-0.0352	-0.0321	-0.0188	0
	-0.1	0	-0.0083	-0.0132	-0.0126	-0.0075	0
	-0.2	0	0.0041	0.0047	0.0039	0.0021	0
	-0.3	0	0.0152	0.0213	0.0192	0.0112	0
	-0.4	0	0.0272	0.0388	0.0354	0.0207	0
	-0.5	0	0.0427	0.0600	0.0543	0.0316	0
$\bar{W}$	0.5	0	0.1480	0.3848	0.6278	0.8045	0.8687
	0.4	0	0.1247	0.3435	0.5722	0.7397	0.8007
	0.3	0	0.1066	0.3116	0.5292	0.6895	0.7481
	0.2	0	0.0939	0.2891	0.4988	0.6541	0.7109
	0.1	0	0.0864	0.2758	0.4810	0.6333	0.6891
	0	0	0.0842	0.2719	0.4757	0.6271	0.6827
	0	0	0.0842	0.2719	0.4757	0.6271	0.6827
	-0.1	0	0.0864	0.2758	0.4809	0.6333	0.6891
	-0.2	0	0.0920	0.2857	0.4942	0.6488	0.7053
	-0.3	0	0.1009	0.3015	0.5156	0.6737	0.7315
	-0.4	0	0.1133	0.3234	0.5451	0.7081	0.7675
	-0.5	0	0.1290	0.3513	0.5826	0.7519	0.8135
$\bar{\sigma}_x$	0.5	-2.1880	-2.7832	-3.7388	-4.5787	-5.1326	-5.3249
	0.4	-1.8700	-2.2788	-2.9994	-3.6410	-4.0654	-4.2129
	0.3	-1.5102	-1.7660	-2.2622	-2.7094	-3.0062	-3.1093
	0.2	-1.1222	-1.2474	-1.5265	-1.7821	-1.9522	-2.0115
	0.1	-0.7196	-0.7259	-0.7916	-0.8568	-0.9010	-0.9165
	0	-0.3158	-0.2041	-0.0567	0.0683	0.1500	0.1783
	0	-7.4206	-4.5466	-0.8926	2.1976	4.2158	4.9145
	-0.1	-1.9320	-1.1107	0.9150	2.7870	4.0362	4.4712
	-0.2	1.7887	1.9858	2.8525	3.6853	4.2459	4.4415
	-0.3	4.8729	4.9601	4.8367	4.6946	4.5954	4.5605
	-0.4	8.4215	8.0233	6.7864	5.6223	4.8422	4.5703
	-0.5	13.5579	11.3910	8.6189	6.2719	4.7386	4.2078

Table 7.3-8 Normalised stresses given  $T_1 z \sin p_1 x$  for clamped-clamped beam

		$x/L$						
$z/h$		0.0	0.1	0.2	0.3	0.4	0.5	
$\tau_{xz}$ Predictor	0.5	0.3120	0.0258	0.0063	0.0016	0.0004	0	
	0.4	0.1979	-0.0609	-0.0782	-0.0620	-0.0334	0	
	0.3	0.1098	-0.1253	-0.1408	-0.1090	-0.0583	0	
	0.2	0.0474	-0.1674	-0.1814	-0.1395	-0.0745	0	
	0.1	0.0108	-0.1875	-0.2003	-0.1536	-0.0819	0	
	0	0.0000	-0.1855	-0.1975	-0.1513	-0.0807	0	
	0	0.0000	-0.1855	-0.1975	-0.1513	-0.0807	0	
	-0.1	0.0270	0.0734	0.0763	0.0581	0.0310	0	
	-0.2	0.0950	0.2226	0.2305	0.1755	0.0935	0	
	-0.3	0.2046	0.2683	0.2718	0.2060	0.1096	0	
	-0.4	0.3559	0.2111	0.2005	0.1498	0.0794	0	
	-0.5	0.5484	0.0454	0.0112	0.0027	0.0006	0	
	$\tau_{xz}$ Corrector	0.5	0	0	0	0	0	0
		0.4	0.0123	-0.0788	-0.0826	-0.0631	-0.0336	0
0.3		0.0252	-0.1350	-0.1432	-0.1096	-0.0584	0	
0.2		0.0357	-0.1701	-0.1821	-0.1396	-0.0745	0	
0.1		0.0421	-0.1852	-0.1998	-0.1534	-0.0819	0	
0		0.0438	-0.1805	-0.1963	-0.1510	-0.0806	0	
0		0.0438	-0.1805	-0.1963	-0.1510	-0.0806	0	
-0.1		0.0105	0.0825	0.0785	0.0587	0.0311	0	
-0.2		-0.0650	0.2037	0.2259	0.1744	0.0932	0	
-0.3		-0.0811	0.2360	0.2638	0.2040	0.1091	0	
-0.4		-0.0305	0.1831	0.1937	0.1481	0.0790	0	
-0.5		0	0	0	0	0	0	
$\sigma_z$ Predictor		0.5	-0.5538	-0.0384	-0.0223	-0.0183	-0.0174	-0.0172
		0.4	-0.4734	-0.0549	-0.0393	-0.0352	-0.0341	-0.0338
	0.3	-0.3823	-0.0674	-0.0536	-0.0492	-0.0476	-0.0471	
	0.2	-0.2841	-0.0771	-0.0660	-0.0612	-0.0589	-0.0581	
	0.1	-0.1821	-0.0855	-0.0774	-0.0721	-0.0689	-0.0679	
	0	-0.0799	-0.0936	-0.0886	-0.0827	-0.0787	-0.0772	
	0	-0.0989	-0.1184	-0.1141	-0.1085	-0.1045	-0.1031	
	-0.1	-0.0258	-0.0985	-0.0925	-0.0862	-0.0818	-0.0802	
	-0.2	0.0238	-0.0884	-0.0784	-0.0721	-0.0683	-0.0670	
	-0.3	0.0650	-0.0820	-0.0674	-0.0616	-0.0589	-0.0581	
	-0.4	0.1123	-0.0736	-0.0555	-0.0504	-0.0487	-0.0483	
	-0.5	0.1808	-0.0574	-0.0384	-0.0338	-0.0326	-0.0324	
	$\sigma_z$ Corrector	0.5	0	0	0	0	0	0
		0.4	-0.0166	-0.0013	0.0006	0.0013	0.0017	0.0018
0.3		-0.0587	-0.0050	0.0022	0.0049	0.0062	0.0066	
0.2		-0.1162	-0.0106	0.0043	0.0100	0.0126	0.0134	
0.1		-0.1804	-0.0174	0.0068	0.0160	0.0202	0.0215	
0		-0.2435	-0.0247	0.0093	0.0223	0.0281	0.0298	
0		-0.2435	-0.0247	0.0093	0.0223	0.0281	0.0298	
-0.1		-0.2426	-0.0283	0.0095	0.0237	0.0300	0.0319	
-0.2		-0.1862	-0.0229	0.0074	0.0187	0.0237	0.0252	
-0.3		-0.1162	-0.0120	0.0045	0.0108	0.0136	0.0145	
-0.4		-0.0430	-0.0029	0.0016	0.0034	0.0042	0.0045	
-0.5		0	0	0	0	0	0	

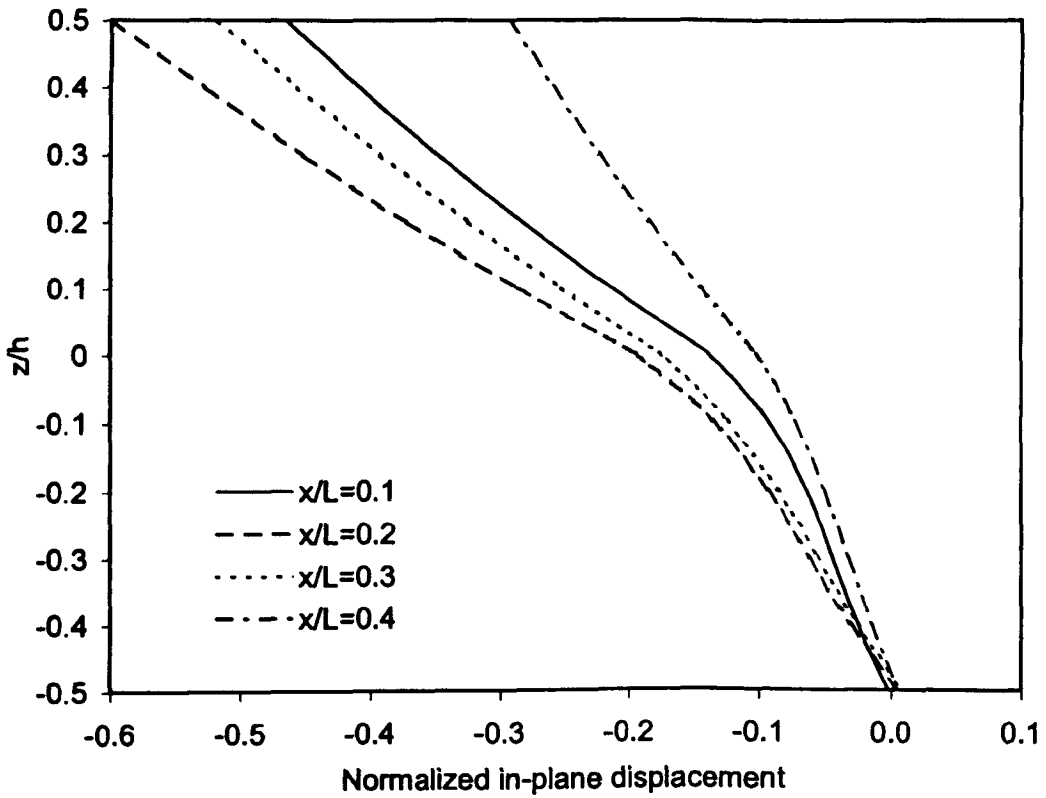


Figure 7.3-7 In-plane displacement distributions in predictor phase for a clamped-clamped beam induced by  $T_0 \sin(p_1 x)$

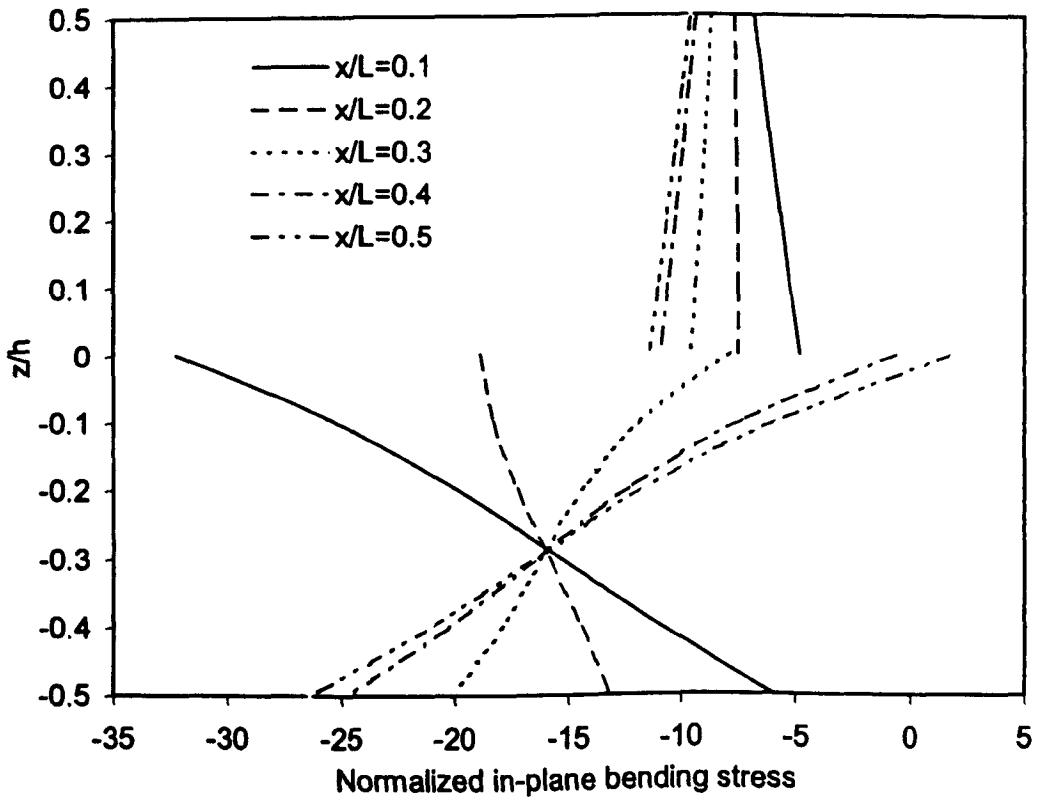


Figure 7.3-8 In-plane bending stress distributions in predictor phase for a clamped-clamped beam induced by  $T_0 \sin(p_1 x)$

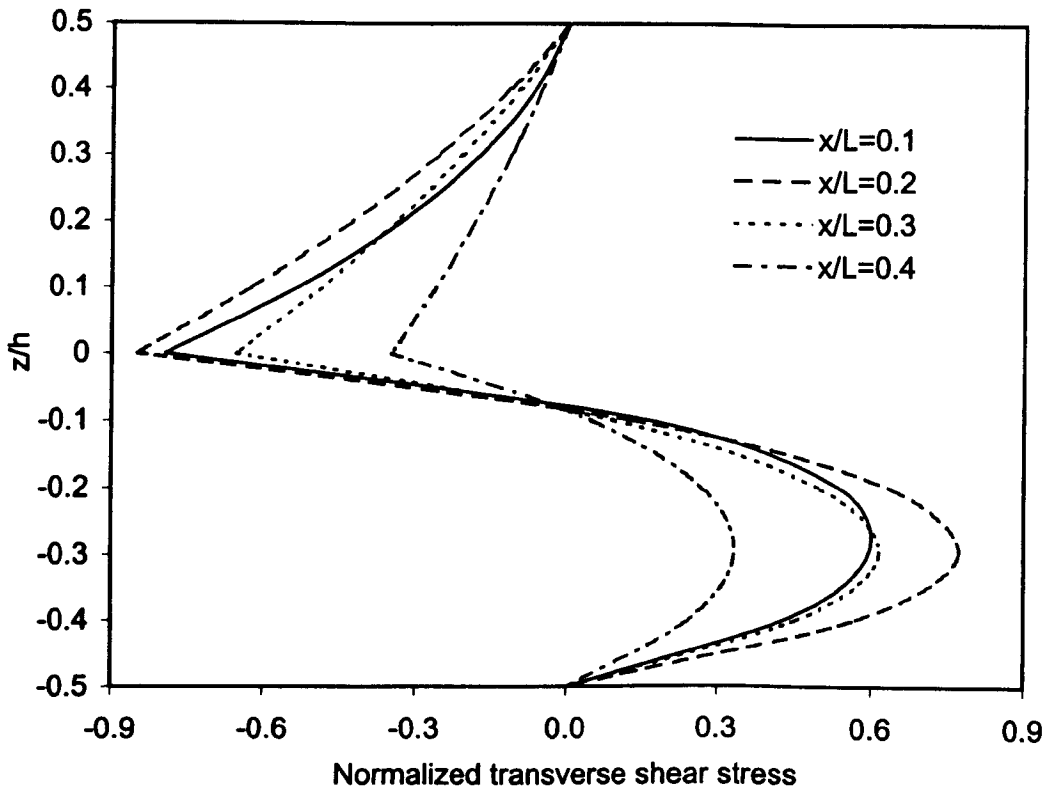


Figure 7.3-9 Transverse shear stress distributions in corrector phase for a clamped-clamped beam induced by  $T_0 \sin(p_1 x)$

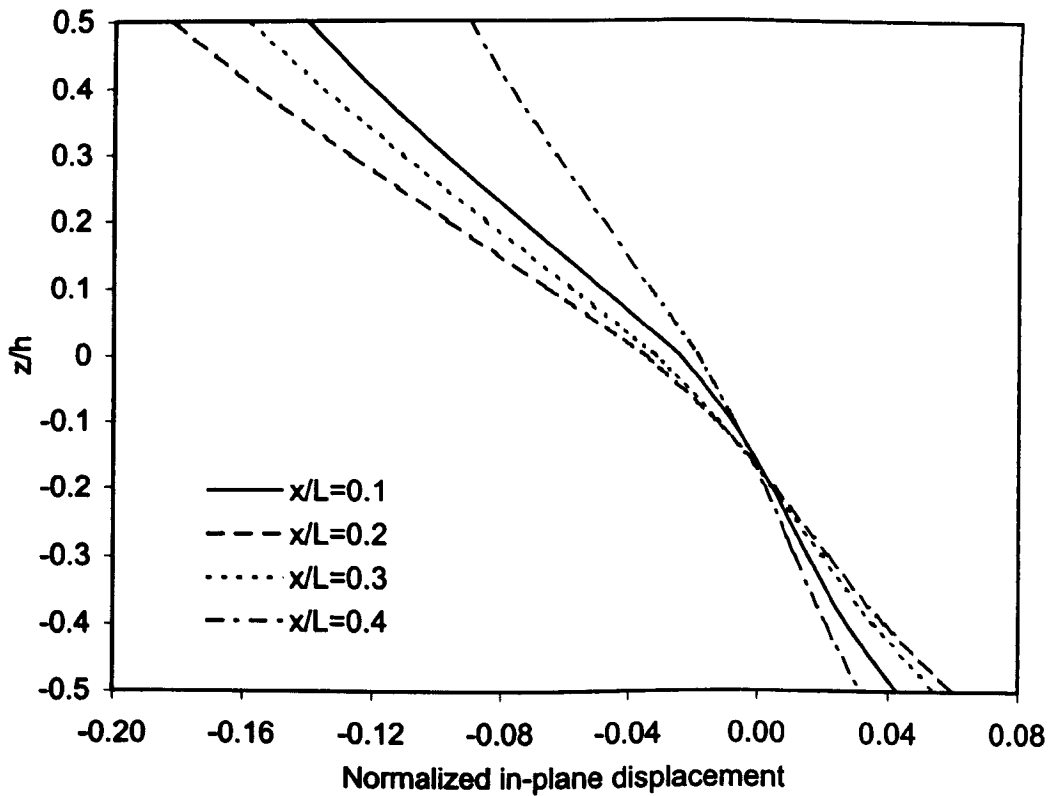


Figure 7.3-10 In-plane displacement distributions in predictor phase for a clamped-clamped beam induced by  $T_1 z \sin(p_1 x)$

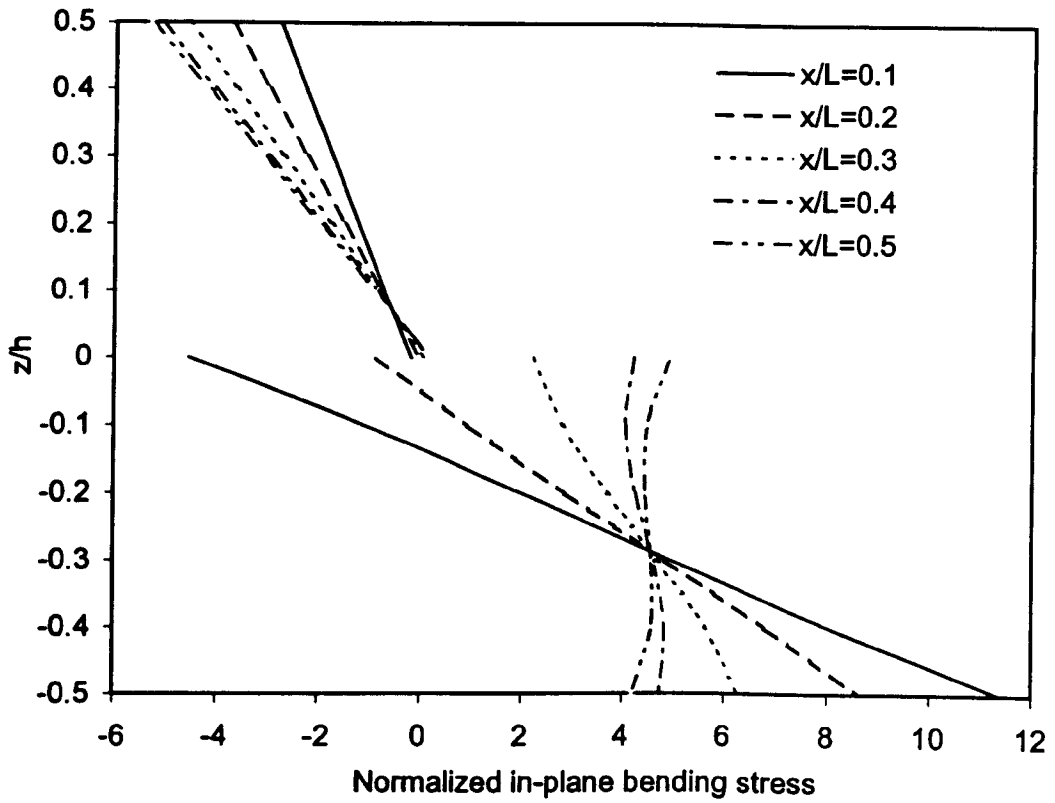


Figure 7.3-11 In-plane bending stress distributions in predictor phase for a clamped-clamped beam induced by  $T_1 z \sin(p_1 x)$

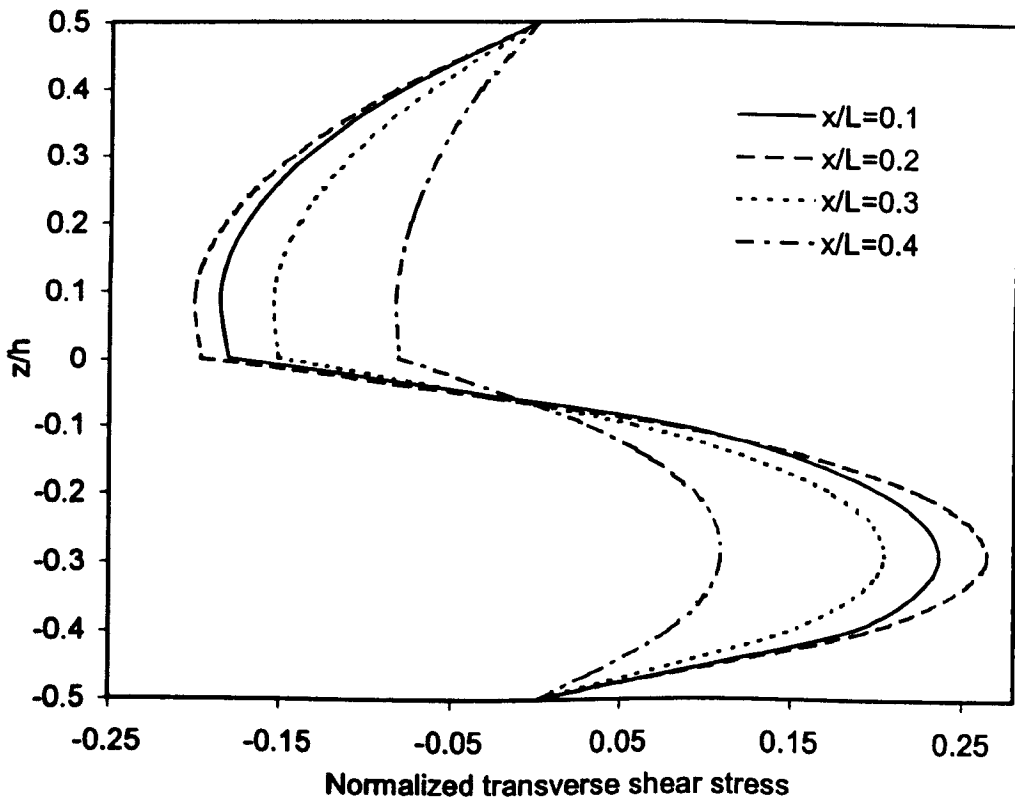


Figure 7.3-12 Transverse shear stress distributions in corrector phase for a clamped-clamped beam induced by  $T_1 z \sin(p_1 x)$

shear stress are illustrated in Figures 7.3-1, 7.3-2 and 7.3-3. Tables 7.3-3 and 7.3-4 present numerical values caused by linear temperature variation. The corresponding distributions of in-plane displacement, in-plane bending stress and transverse shear stress are illustrated in figures 7.3-4, 7.3-5 and 7.3-6. For the case of simply supported beams, the general four-degree-of-freedom beam theory subject thermal loading yields the exact solution [Murakami, 1993].

The exact elasticity solution of general 4-degree-of-freedom beam theory subject to thermal loading allows investigation of other sets of boundary conditions. Due to the symmetry of applied edge boundary conditions, results for a clamped-clamped beam are presented only for the left-half part of the beam ( $0 \leq x/L \leq 0.5$ ). Tables 7.3-5 and 7.3-6 present numerical values of normalized displacements, in-plane bending stress and transverse shear and normal stress given uniform temperature variation. Corresponding figures of in-plane displacement and in-plane bending stress in predictor phase, and transverse shear stress in corrector phase are illustrated in Figures 7.3-7, 7.3-8 and 7.3-9. Tables 7.3-7 and 7.3-8 present numerical values for given a linear temperature variation, and the corresponding figures of in-plane displacement, in-plane bending stress in predictor phase and transverse shear stress in corrector phase are illustrated in Figures 7.3-10, 7.3-11 and 7.3-12.

Tables 7.3-6 and 7.3-8 show clearly that, the through-thickness distributions of shear stress predictor phase are continuous at the inter-laminar interface, in the main due to its specific lay-up. Further, it satisfies exactly point by point zero transverse shear stress at the middle cross-section of the beam. It should be noted that there is a small and away from the edge negligible shear stress in predictor phase on both top and bottom lateral surfaces. However, this is not considered as a serious disadvantage of the present method. Although this is not expected to influence the accuracy of numerical results, it does have an additive

effect on the small error given the singular nature of the corner edge points. With disregard to the shear stress prediction in the vicinity of clamped edges, the difference of shear stress predictor and corrector phases is always much smaller than 1% in between of  $0.2 \leq x/L \leq 0.8$  caused by uniform or linear temperature variations. These further verify the accuracy of prediction of the transverse shear stress, and then the displacements and stresses in predictor phase. The transverse normal stress predictor phase caused by both uniform and linear temperature variations neither satisfies the lateral surface boundary conditions nor the inter-laminar interface continuity, but is dramatically improved in corrector phase.

## **7.7 Conclusions**

A new method for accurate stress analysis of laminated composite beams subject to thermal loading has been proposed. The method is based on G4BT and appropriate specification of through-thickness shape functions, which are associated with unknown displacement components. These allow consideration of the effects of both transverse shear and transverse normal deformation. Further, it involves four unknown displacement functions (degrees of freedom), each one of which is assigned a certain physical meaning. In particular applications, these are determined from the solution of four one-dimensional Navier-type equations of equilibrium, which form a tenth order set of simultaneous ordinary differential equations with respect to the axial co-ordinate parameter,  $x$ .

The method produces an excellent choice of both shape functions involved, and it leads to the exact elasticity solution presented by Murakami [1993] subject to thermal loading for simply supported infinite strips. By means of those shape functions, exact through-thickness displacement and stress distributions are "extracted" from the well-

known elasticity solution and are appropriately "fitted" into the corresponding distributions assumed for the development of general four-degree-of-freedom beam theory. Hence, the main physical characteristics of an exact elasticity solution are successfully incorporated into the proposed beam theory. Implementation of these new types of shape function is not difficult to achieve, as shape functions enter general four-degree-of-freedom beam theory only by means of the constitutive equations. Therefore, as far as accurate stress analysis of complicated material configurations is concerned (multi-layered beams), implementation of even more complicated forms of such shape functions is not regarded as a possible drawback of the proposed method.

At the edges of clamped-clamped beams, the displacement distributions exactly satisfy in a three-dimensional point-by-point sense, the same as the edge boundary conditions applied. The shear stress predictor phase is predicted to be continuous at the material interface, in the main due to the specific lay-up chosen. It is able to satisfy accurately, but not exactly, the stress boundary conditions imposed on the lateral planes of the beam. The practically negligible non-zero shear stress predictor phase on lateral surfaces cannot be considered as a serious disadvantage of the present method. This is because the values of transverse stresses are at least one order of magnitude lower than the values of the bending stresses whose distributions of which are considered to be extremely accurate. Furthermore, the accuracy of this method was tested by comparing the transverse shear stress predictor and corrector phases obtained through a predictor-corrector method [Soldatos and Liu, 2001] [Liu and Soldatos, submitted]. The transverse shear stress distributions of both predictor and corrector phases maintain excellent agreement in cross-sections away from the clamped edge.

Nevertheless, a procedure to improve or even entirely eliminate the effects of the slight inaccuracy given this method, has been outlined in [Soldatos and Watson, 1997a].

This would require the solution of a highly non-linear system of simultaneous algebraic equations, the number of which depends on the number of the layers in a particular laminate. Such a laborious and numerically complicated procedure was not employed in the present study, mostly because it is currently uncertain whether its possible success will be found to have any practical importance. The possibility, however, has been left open for a future extension of the present method towards that direction. It should be finally noted that, in its present form, the proposed model has been outlined and is therefore only available in connection with geometrically linearly elastic problems. However, the possibility of extending its applicability for the accurate stress analysis of beams subjected geometrically non-linear deformations is wide open.

## Chapter 8

### Conclusions

A specific displacement field assumption of certain conventional plate/beam theory can be thought as the truncations of the displacement field in a Taylor series expansion. Classical plate/beam theories and uniform shear deformable plate/beam theories take the first two terms of this Taylor series. Parabolic shear deformable plate/beam theories consider the first four terms of this Taylor series. In principle, it is possible to extend the displacement field in terms of the thickness coordinate up to any desired degree. However, due to the algebraic complexity and computer effort involved with higher-order theories in return of marginal gain in accuracy, conventional theories [Timoshenko, 1921] [Bickford, 1982] only involve limited terms truncated from Taylor series. Further shape functions of a conventional plate/beam theory can be determined by its displacement field incorporated with particular assumptions and restrictions (Chapter1 and Chapter2).

The so called 'degree' of a certain plate/beam theory can be counted and identified from the number of the unknown functions left in the displacement field during the problem simplification. These theories are based on the appropriate specification of through-thickness shape functions, which are associated with unknown displacement components. Through them, it enables the consideration of the effects of both transverse shear and transverse normal deformation. Further, by involving a number of unknown functions of displacement components (degrees of freedom), it also enable the three dimensional elasticity can be solved one- or two- dimensional, Navier-type equations of equilibrium, with respect to the axial co-ordinate parameter,  $x$ .

Classical plate/beam theories neglect the transverse shear stress, while uniform shear deformable plate/beam theories consider transverse shear stress as a constant through thickness. Parabolic shear deformable plate/beam theories improve the predictions by taking into account the zero shear stresses on lateral planes but not interlaminar stress and displacement continuity at interfaces. Non-linear choices of the shape functions (parabolic or hyperbolic) yield closer results to corresponding exact 3D solutions than lower order shape functions (classical and uniform). The shape functions of G3BT [Soldatos and Watson, 1997a], G4BT [Soldatos and Watson, 1997b-c] and G5BT [Shu and Soldatos, 2000] adopted exponential variation along the  $z$  – axis and sinusoidal variation in the  $x$  – direction. They are high order shape functions and suitable for more accurate stress analysis due to their shape functions taken account of both lateral plane stress boundary conditions and interlamina stress and displacement continuity at interfaces.

A predictor-corrector method (Chapter4) can improve the accuracy of transverse stress analysis results. The assessment performed in this study has clearly verified the fact that the shear stress distributions obtained through the predictor phase of conventional theories (USDT [Timoshenko, 1921] and PSDT [Bickford, 1982] are very inaccurate. Contrary to this, the predictor phase of the generalized G3BT [Soldatos and Watson, 1997a], G5BT give practically identical shear stress results with its corrector counterpart, at least as far as simply supported beams are concerned. Hence the predictor phase of G3T and G5BT [Soldatos and Watson, 1997a] [Shu and Soldatos, 2000] are already much more accurate than even the corrector phase of either USDT or PSDT. In addition, for the problem of cross-ply laminates, G5BT degenerates to and yields identical results with G3BT. In dealing however with simply supported beams only, the generalized G4T [Soldatos and Watson, 1997b, c] yields straight away the exact elasticity stress distributions and, therefore, it does not need the application of corrector phase.

The generalized plate/beam theories [Soldatos and Watson, 1997a-c] [Shu and Soldatos, 2000] discussed in this study are all displacement field based theories. The general four-degree-of-freedom beam theory (G4BT) takes transverse shear and transverse normal deformation into consideration. The general five-degree-of-freedom beam theory (G5BT) and general three-degree-of-freedom beam theory (G3BT) are all shear deformable theories that ignore transverse normal deformation. G3BT, G4BT and G5BT are all suitable for stress analysis of cross-ply laminates, while G5BT is also suitable for stress analysis of angle-ply laminates involved in cylindrical bending. Due to G3BT and G5BT use appropriate reduced stiffnesses, they can predict transverse normal stress distributions only through corrector phase. As shown in Section 3.6, the conventional plate/beam theories (including Classical beam theory, Uniform shear deformable theory (USDT) [Timoshenko, 1921] and parabolic shear deformable theory (PSDT) [Bickford, 1982]) can be considered as simple and special cases of G5BT or G3BT determined by the number of their non-zero displacement components and shape functions.

For beams with more complicated edge boundary conditions, the stress distributions obtained through the predictor phase of either G3T, G4T or G5T may be not as accurate as their simply supported counterparts. In their corrector phases, however, G3T, G4T and G5T improve considerably their initial predictions and produce almost identical transverse shear and transverse normal stress distributions, at least for the particular material arrangement considered in this study. For cross-ply laminates tested, this remarkable agreement of the corresponding numerical results obtained through the corrector phase of these three generalized theories appears to be in favour of G3T, which uses a smaller number of degrees of freedom. As compared with corresponding results due to Vel and Batra (2000), there is a very good agreement of corresponding displacement

values and an excellent agreement of corresponding bending stress values, which were provided based on predictor phase of both G3T and G4T.

G5BT is suitable for stress analysis for angle-ply laminates. When varying angles, span and stiffness ratio at the selected points (Chapter 6), the correction percentage of the maximum shear stress always remains less than about 3% and 4% for the clamped-clamped beam and clamped-free beam, respectively. These excellent agreement of shear stress distributions obtained in both predictor and corrector phases, confirms its great applicability and feasibility.

G4BT is also suitable for accurate stress analysis for cross-ply laminates subject to thermal loading. This method produces an excellent choice of both shape functions involved, as it led to the exact elasticity solution presented by Murakami [1993] subject to thermal loading for simply supported infinite strips. These allow consideration of the effects of both transverse shear and transverse normal deformation. The accuracy of this method was tested by comparing the transverse shear stress predictor phase and its corrector phases counterparts obtained through a predictor-corrector method [Soldatos and Liu, 2001] [Liu and Soldatos, submitted]. As clamped-clamped beam concerned, the transverse shear stress distributions of both predictor and corrector phases maintain excellent agreement in cross-sections away from the clamped edge.

Nevertheless, a procedure to improve or even entirely eliminate the effects of the slight inaccuracy given these general beam theories, has been outlined [Soldatos and Watson, 1997a]. This would require the solution of a highly non-linear system of simultaneous algebraic equations, the number of which depends on the number of the layers in a particular laminate. Such a laborious and numerically complicated procedure was not employed in the present study, mostly because it is currently uncertain whether its possible success will be found to have any practical importance. The possibility, however,

has been left open for a future extension of the present method towards in that direction. It should be finally noted that, the discussed theories have been outlined and are therefore only available in connection with geometrically linearly elastic problems. However, the possibility of extending their applicability for the accurate stress analysis of beams subjected geometrically non-linear deformations is wide open.

## Appendix 1:

### General solution of general three-degree-of-freedom beam theory equations

The general solution of the ordinary differential equations (3.5-3) is given as follows:

$$u_0 = \frac{1}{E_1} [E_3(K_1 e^{\mu x} + K_2 e^{-\mu x}) + D_{11}^c(K_3 x + K_4) - B_{11}^c(K_5 x^2 + K_6 x + K_7) + \frac{2K_5 E_2 E_3}{A_{55}^a E_1}] + A \cos p_m x,$$

$$w_0 = \frac{1}{E_1} \left[ \frac{E_2}{\mu} (K_1 e^{\mu x} - K_2 e^{-\mu x}) + B_{11}^c \left( \frac{1}{2} K_3 x^2 + K_4 x \right) - A_{11}^c \left( \frac{1}{3} K_5 x^3 + \frac{1}{2} K_6 x^2 + K_7 x \right) + K_8 + \frac{2K_5 E_2^2}{A_{55}^a E_1} \right] + C \sin p_m x,$$

$$u_1 = K_1 e^{\mu x} + K_2 e^{-\mu x} + \frac{2K_5 E_2}{A_{55}^a E_1} + B \cos p_m x, \quad (\text{A1-1})$$

where

$$E_1 = A_{11}^c D_{11}^c - (B_{11}^c)^2, \quad E_2 = A_{11}^c D_{11}^a - B_{11}^c B_{11}^a, \quad E_3 = B_{11}^c D_{11}^a - D_{11}^c B_{11}^a, \\ \mu = \sqrt{\frac{A_{55}^a E_1}{B_{11}^a E_3 - D_{11}^a E_2 + D_{11}^{aa} E_1}}, \quad (\text{A1-2})$$

and  $K_i$  ( $i=1, 2, \dots, 8$ ) are arbitrary constants of integration to be determined when a set of edge boundary conditions (Equation 3.5-3) is specified. The remaining constants  $A$ ,  $B$  and  $C$  are the coefficients of the particular integrals of Equation (3.5-3) with the form of (3.5-6) and, as such, are identical to the solution of the simply supported beam.

## Appendix 2:

### General solution of general four-degree-of-freedom beam theory equations

The general solution of the system of ordinary differential equations (3.4-3) can be written in the following form, which is independent of the choice of the shape functions:

$$\begin{aligned}
 u_0 &= \frac{1}{F_1} \left\{ \sum_{i=1}^4 \frac{1}{\mu_i} [A_{55}^{aa} F_1 F_5 + \mu_i^2 (F_3 G_2 - F_5 G_1)] K_i e^{\mu_i x} + Q_3 K_5 x - Q_2 \left( \frac{1}{2} K_6 x^2 + K_7 x \right) + K_8 \right\} \\
 &\quad + A \cos p_m x, \\
 w_0 &= \frac{1}{F_1} \left\{ \sum_{i=1}^4 \frac{1}{\mu_i} [A_{55}^{aa} F_1 F_4 + \mu_i^2 (F_2 G_2 - F_4 G_1)] K_i e^{\mu_i x} \right\} \\
 &\quad + \frac{1}{F_1} \left\{ \frac{1}{2} Q_2 K_5 x^2 - Q_1 \left( \frac{1}{6} K_6 x^3 + \frac{1}{2} K_7 x^2 \right) + K_9 x + K_{10} \right\} + C \sin p_m x, \\
 u_1 &= \sum_{i=1}^4 \mu_i G_2 K_i e^{\mu_i x} + \frac{F_2 G_4 - F_4 G_2}{A_{55}^{aa} F_1 G_4} K_6 + B \cos p_m x, \\
 w_1 &= \sum_{i=1}^4 (A_{55}^{aa} F_1 - \mu_i^2 G_1) K_i e^{\mu_i x} + \frac{F_5}{G_4} K_5 - \frac{F_4}{G_4} (K_6 x + K_7) + D \sin p_m x, \tag{A2-1}
 \end{aligned}$$

where,

$$\begin{aligned}
 F_1 &= A_{11}^c D_{11}^c - B_{11}^{c^2}, & G_1 &= B_{11}^a F_3 - D_{11}^a F_2 + D_{11}^{aa} F_1, & Q_1 &= A_{11}^c + \frac{F_4^2}{G_4}, \\
 F_2 &= A_{11}^c D_{11}^a - B_{11}^c B_{11}^a, & G_2 &= B_{11}^a F_5 - D_{11}^a F_4 + (D_{13}^{ab} - A_{55}^{ab}) F_1, & Q_2 &= B_{11}^c + \frac{F_4 F_5}{G_4}, \tag{A2-2} \\
 F_3 &= B_{11}^c D_{11}^a - D_{11}^c B_{11}^a, & G_3 &= B_{13}^b F_3 - D_{13}^b F_2 + (D_{13}^{ab} - A_{55}^{ab}) F_1, \\
 F_4 &= A_{11}^c D_{13}^b - B_{11}^c B_{13}^b, & G_4 &= B_{13}^b F_5 - D_{13}^b F_4 + D_{33}^{bb} F_1, & Q_3 &= D_{11}^c + \frac{F_5^2}{G_4}, \\
 F_5 &= B_{11}^c D_{13}^b - D_{11}^c B_{13}^b,
 \end{aligned}$$

and  $\mu_i$  are the four roots of the following equation:

$$A_{55}^{bb} F_1 G_1 \mu^4 - (G_1 G_4 - G_2 G_3 + A_{55}^{bb} A_{55}^{aa} F_1^2) \mu^2 + A_{55}^{aa} F_1 G_4 = 0. \quad (\text{A2-3})$$

The trigonometric terms in the displacement general solution represent the particular integral of differential equations (3.4-3) with the form of (3.4-6) for the corresponding solution of simply supported beams. Their constant coefficients are determined from the solution of (3.6-17). In the particular case of a beam having both edges simply supported, all 10 arbitrary constants of integration  $K_i$  ( $i = 1, 2, \dots, 10$ ) take zero values and equations (3.4-3) are naturally reduced to their appropriate trigonometric form. The ten arbitrary constants of integration  $K_i$  are free to be determined by means of an appropriate set of boundary conditions (Equation 3.4-5) imposed at the edges  $x = 0$  and  $x = L$  of the beam.

### Appendix 3:

## General solution of general five-degree-of-freedom beam theory equations

Regardless of the particular form of the shape functions employed, the general solution of the ordinary differential equations (3.3-3) can be written as follows:

$$\begin{aligned}
 u &= \sum_{i=1}^4 (E_1 E_{7i} + E_2 E_{8i} + E_5 \mu_i) K_i e^{\mu_i x} + K_9 + K_{10} x + E_5 K_8 x^2 + A \cos p_m x, \\
 v &= \sum_{i=1}^4 (E_3 E_{7i} + E_4 E_{8i} + E_6 \mu_i) K_i e^{\mu_i x} + K_{11} + K_{12} x + E_6 K_8 x^2 + C \cos p_m x, \\
 u_1 &= \sum_{i=1}^4 E_{7i} K_i e^{\mu_i x} + 2 \frac{C_3 A_{4422} - C_6 A_{4512}}{A_{4422} A_{5511} - A_{4512}^2} K_8 + B \cos p_m x, \\
 v_1 &= \sum_{i=1}^4 E_{8i} K_i e^{\mu_i x} + 2 \frac{C_6 A_{5511} - C_3 A_{4512}}{A_{4422} A_{5511} - A_{4512}^2} K_8 + D \cos p_m x, \\
 w &= \sum_{i=1}^4 K_i e^{\mu_i x} + K_5 + K_6 x + K_7 x^2 + \frac{1}{3} K_8 x^3 + E \sin p_m x,
 \end{aligned} \tag{A3-1}$$

where  $K_i$  ( $i=1, 2, \dots, 12$ ) are arbitrary constants of integration to be determined when a set of edge boundary conditions (Equation 3.3-5) are specified. Moreover,  $\mu_i$  ( $i=1, 2, 3, 4$ ) are the four roots of the following quartic equation:

$$\begin{aligned}
 &(C_1 C_5 C_9 + C_2 C_6 C_7 + C_3 C_4 C_8 - C_1 C_6 C_8 - C_2 C_4 C_9 - C_3 C_5 C_7) \mu^4 + \\
 &[(C_3 C_7 - C_1 C_9) A_{4422} + (C_6 C_8 - C_5 C_9) A_{5511} + \\
 &(C_9 C_2 + C_9 C_4 - C_3 C_8 - C_6 C_7) A_{4512}] \mu^2 + C_9 (A_{4422} A_{5511} - A_{4512}^2) = 0,
 \end{aligned} \tag{A3-2}$$

where,

$$\begin{aligned}
 C_1 &= B_{111}E_1 + B_{161}E_3 + D_{1111}, & C_2 &= B_{111}E_2 + B_{161}E_4 + D_{1612}, \\
 C_3 &= B_{111}E_5 + B_{161}E_6 - D_{111}, & C_4 &= B_{162}E_1 + B_{662}E_3 + D_{1612}, \\
 C_5 &= B_{162}E_2 + B_{662}E_4 + D_{6622}, & C_6 &= B_{162}E_5 + B_{662}E_6 - D_{162}, \\
 C_7 &= B_{11}E_1 + B_{16}E_3 + D_{111}, & C_8 &= B_{11}E_2 + B_{16}E_4 + D_{162}, \\
 C_9 &= B_{11}E_5 + B_{16}E_6 - D_{11},
 \end{aligned} \tag{A3-3}$$

and,

$$\begin{aligned}
 E_1 &= \frac{A_{16}B_{161} - A_{66}B_{111}}{A_{11}A_{66} - A_{16}^2}, & E_2 &= \frac{A_{16}B_{662} - A_{66}B_{162}}{A_{11}A_{66} - A_{16}^2}, & E_3 &= \frac{A_{16}B_{111} - A_{11}B_{161}}{A_{11}A_{66} - A_{16}^2}, \\
 E_4 &= \frac{A_{16}B_{162} - A_{11}B_{662}}{A_{11}A_{66} - A_{16}^2}, & E_5 &= \frac{A_{66}B_{11} - A_{16}B_{16}}{A_{11}A_{66} - A_{16}^2}, & E_6 &= \frac{A_{11}B_{16} - A_{16}B_{11}}{A_{11}A_{66} - A_{16}^2}, \\
 E_7 &= \frac{C_6(C_2\mu_i^2 - A_{4512}) - C_3(C_5\mu_i^2 - A_{4422})}{(C_1\mu_i^2 - A_{5511})(C_5\mu_i^2 - A_{4422}) - (C_2\mu_i^2 - A_{4512})(C_4\mu_i^2 - A_{4512})}, \\
 E_8 &= \frac{C_3(C_4\mu_i^2 - A_{4512}) - C_6(C_1\mu_i^2 - A_{5511})}{(C_1\mu_i^2 - A_{5511})(C_5\mu_i^2 - A_{4422}) - (C_2\mu_i^2 - A_{4512})(C_4\mu_i^2 - A_{4512})}.
 \end{aligned} \tag{A3-4}$$

The remaining constants,  $A$ ,  $B$ ,  $C$ ,  $D$  and  $E$ , appearing in equations (A3-1) are the coefficients of terms that represent particular integrals of the set of equations (3.3-3). As such, these terms are identical to the solution of the simply supported beam obtained with the form of (Equation 3.3-7). For plates subjected to a different set of edge boundary conditions, corresponding values to those constants,  $K_i$  ( $i=1, 2, \dots, 12$ ) are determined by applying that set of boundary conditions to equations (Equation 3.3-5).

## References

- Ali, J.S.M., Bhaskar, K., Varadan, T.K. 1999. A new theory for accurate thermal/mechanical flexural analysis of symmetric laminated plates. *Composite Structures*, 45:227-232.
- Bhimaraddi, A., Stevens, L.K. 1984. A higher order theory for free vibration of orthotropic, homogeneous and laminated rectangular plates. *Journal of Applied Mechanics*, 51:195-198.
- Bickford, W.B. 1982. A consistent higher-order beam theory. *Developments in Theoretical and Applied Mechanics*, 11:137-142.
- Cauchy, A. 1828. Sur l'équilibre et le mouvement d'une plaque solid. *Exercise de Mathematique*, 3.
- Cho, K.N., Striz, A.G., Bert, C.W. 1989. Thermal stress analysis of laminate using higher-order theory in each layer. *Journal of Thermal Stresses*, 12:321-332.
- Cho, M., Pannerter, R.R. 1993. Efficient higher order composite plate theory for general lamination configurations. *AIAA Journal*, 31:1299-1306.
- Chow, T.S. 1971. On the propagation of flexural waves in an orthotropic laminated plates and its response to an impulsive load. *Journal of Composite Materials*, 5:307-19.
- Coper, G.R. 1966. The shear coefficient in Timshenko's beam theory. *Journal of Applied Mechanics*, June:335-40.
- DiSciuva, M. 1986. Bending, vibration and buckling of simply supported thick multilayered orthotropic plates: An evaluation of a new displacement model. *Journal of Sound Vibration*, 105(3):425-42.

- DiSciuva, M. 1987. An improved shear-deformation theory for moderately thick multilayered anisotropic shells and plates. *Journal of Applied Mechanics*, 54:589-596.
- Heuer, R. 1992. Static and dynamic analysis of transversely isotropic, moderately thick sandwich beams by analogy. *Acta Mechanica*, 91:1-9.
- Jane, K.C., Hong, C.C. 2000. Interlaminar stresses of a rectangular laminated plate with simply supported edges subject to free vibration. *International Journal of Mechanical Science*, 42:2031-2039.
- Jones, R.M. 1975. *Mechanics of composite materials*. Hemisphere Publishing Corporation, New York.
- Jones, R.M. 1999. *Mechanics of composite materials*. Taylor & Francis Ltd, London.
- Khdeir, A.A., Reddy, J.N. 1991. Thermal stresses and deflections of cross-ply laminated plates using refined plate theories. *Journal of Thermal Stresses*, 14:419-438.
- Khdeir, A.A., Reddy, J.N. 1999. Jordan canonical form solution for thermally induced deformations of cross-ply laminated composite beams. *Journal of Thermal Stresses*, 22:331-346.
- Kirchhoff, G. 1850. Über das Gleichgewicht und die bewegung einer elastischen Scheibe. *J. Reine Ang. Math.*, 40:51-88
- Lee, K.H., Senthilnathan, N.R., Lim, S.P., Chow, S.T. 1990. An improved zig-zag model for the bending of laminated composite plates. *Composite Structures*, 15:137-148.
- Li S. 1996. Rigidities of one-dimensional laminates of composite materials. *Journal of Engineering Mechanics*, April:371-374

- Liu, S.L., Soldatos, K.P. 2001. On the improvement of transverse stress distributions in cross-ply laminated beams: Advanced versus conventional beam theories. International Journal of Mechanical Science (submitted)
- Love, A.E.H., 1952. A treatise on the mathematical theory of elasticity. Cambridge University Press, 4<sup>th</sup> Edition.
- Mindlin, R.D. 1951. Influence of rotatory inertia and shear on flexural vibrations of isotropic elastic plates. Journal of Applied Mechanics, 18:31-38.
- Murakami, H. 1993. Assessment of plate theories for treating the thermomechanical response of layered plates. Composites Engineering, 3:137-149.
- Noor, A.K., Burton, W.S. 1990a. Assessment of computational models for multilayered composite shells. Applied Mechanics Review, 43:67-97.
- Noor, A.K., Burton, W.S. 1990b. Predictor-corrector procedures for stress and free vibration analyses of multilayered composite plates and shells. Computer Methods in Applied Mechanics and Engineering, 82:341-63.
- Noor, A.K., Burton, W.S. 1991. Predictor-corrector procedure for thermal buckling of multilayered composite plates. Computers and Structures, 40(5):1071-1084.
- Noor, A.K., Burton, W.S. 1992. Computational models for high-temperature multilayered composite plates and shells. Applied Mechanics Reviews, 45:419-446.
- Noor, A.K., Kim, Y.H., Peters, J.M. 1994. Transverse shear stresses and their sensitivity coefficients in multilayered composite panels. AIAA Journal, 32:1259-1269.

- Noor, A.K., Malik, M. 1999. Accurate determination of transverse normal stresses in sandwich panels subjected to thermomechanical loadings. *Computer Methods in Applied Mechanics and Engineering*, 178:431-43.
- Novozhilov, V.V. 1964. *Thin shell theory*. P. Noordhoff ltd, Groningen.
- Pagano, N.J. 1969. Exact solution for composite laminates in cylindrical bending. *Journal of Composite Materials*, 3:398-411.
- Pagano, N.J. 1970. Influence of shear coupling in cylindrical bending of anisotropic laminates. *Journal of Composite Materials*, 4:330-343.
- Pell, W.H. 1946. Thermal deflections of anisotropic thin plates. *Quarterly of Applied Mathematics*, 4:27-44.
- Poisson, S.D. 1829. *Memoire sur l'equilibre et le mouvement des corps solides*. *Memoire de l'Academia de Science*, 8.
- Raman, P.M., Davalos, J.F. 1996. Static shear correction factor for laminated rectangular beams. *Composites*, 27(B):285-93.
- Reddy, J.N. 1984. A simple higher-order theory for laminated composite plates. *Journal of Applied Mechanics*, 51:745-752.
- Reddy, J.N. 1997. *Mechanics of laminated composite plates: theory and analysis*. CRC Press, Inc, New York.
- Reddy, J.N., Bert, C.W., Hsu, Y.S., Reddy, V.S. 1980. Thermal bending of thick rectangular plates of bimodulus composite materials. *Journal of Mechanical Engineering Science*, 22 (6):297-304.
- Reddy, J.N., Hsu, Y.S., 1980. Effects of shear deformation and anisotropy on the thermal bending of layered composite plates. *Journal of Thermal Stresses*, 3:475-493.

- Reissner, E. 1945. The effect of transverse shear deformations on the bending of elastic plates. *Journal of Applied Mechanics*, 12:A69-A77.
- Ren, J.G. 1986. Bending theory of laminated plate. *Composites Science and Technology*, 27:225-248
- Savithri, S., Varadan, T.K. 1990. Free vibration and stability of cross-ply laminated plates. *Journal of Sound Vibration*, 141(3):516-20.
- Savoia, M., Reddy, J.N. 1995. Three-dimensional thermal analysis of laminated composite plates. *International Journal of Solids and Structures*, 32:593-608.
- Savoia, M., Reddy, J.N. 1997. Three-dimensional thermal analysis of laminated composite plates-closure. *International Journal of Solids and Structures*, 34:4653-4654.
- Shu X., Soldatos K.P. 2000. Cylindrical bending of angle-ply laminates subjected to different sets of edge boundary conditions. *International Journal of Solids and Structures*, 37:4289-4307.
- Sokolnikoff, I.S. 1956. *Mathematical theory of elasticity (Second edition)*. McGraw-Hill Book Company, Inc, New York.
- Soldatos, K. P. and Timarci, T. 1993: A unified formulation of laminated composite shear deformable five-degrees- of-freedom cylindrical shell theories. *Composite Structure* 25, 165-171
- Soldatos, K.P. 1992. A transverse shear deformation theory for homogeneous monoclinic plates. *Acta Mechanica*, 94:195-220.
- Soldatos, K.P. 1993. Vectorial approach for the formulation of variationally consistent higher-order plate theory. *Composite Engineering*, 3(1):3-17.

- Soldatos, K.P. 1995. Generalization of variationally consistent plate theories on the basis of a vectorial formulation. *Journal of Sound Vibration*, 183:819-839.
- Soldatos, K.P., Liu, S.L. 2001. On the generalised plane strain deformations of thick anisotropic composite laminated plates. *International Journal of Solids and structures*, 38:479-482.
- Soldatos, K.P., Watson, P. 1997a. A method for improving the stress analysis performance of one- and two-dimensional theories for laminated composites. *Acta Mechanica*, 123:163-186.
- Soldatos, K.P., Watson, P. 1997b. Accurate stress analysis of laminated plates combining a two-dimensional theory with the exact three-dimensional solution for simply supported edges. *Mathematics and Mechanics of Solids*, 2:459-489.
- Soldatos, K.P., Watson, P. 1997c. A general theory for the accurate stress analysis of homogeneous and laminated composite beams. *International Journal of Solids and structures*, 22:2857-2885.
- Srinivas, S., Rao, A.K. 1970. Bending, vibration and buckling of simply supported thick orthotropic rectangular plates and laminates. *International Journal of Solids and structures*, 6:1466-1481.
- Srinivas, S., Rao, A.K. 1972. A note on flexure of thick rectangular plates and laminates with variation of temperature across thickness. *Bulletin of the Polish Academy of Sciences, Technical Sciences*, 20:229-234.
- Stavsky, Y. 1963. Thermoelasticity of heterogeneous anisotropic plates. *Journal of Engineering Mechanics Division, Proceedings of ASCE*, 89:89-105.
- Sun, C.T., Whitney, J.M., Whitford, L. 1975. Dynamic response of laminated composite plates. *AIAA Journal*, 13(10):1259-1260.

- Tauchert, T.R. 1980. Thermoclastic analysis of laminated orthotropic slabs. *Journal of Thermal Stresses*, 3:117-132.
- Tauchert, T.R. 1991. Thermally induced flexure, buckling, and vibration of plates. *Applied Mechanics Reviews*, 44:347-360.
- Thangjitham, S., Choi, H.J. 1991. Thermal stresses in a multilayered anisotropic medium. *Journal of Applied Mechanics*, 58:1021-1027.
- Timarci, T. and Soldatos, K.P. 1995. Comparative dynamic studies for symmetric cross-ply circular cylindrical shells on the basis of a unified shear deformable shell theory, *Journal of Sound and Vibration* 187, 609-624.
- Timoshenko, S.P. 1921. On the correction for shears of the differential equation for transverse vibrations of prismatic bars. *Philosophical Magazine*, 41:744-746.
- Touratier, M. 1992. A refined theory of laminated shallow shells. *International Journal of Solids and Structures*, 29:1401-1415
- Tungikar, V.B., Rao, K.M. 1994. Three dimensional exact solution of thermal stresses in rectangular composite laminate. *Composite Structures*, 27:419-430.
- Vel, S.S., Batra, R.C. 2000. The generalized plane strain deformations of thick anisotropic composite laminated plates. *International Journal of Solids and structures*, 37:715-733.
- Vel, S.S., Batra, R.C. 2001. Generalized plane strain thermoelastic deformation of laminated anisotropic thick plates. *International Journal of Solids and Structures*, 38:1395-1414
- Whitney, J.M. 1973. Shear correction factors for orthotropic laminates under static load. *Journal of Applied Mechanics*, March:302-304.

Whitney, J.M. 1987. *Structural Analysis Of Laminated Anisotropic Plates*. Technomic Publishing Company, Inc.

Wu, C.H., Tauchert, T.R. 1980a. Thermoelastic analysis of laminated plates 1: symmetric specially orthotropic laminates. *Journal of Thermal Stresses*, 3:247-259.

Wu, C.H., Tauchert, T.R. 1980b. Thermoelastic analysis of laminated plates 2: antisymmetric cross-ply and angle-ply laminates. *Journal of Thermal Stresses*, 3:365-378.